200

Multi-scale system pharmacology modelling pipeline to assess the prophylactic efficacy of NRTIs against HIV-1

Mr Sulav Duwal[1], Mr Vikram Sunkara[2], Mr Max von Kleist[1]

[1]Freie University Berlin, Berlin, Germany, [2]Zuse Institute Berlin, Berlin, Germany

Aims: Pharmacointervention strategies are promising tools to curb the HIV-1 epidemic. Two strategies have recently been proposed: (i) Treatment-as-prevention (TasP) targets potential transmitters by reducing the patients' virus load and thereby also their contagiousness. However, onwards transmission may preferentially occur early after infection when the individual is unaware of his/her serologic status and may not have initiated treatment [1]. (ii) Pre-exposure prophylaxis (PrEP) targets uninfected individuals at risk. Prophylactic drug intake reduces infection probabilities following viral exposure and has proven to effectively prevent vertical transmission [2]. Nucleotide reverse transcriptase inhibitors (NRTIs) are currently intensively investigated as PrEP compounds. While PrEP efficacy depends on a number of factors (e.g. the viral exposure, PK-PD, transmitted drug resistance), our primary focus was to build a modular multi-scale system pharmacology modelling pipeline allowing to combine parameters related to target-site pharmacokinetics (module I), the molecular mechanism of action (MMOA, module II), viral exposure and transmitter virology (module IV) to evaluate PrEP efficacy (module III) for the NRTIs tenofovir (TFV), emtricitabine (FTC) and lamivudine (3TC). Moreover, the pipeline allows to translate in vitro testable parameters to measures of PrEP efficacy (modules II-III).

Methods: While the PK and MMOA modules (I & II) have been developed and validated against clinical data in a previous work [3,4], here we analyze the effects of NRTIs in reducing infection (module III). In this regard, we derived a stochastic master equation, allowing to resolve the probability- and timing of infection after exposure. With regard to module IV, we developed a statistical model that computes viral exposure distributions in the recipient depending on the viral load of the transmitter, and the mode of transmission. The model was parametrized by available data from a large observational study (German Seroconverter Study), complemented and validated by literature data.

Results: Combining all modules allowed to estimate the PrEP-efficacy for various schedules ('on demand' or 'chronic' administration with single drugs or combinations) in relation to the timing of viral exposure, with wild type or mutant strains. In contrast to the current beliefs [5], our pipeline revealed that FTC and 3TC were superior to TFV in inhibiting sexual infection with wild type virus, which was particularly evident for PrEP 'on demand'. However, due to its intracellular half-life TFV is more pharmacologically forgiving, in cases of incomplete or poor adherence.

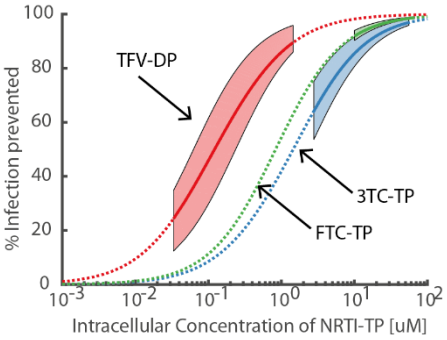

Figure 1: Concentration vs. Transmission Risk Reduction. The dotted lines represent the mean protection (% infection prevented) following homosexual intercourse for various intracellular concentrations of active NRTI-triphosphates. The solid lines present the mean efficacies for clinically relevant concentration ranges (when 300mg TDF, 200mg FTC or 300mg 3TC were applied once daily). The shaded regions represent the interquartile range of the predicted risk reduction, when variability in microscopic parameters (module II) and virus exposure (module IV) were taken into account.

Conclusion: In this work, we present the first framework allowing to estimate PrEP efficacy by integrating target-site PK (module I), MMOA (module II) and viral exposure (module IV). This framework allows to *in silico* assess a variety of phenomena, including pharmacologic limitations, mode of- and timing of viral challenge with respect to PrEP administration, as well as impacts on transmitted drug resistance. The framework can be extended to other antiviral classes to screen for PrEP candidates. In addition, the model can be used to explore TasP efficacy with- or without PrEP and can therefore inform- and extend epidemiologic models.

References:

1. Yousef KP, Meixenberger K, Smith MR, Somogyi S, Gromöller S, Schmidt D, Gunsenheimer-Bartmeyer B, Hamouda O, Kücherer C and von Kleist M (2016) JAIDS (under revision)
2. Frank* M, von Kleist* M, Kunz A, Harms G, Schütte C and Kloft C. (2011) Antimicrob. Agents Chemother 55, 5529,
3. von Kleist M, Metzner P, Marquet R and Schütte C (2012) PLoS Comp. Biol. 8: e1002359
4. Duwal S, von Kleist M (2016) European Journal of Pharmaceutical Sciences
5. Hendrix CW (2013) Cell.

201

Joint modelling of plasma and fecal moxifloxacin pharmacokinetics in healthy volunteers

Dr Charles Burdet[1,2], Dr Thu-Thuy Nguyen[1], Dr Jean de Gunzburg[3], Dr Annie Ducher[3], Dr Marion Ghidi[3], Pr Xavier Duval[1,2], Dr Marina Varastet[3], Pr Antoine Andremont[1,2], Pr France Mentré[1,2]

[1]INSERM & Paris Diderot University, UMR 1137, Paris, France, [2]AP-HP, Bichat Hospital, Paris, France, [3]Da Volterra, Paris, France

Aims: Antibiotic administration leads to fecal microbiota disruption with emergence of antimicrobial resistance [1]. Animal data suggest that emergence of bacterial resistance can be predicted from fecal antibiotic exposure [2]. We developed a joint model of plasma and fecal pharmacokinetics of the fluoroquinolone antimicrobial moxifloxacin after oral administration in humans.

Methods: Twenty-two healthy volunteers were recruited in a randomized clinical trial (sponsor Da Volterra) and received either a 5-day course of moxifloxacin (n=14) or no moxifloxacin (n=8, used as a control group for microbiota analysis). Moxifloxacin dosing regimen (400 mg OAD) was similar to that usually administered in infected patients. Moxifloxacin plasma concentrations were determined at D1 and D5. Eleven fecal samples were obtained from D1 to D16 for measures of moxifloxacin concentrations. Nonlinear mixed-effects modelling was performed to characterize the pharmacokinetic properties of moxifloxacin and its fecal excretion. The weight of feces was fixed to 200 g/day. Model selection was performed by visual inspection of various goodness of fit plots and the Bayesian Information Criteria. Analysis was performed using the SAEM algorithm and the Monolix software (Lixoft, France) [3]. Population parameters and their residual standard errors are reported.

Results: We present here the results of the pharmacokinetic modelling. Moxifloxacin plasma concentrations were best described by a 2 compartment model with first order absorption and linear elimination, with a lag time. Fecal concentrations were modeled using a fecal compartment connected to the peripheral compartment. Goodness-of-fit of this model was satisfactory. In the plasma model, T_{lag} and k_a were estimated to 0.348 h (RSE=18%) and 3.241 h^{-1} (55%). k was estimated to 0.067 h^{-1} (5%), k_{12} to 0.021 h^{-1} (18%) and k_{21} to 0.038 h^{-1} (25%). The volume of distribution V in the central compartment was estimated to 98.9 L (5%). The rate of entry of moxifloxacin in the fecal compartment was estimated to 0.023 h^{-1} (15%), and the rate of elimination from the fecal compartment to 0.067 h^{-1} (14%). Variabilities (expressed in CV%) were estimated below 40% for all parameters, with the exception of k_a for which a high variability was estimated (160%). Retained residual error model was proportional for the plasma concentrations (23%) and combined for the fecal concentrations (with a residual error of 53%).

Conclusion: We developed the first joint model of moxifloxacin pharmacokinetics in plasma and feces. The administration of moxifloxacin modifies the composition of the fecal microbiota, as it was shown for other antimicrobials [4, 5]. This might allow for resistant strains or other pathogenic bacteria to colonize the gut. The next step is to investigate the link between the moxifloxacin fecal exposure and the bacterial microbiota diversity measured by the Shannon index.

References:

1. Andremont A. Commensal Flora May Play Key Role in Spreading Antibiotic Resistance. ASM News 2003; 69(12): 601-7.
2. Nguyen TT, Guedj J, Chachaty E, de Gunzburg J, Andremont A, Mentre F. Mathematical modeling of bacterial kinetics to predict the impact of antibiotic colonic exposure and treatment duration on the amount of resistant enterobacteria excreted. PLoS Comput Biol 2014; 10(9): e1003840.
3. Kuhn E, Lavielle M. Maximum likelihood estimation in nonlinear mixed effects models. Comput Statist Data Anal 2005; 49: 1020-38.
4. Fantin B, Duval X, Massias L, et al. Ciprofloxacin dosage and emergence of resistance in human commensal bacteria. J Infect Dis 2009; 200(3): 390-8.
5. Michea-Hamzehpour M, Auckenthaler R, Kunz J, Pechere JC. Effect of a single dose of cefotaxime or ceftriaxone on human faecal flora. A double-blind study. Drugs 1988; 35 Suppl 2: 6-11.

202

Favipiravir pharmacokinetics in non-human primates: insights for future efficacy studies against hemorrhagic fever viruses

Vincent Madelain[1], Dr Jérémie Guedj[1], Pr France Mentré[1], Dr Thi Huyen Tram Nguyen[1], Frédéric Jacquot[2], Dr Koichi Yamada[3], Dr Yousuke Furuta[3], Dr Takumi Kadota[3], Dr Anne-Marie Taburet[4], Pr Xavier de Lamballerie[5,6], Dr Hervé Raoul[2]

[1]INSERM , Université Paris Diderot, IAME, UMR 1137, Sorbonne Paris Cité, F-75018 Paris, FRANCE, [2]Laboratoire P4 Inserm-Jean Mérieux, US003 Inserm, 69365 Lyon, France, [3]Dept Research Laboratory of Toyama Chemical Co Ltd, Toyama, Japan, [4]Hopital Bicêtre, Assistance Publique-Hôpitaux de Paris; INSERM U1184, Center for Immunology of Viral Infections and Autoimmune Diseases, CEA, Université Paris-Sud, Kremlin Bicêtre, France, [5]UMR "Emergence des Pathologies Virales" (EPV: Aix-Marseille university - IRD 190 - Inserm 1207 - EHESP), Marseille, France, [6]Institut Hospitalo-Universitaire Méditerranée Infection, Marseille, France

Aims: Favipiravir is an antiviral nucleotide analogue with strong antiviral effectiveness against several hemorrhagic fever viruses *in vitro* and in small animals. This drug was evaluated in Ebola virus infected patient (1), but its efficacy in non-human primates (NHPs) has not been previously assessed. Here, in order to prepare efficacy studies, we aimed to characterize for the first time the pharmacokinetics (PK) of favipiravir administered intravenously for up to 2 weeks at various doses.

Methods: PK studies of favipiravir in Cynomolgus macaques from Chinese and Mauritian origin were performed in Japan and France, respectively. Favipiravir was given by short infusion up to 14 days, with a loading dose of 200-250 mg/kg BID at day 1 followed by a maintenance dose of 60, 100 or 150 mg/kg BID (Chinese NHPs) and 100, 150 or 180 mg/kg BID (Mauritian NHPs). Following a population approach, a PK model was developed to estimate the effect of dose, sex, breed, and to predict by simulation the exposure achieved in various dosing regimen. Assuming a protein binding rate of 50% (2), we proposed doses of favipiravir needed to achieve free concentrations close or above EC_{50} values reported for Ebola virus (50 µg/L), Rift Valley fever and Lassa viruses (5 µg/L) and for Crimea-Congo virus (1 µg/L).

Results: No serious abnormality in the 30 NHPs studied was observed at any of the doses tested. PK was highly non-linear over doses and time with a 20-50% reduction in average concentration at day 14 compared to day 7. This non-linearity was explained in the model by a time-dependent elimination mediated by aldehyde oxidase, the main enzyme involved in favipiravir metabolism (3). The clearance rate was also affected by genetic background, with concentrations much lower in Mauritian than in Chinese NHPs. Consequently maintenance doses of 150 and 130 mg/kg BID in NHPs of Mauritian and Chinese origin, respectively, may be needed to maintain concentration above or close to favipiravir's EC_{50} against EBOV until day 14 (Table 1). Lower maintenance doses of 130 and 100 mg/kg BID in NHPs of Mauritian and Chinese origin, respectively, should be sufficient for Rift valley fever, Lassa and Crimea-Congo viruses.

Table 2: Model predictions for favipiravir plasma free concentrations (Median [5%;95%]).

	Day 7			Day 14		
	C_{trough} (µg/mL)	C_{max} (µg/mL)	C_{ave} (µg/mL)	C_{trough} (µg/mL)	C_{max} (µg/mL)	C_{ave} (µg/mL)
Mauritian NHPs						
60mg/kg	0.0 [0.0-1.8]	71.2 [53.5-91.6]	6.4 [2.7-23.5]	0.0 [0.0-0.3]	68.0 [50.8-88.2]	4.5 [2.1-15.9]
100mg/kg	1.5 [0.0-35.8]	132.2 [97.2-186.0]	33.8 [6.6-92.4]	0.1 [0.0-25.0]	123.2 [91.3-172.9]	16.6 [4.1-78.5]
130mg/kg	15.5 [0.0-82.9]	189.5 [132.7-280.0]	74.6 [12.8-165.1]	2.3 [0.0-63.7]	169.5 [122.5-259.1]	41.0 [6.1-143.6]
150mg/kg	30.3 [0.0-112.7]	229.9 [159.0-344.6]	107.6 [19.7-211.7]	8.5 [0.0-94.4]	204.4 [143.8-320.5]	66.0 [7.6-190.3]
180mg/kg	58.9 [0.3-159.0]	298.9 [197.8-439.3]	156.1 [38.0-285.5]	26.1 [0.0-137.8]	261.6 [176.6-420.5]	109.9 [10.0-262.0]
Chinese NHPs						
60mg/kg	0.6 [0.0-13.5]	80.0 [60.5-104.4]	16.8 [6.6-44.2]	0.1 [0.0-7.4]	77.2 [59.3-98.9]	11.6 [4.9-35.6]
100mg/kg	17.2 [0.1-66.0]	151.3 [108.2-217.5]	62.1 [17.0-127.8]	4.7 [0.0-53.7]	138.9 [103.2-203.6]	39.5 [10.1-113.0]
130mg/kg	43.4 [1.5-111.8]	217.0 [150.3-314.3]	108.0 [32.2-197.2]	19.6 [0.0-94.5]	193.8 [140.0-298.7]	76.2 [14.4-184.2]
150mg/kg	61.8 [4.4-145.1]	263.7 [179.8-379.4]	142.1 [46.7-246.7]	33.7 [0.0-128.0]	232.2 [164.0-359.5]	107.1 [19.1-227.7]
180mg/kg	93.8 [10.5-198.3]	335.3 [227.2-479.2]	191.8 [72.8-319.5]	59.7 [0.0-180.4]	296.8 [202.5-452.4]	152.7 [25.2-299.4]

Conclusion: Our results shows that favipiravir PK was largely nonlinear over doses and time, leading to a large decrease in concentrations after day 7, that could be captured by a mechanistic enzyme based model. In absence of intracellular data, dose recommendation was based on protein unbound plasma concentrations, but the relevance of this approach will need further efficacy studies.

References:

1. Sissoko D, Laouenan C, Folkesson E, M'Lebing A-B, Beavogui A-H, Baize S, et al. Experimental Treatment with Favipiravir for Ebola Virus Disease (the JIKI Trial): A Historically Controlled, Single-Arm Proof-of-Concept Trial in Guinea. PLoS Med. 2016 Mar;13(3):e1001967.
2. Mentré F, Taburet A-M, Guedj J, Anglaret X, Keïta S, de Lamballerie X, et al. Dose regimen of favipiravir for Ebola virus disease. Lancet Infect Dis. 2015 Feb;15(2):150–1.
3. Madelain V, Nguyen THT, Olivo A, de Lamballerie X, Guedj J, Taburet A-M, et al. Ebola Virus Infection: Review of the Pharmacokinetic and Pharmacodynamic Properties of Drugs Considered for Testing in Human Efficacy Trials. Clin Pharmacokinet. 2016 Jan 21;

203

Population pharmacokinetics of artesunate and dihydroartemisinin in patients with sensitive and resistant malaria infection

Miss Thanaporn Wattanakul[1,2], Debashish Das[1,3], Rupam Tripura[1], Aung Pyae Phyo[4], Khin Maung Lwin[4], Poravuth Yi[5], Nicholas P. J. Day[1,2], Duong Socheat[5], Chea Nguon[5], Nicholas J. White[1,2], François Nosten[1,2,4], Arjen M. Dondorp[1,2], Joel Tarning[1,2]

[1]Mahidol-Oxford Tropical Medicine Research Unit, Faculty of Tropical Medicine, Mahidol University, Bangkok, Thailand, [2]Centre for Tropical Medicine and Global Health, Nuffield Department of Medicine, University of Oxford, Oxford, United Kingdom, [3]WorldWide Antimalarial Resistance Network, Oxford, United Kingdom, [4]Shoklo Malaria Research Unit, Mae Sot, Thailand, [5]The National Center for Parasitology, Entomology and Malaria Control, Phnom Penh, Cambodia

Aims: Artemisinin-resistant *falciparum* malaria is now prevalent in Southeast Asia. Understanding the pharmacokinetic and pharmacodynamic properties of artesunate and its active metabolite, dihydroartemisinin, in patients with sensitive and resistant malaria is essential to achieve effective and safe treatment. The aim of this work was to characterize the pharmacokinetic properties of artesunate and dihydroartemisinin in patients with sensitive and resistant malaria infections in Myanmar, Cambodia and Thailand.

Methods: A total of 4,217 plasma concentrations of artesunate and dihydroartemisinin from 153 patients from the clinical efficacy study (1) were modeled simultaneously using nonlinear mixed-effects modelling. The model building was conducted using the first-order conditional estimation method with interactions. The first observed serial concentration below the limit of quantification (LLOQ) for each patient was substituted by half of the LLOQ (LLOQ/2), the rest were omitted. Full *in vivo* conversion of artesunate into dihydroartemisinin was assumed and different structural disposition models were evaluated. Several absorption models were investigated i.e. zero-order, first-order, first-order with lag time, and transit absorption models. A stepwise covariate search was used to evaluate the relationship between pharmacokinetic parameters and patient characteristics. Model diagnostics and evaluation were performed using Xpose version 4.0, Pirana, and Pearl-speaks-NONMEM (PsN; version 4.4.8).

Results: A one-compartment disposition model for both artesunate and dihydroartemisinin provided the best fit to the data. An additional disposition compartment, for both artesunate and dihydroartemisinin, resulted in a decreased objective function value (ΔOFV = -205). However, the visual predictive check showed substantial model misspecification in the terminal phase for both compounds, as compared to a simpler one-compartment structural model. Furthermore, the median elimination half-life of dihydroartemisinin was unreasonable long when described using a two-compartment disposition model (16 hours compared to literature values of 30-60 minutes). The one-compartment disposition model was therefore carried forward for both compounds. The absorption of artesunate was best described by a transit absorption model with two transit compartments. Introducing inter-occasion variability on absorption parameters (i.e relative bioavailability and mean transit time) improved the model fit substantially. Body weight was implemented as an allometric function on all clearance (power fixed to 0.75) and volume (power fixed to 1) parameters and resulted in improvement of model fit (ΔOFV = -6.65). Alanine aminotransferase and split dosing regimen (i.e twice daily vs once daily dosing) affected artesunate clearance and dihydroartemisinin clearance significantly during the forward covariate addition (p-value < 0.05) but failed to be retained in the more stringent backward elimination step (p-value < 0.001).

Conclusion: The pharmacokinetic properties of artesunate and dihydroartemisin were adequately described by a flexible transit-compartment absorption of artesunate followed by one-compartment disposition models with full *in vivo* conversion of artesunate into dihydroartemisinin. The pharmacokinetic properties of artesunate and dihydroartemisinin were not different in patients with sensitive and resistant malaria infection.

References:

1. Das D, Tripura R, Phyo AP, Lwin KM, Tarning J, Lee SJ, et al. Effect of high-dose or split-dose artesunate on parasite clearance in artemisinin-resistant falciparum malaria. Clinical infectious diseases: an official publication of the Infectious Diseases Society of America. 2013;56(5):e48-58.

204

Model-based assessment of benefits and risks of rt-PA treatment in acute ischemic stroke

Jinju Guk[1,2], Dongwoo Chae[1,2], Hankil Son[1], Kyungsoo Park[1]

[1]Department Of Pharmacology, Yonsei University College Of Medicine, Seoul, South Korea, [2]Brain Korea 21 plus Project for Medical Science, Yonsei University, Seoul, South Korea

Aims : Recombinant tissue plasminogen activator (rt-PA) is only approved by FDA to treat acute ischemic stroke as first-line therapy. But based upon revascularization rate as low as 20-40% and a severe adverse event of hemorrhage frequently occurring during the course of rt-PA therapy, many studies have been conducted to identify the characteristics of patients who are prone to treatment failure and/or the occurrence of hemorrhagic adverse event. However, there have been no studies to quantitatively evaluate the effectiveness of rt-PA therapy for patients with stroke in hyperacute phase (first 24 hours after stroke) which is a crucial period in determining patient survival. Therefore, the aims of this study were to assess the benefits and risks of rt-PA alone treatment in acute ischemic stroke using a pharmacometrics approach.

Methods: Data was collected from electronic medical records of Severance Hospital, Seoul in South Korea. A total of 336 patients were eligible. For treatment effect, Item Response Theory (IRT) based disease progression model was adopted to describe time course of The National Institutes of Health Stroke Scale (NIHSS) score. For treatment risks, the incidence of and time to additional intervention for reperfusion therapies were modeled using logistic and time-to-event (TTE) models. Finally, time to hemorrhage events was modeled using another TTE model. All of model building strategies were performed using NONMEM7.3 with Laplacian method.

Results: NIHSS score was well characterized by partial credit model (PCM) and disease progression for longitudinal change of stroke severity over the first-24 hours after the initiation of rt-PA treatment was described using asymptotic exponential function. In the incidence model for additional intervention following the failure of rt-PA treatment, high baseline NIHSS score and infarction in middle cerebral artery regions were identified as influencing factors ($p<0.0001$ and $p=0.0008$, respectively). As for TTE model for additional intervention, gompertz hazard function best described the data, with the hazard increasing with baseline NIHSS score ($p=0.0009$). As for TTE model for the hemorrhage event for those who were treated with rt-PA only, weibull hazard function best described the data, with the hazard increasing with time-varying longitudinal change of NIHSS score ($p=0.0006$).

Conclusion: This work suggests that IRT based disease progression model could be used to describe the effectiveness of rt-PA alone for hyperacute phase. It also suggests that management of drug induced risks such as failure with rt-PA treatment and hemorrhage event would also take advantages of pharmacometric approaches in that risks and time to adverse events can be predicted. To sum up, pharmacometric using clinical data can not only provide references for future clinical trials but also apply for the tailored care as a supportive tool in current clinical situations.

205

An optimal sampling schedule for children receiving cephazolin +/- vancomycin for cardiopulmonary bypass

Dr Jacqueline Hannam[1], Professor Brian Anderson[1], Professor Nick Holford[2]

[1]Department of Anaesthesiology, University of Auckland, Auckland, New Zealand, [2]Department of Pharmacology and Clinical Pharmacology, University of Auckland, Auckland, New Zealand

Aims: We aimed to optimise a sampling schedule designed to determine cephazolin and vancomycin PK in critically ill children undergoing cardiopulmonary bypass (CPB).

Methods: Models with allometric scaling and maturation on clearance were identified for vancomycin[1] and cephazolin.[2] Age was simulated using a mean (%CV) value of 5 (0.6) y with weight predicted from age.[3] Doses and dose durations were assumed to vary by 10%. WinPOPT (University of Otago, New Zealand) was used to estimate optimal times for up to 8 samples per patient. We assumed 10 subjects (Group A) receive two doses of cephazolin 50 mg/kg 6-hourly (no CPB, Fig 1), while 50 subjects (Group B) undergo a procedure with CPB (CPB starts 1h post-induction, duration 1.5h). Group B subjects receive cephazolin 50 mg/kg at induction and 5 min after CPB ends (t=2.55h) with 15 subjects also receiving 15mg/kg vancomycin at induction. Optimal sampling times for detecting CPB related changes were considered separately. Designs were selected by comparing criterions and estimated standard errors (SE).

Results: For Group A the best schedule allocated seven samples over dose 1 and one sample over dose 2 (see Table 1), while in Group B, the best schedule allocated 6 samples over dose 1 and a further two over dose 2. SEs for cephazolin parameters were <30% with the exception of V2 (50%). SEs for vancomycin were all <35%. Five samples taken directly from the CPB circuit had greatest efficiency in detecting CPB related changes within the design constraints.

Figure 3

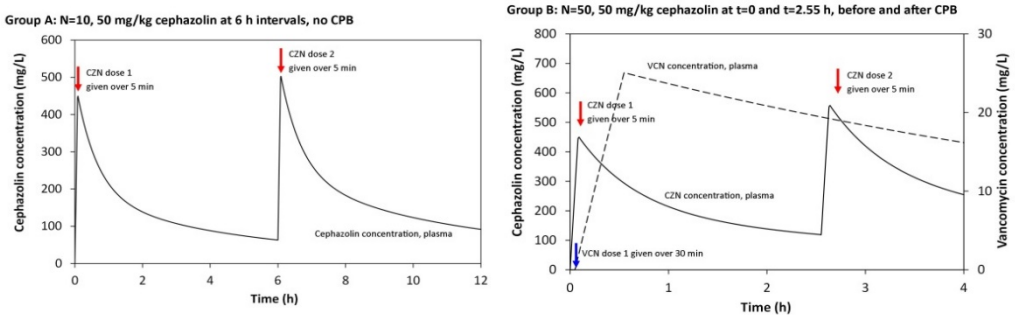

Table 1

Group A Design; criterion (% efficiency)		Group B Design; criterion (% efficiency)	
A1	8 samples over dose 1, 20.49 (ref)	B1	8 samples over dose 1; 16.97 (ref)
A2	7 s samples over dose 1, 1 over dose 2; 30.33 (100%)	B2	7 samples over dose 1, 1 over dose 2; 35.35 (208%)
A3	6 samples over dose 1, 2 over dose 2; 28.90 (95%)	B3	6 samples over dose 1, 2 over dose 2; 37.08 (219%)
A4	5 samples over dose 1, 3 over dose 2; 29.78 (98%)	B4	5 samples over dose 1, 3 over dose 2; 36.78 (217%)
A5	4 samples over dose 1, 4 over dose 1; 29.42 (97%)	B5	4 samples over dose 1, 4 over dose 2; 36.12 (213%)

Final sample times (h post dose)	Dose 1	Dose 2
Group A	0.127, 0.43, 0.43, 1.3, 3.18, 6, 6 h	6 h
Group B	0.001, 0.001, 0.098, 0.37, 0.37, 0.924, 1.5 h	0.37, 1.5 h

Conclusion: This design may be used to plan a clinical study of 50 children receiving cephazolin +/- vancomycin, some of which will also receive a procedure involving CPB.

References:

1. Anderson BJ, Allegaert K, Van den Anker JN, et al. Vancomycin pharmacokinetics in preterm neonates and the prediction of adult clearance. Br J Clin Pharmacol 2007; 63: 75-8.
2. Denti P, Dresner A, Castel S, et al. Population pharmacokinetics of cefazolin in children undergoing elective cardiac surgery. Population Approach Group Europe. Alicante, Spain, 2014.
3. Sumpter AL, Holford NH. Predicting weight using postmenstrual age--neonates to adults. Paediatr Anaesth 2011; 21: 309-315.

206

Repeated time-to-event analysis of Pseudomonas aeruginosa and Aspergillus fumigatus acquisitions in children with cystic fibrosis

Mrs Sabariah Noor Harun[1,2], Prof Claire Wainwright[3,4], Prof Nick Holford[1,5], Dr Stefanie Hennig[1]

[1]School of Pharmacy,The University of Queensland, Brisbane, Australia, [2]School of Pharmaceutical Sciences, Universiti Sains Malaysia , USM, Malaysia, [3]School of Medicine, The University of Queensland, Brisbane, Australia, [4]Department of Respiratory and Sleep Medicine Lady Cilento Children's Hospital, Brisbane, Australia, [5]Department of Pharmacology & Clinical Pharmacology, University of Auckland, New Zealand

Aims: To describe the hazard of having *Aspergillus fumigatus* positive cultures in young children (≤ 5 years of age) with cystic fibrosis (CF) and to investigate the predictive factors influencing the hazard, specifically the influence of prior *Pseudomonas aeruginosa* positive culture.

Methods: Data on repeated *Aspergillus fumigatus* and *Pseudomonas aeruginosa* cultures were obtained from 80 children in the Australasian Cystic Fibrosis Bronchoalveolar lavage (BAL) study (1). A repeated time to event (RTTE) model was developed to describe the hazard of *Pseudomonas aeruginosa and Aspergillus fumigatus* positive culture events by fitting a parametric hazard model using NONMEM version 7.2. The predicted probability of having a *Pseudomonas aeruginosa* positive culture prior to the time of having a *Aspergillus fumigatus* positive culture was tested as an influence on the hazard of having an *Aspergillus fumigatus* positive culture. Other time varying (e.g. number of antibiotic therapy courses received prior the event) and time constant covariates (e.g. sex and meconium ileus) were also tested.

Results: The median age of having the first positive culture was 2.38 years for *Pseudomonas aeruginosa and* 3.69 years for *Aspergillus fumigatus*. The baseline hazard of having recurrent *Pseudomonas aeruginosa* and *Aspergillus fumigatus* positive cultures in the first five years of life of children with CF increased with time and was described by a Gompertz model. The hazard of *Pseudomonas* aeruginosa events doubled after the first event. The hazard of recurrent *Aspergillus fumigatus* events was found to be increased by the use of combination treatment with intravenous and inhalation tobramycin to eradicate *Pseudomonas aeruginosa* infection (Table 1). The probability of having *Pseudomonas aeruginosa* events had no detectable influence on the hazard of having *Aspergillus fumigatus* events.

Table 1: Hazard estimates and their uncertainty from a combined *Pseudomonas aeruginosa* and *Aspergillus fumigatus* positive culture repeated time to event model

		***Pseudomonas aeruginosa* positive culture**			***Aspergillus fumigatus* positive culture**		
		Final model estimate	**Bootstrap**		**Final model estimate**	**Bootstrap**	
			Median	**95% CI**		**Median**	**95% CI**
Parameter	**Units**						
Hazard of first event	$year^{-1}$	0.13	0.13	0.08-0.19	0.03	0.02	0.01-0.05
Hazard of subsequent event	$year^{-1}$	0.25	0.25	0.12-0.39	-	-	-
β_{Time}	$year^{-1}$	0.13	0.13	0.01-0.32	0.35	0.35	0.16-0.53
(half-life)*	year	(0.19)	(0.19)	(0.01-0.46)	(0.50)	(0.50)	(0.23-0.77)
$\beta_{eradication\ therapy}$		-	-	-	1.29	1.32	0.66-2.16
(hazard ratio)#					(3.63)	(3.74)	(1.93-8.69)

** Gompertz parameter converted to half-life by dividing the estimate into ln (2)*

 # Hazard ratio calculated from exp ($\beta_{eradication\ therapy}$)

Conclusion: Eradication therapy for *Pseudomonas aeruginosa* infection was a more important influence on the hazard of having a *Aspergillus fumigatus* positive culture than the probability of having a *Pseudomonas aeruginosa* positive culture itself. However, because eradication therapy is important in children with CF, stopping the treatment is not clinically feasible in order to to reduce the risk of *Aspergillus fumigatus* positive culture. Further studies to determine the effect of antifungal treatment on the hazard of having *Aspergillus fumigatus* positive culture and the impact of *Aspergillus fumigatus* positive culture on disease progression are warranted.

References:

1. Wainwright CE, Vidmar S, Armstrong DS, Byrnes CA, Carlin JB, Cheney J, et al. Effect of bronchoalveolar lavage-directed therapy on Pseudomonas aeruginosa infection and structural lung injury in children with cystic fibrosis: a randomized trial. JAMA : the journal of the American Medical Association. 2011;306(2):163-71.

207

A pilot study to investigate the relationship between doxorubicin and doxorubicinol pharmacokinetics and cardiotoxicity in children and adolescents with cancer

Stefanie Hennig[1], Kuhan Kunarajah[2], Ross Norris[1,3,4], Michael Lobb[3], Bruce Charles[1,3], Ross Pinkerton[5] and Andrew S. Moore[2,5,6]

[1]*School of Pharmacy, The University of Queensland, Pharmacy Australia Centre of Excellence (PACE), Brisbane, Australia,* [2]*Diamantina Institute and Queensland Children's Medical Research Institute, The University of Queensland, Brisbane, Australia,* [3]*Australian Centre for Paediatric Pharmacokinetics, Mater Pharmacy Services, Brisbane, Australia,* [4]*School of Pharmacy, Griffith University, Gold Coast, Australia,* [5]*Queensland Children's Cancer Centre, Children's Health Queensland Hospital and Health Service, Brisbane, Australia,* [6]*UQ Child Health Research Centre, The University of Queensland, Brisbane, Australia*

Aims: The primary aim of this pilot study was to assess the relationship between doxorubicin (dox) and doxorubicinol (doxinol) pharmacokinetics (PK) and markers of cardiotoxicity (cardiac troponin I (cTnI)), determine PK variability and identify covariates explaining the variability in the PK in children and adolescents with cancer.

Methods: A prospective pilot study measured plasma dox and doxinol and cardiac troponin I (cTnI) in children undergoing chemotherapy treatment at the Royal Children's Hospital, now Lady Cilento Children's Hospital, Brisbane, Australia. A population parent-metabolite pharmacokinetic (PK) model for dox and doxinol as well as a turnover-model for cTnI were developed using a non-linear mixed effects modelling approach (NONMEM v7.3). A population PK model of dox and doxinol was developed first, guided by previous models in the literature (1, 2), whose exposure was then stimulating the release of cTnI into the blood. Between subject variability (BSV) and between occasion variability (BOV) were estimated. A covariate analysis to identify influential factors explaining variability was performed.

Results: 17 children (6 female) aged 3.4 - 14.7 years (median 7.0) being treated for a variety of cancers had blood sampled after 1 or 2 two doses of dox (total of 24 doses of dox). Eleven patients had received doses of anthracyclines prior to the fist observed dose in this study, six patients didn't (median cumulative prior dose 90 mg/m^2, range 0-225 mg/m^2). The median dox dose administered was 30 mg/m^2 (range 25-75 mg/m^2) given over 1 h (range 0.25 – 72.5 h). First samples were taken from 0.5 to 336 h after the start of the infusion. Measured dox concentrations (n=100) ranged from 0.01 – 39.4 mcg/L, doxinol concentrations (n=120) ranged from 0.01 – 57.7 mcg/L, and cTnI (n=104) ranged from 0.05 – 0.1 ng/mL. The best fit of the model to the data shown in Figure 1. Dox clearance from the central compartment was estimated as 58.9 L/h/1.8 m^2 for an average 8.4-yearold (BSV= 19.8%, BOV=9%), central volume of distribution was 33.4 L/1.8 m^2. Doxinol clearance was 18.1 L/h/1.8 m^2 (BSV= 28.8%), and volume of distribution was 454 L/1.8 m^2. Body surface area (BSV) was added as a covariate on all clearance and distribution parameters for dox and doxinol, as well as age on dox clearance. Dox and doxinol exposure stimulated the release of cTnI into the blood, which was modelled via an E_{max} function(3). E_{max} = 0.557, K_{deg} = 0.18 h^{-1} ($t_{1/2}$=3.8), EC_{50}=9.1 microg/L, Baseline = 15 pg/mL (fixed, BSV= 7.5%, BOV= 45%). The baseline increased by 0.1% with every 1 mg/m^2 increase in prior cumulative anthracyclines doses.

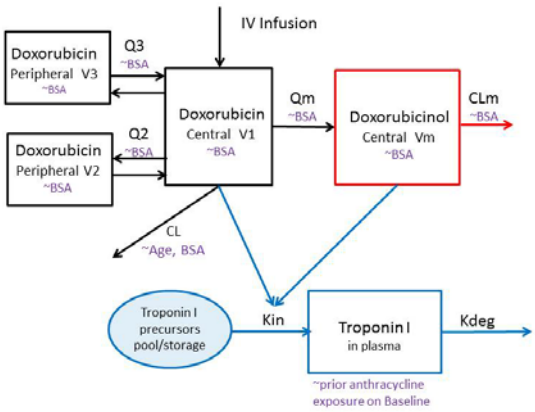

Figure 1: Final model (dox =black, doxinol = red, cTnI = blue, significant covariates = purple)

Conclusion: The PK of dox and doxinol was described satisfactorily, and parameter estimates were comparable to those previously reported in similar patients (1, 2). This pilot study further found that prior anthracycline exposure increased the risk of anthracycline exposure-induced cardiotoxicity; however this effect should be evaluated further. The study contributes to an improved understanding the dose-concentration-toxicity relationship in children with cancer.

References:

1. Kontny NE, Wurthwein G, Joachim B, Boddy AV, Krischke M, Fuhr U, et al. Population pharmacokinetics of doxorubicin: establishment of a NONMEM model for adults and children older than 3 years. Cancer Chemother Pharmacol. 2013;71(3):749-63.
2. Voller S, Boos J, Krischke M, Wurthwein G, Kontny NE, Boddy AV, et al. Age-Dependent Pharmacokinetics of Doxorubicin in Children with Cancer. Clin Pharmacokinet. 2015;54(11):1139-49.
3. Mikaelian I, Dunn ME, Mould DR, Hirkaler G, Geng W, Coluccio D, et al. Differential analysis of transient increases of serum cTnI in response to handling in rats. Pharmacol Res Perspect. 2013;1(2):e00011.

208

Development of a biomarker-based prediction model of disease progression during chemotherapy in young adolescents

Ms Young A Heo[1,2], Dr Kyungsoo Park[1]

[1]Department of Pharmacology, Yonsei University College of Medicine, Seoul, South Korea, [2]Brain Korea 21 Plus Project for Medical Science, Yonsei University, South Korea

Aims: This study aims to develop a quantitative semi-mechanistic model to describe the disease progression of leukemia during chemotherapy using circulating biomarkers in Korean adolescent population.

Methods: A routine clinical data set for 89 patients who were diagnosed as acute lymphoblastic leukemia (ALL) or acute myeloid leukemia (AML) for the first time between the age of 1 – 20 was collected from Severance hospital electric medical records (EMR) system. Lymphocyte (LYM) and platelet counts (PLT) were dependent variables, and age, WBC count, bone marrow transplantation and other laboratory results such as creatinine, ASL and ALT levels were covariates to be tested. A mechanistic model was used to describe LYM change with time during chemotherapy. A K-PD model was used to describe drug kinetics as blood concentration data were not available. LYM production was described by a single compartment representing proliferative cells, 3 transit compartments representing LYM maturation, and a single compartment representing blood LYM, where LYM production was assumed to be influenced by negative feedback from blood LYM and reduced by chemotherapy. Population modeling approach was performed using NONMEM 7.3.

Results: Due to data's hetrogeneity, patients treatment options were grouped into risk based protocol, standard risk (SR) and high risk (HR) based on the clinical practice. Drug effect was described by a linear model of effec-cite concenrtation obtianed from K-PD model, where drug doses were BSA standardized due to the use of multiple cytotoxic drugs during the treatment. Estimated parameters were 0.581, 0.458 and 1.19 for the slope of drug effect model for the subgroup of ALL_SR, ALL_HR and AML_HR, respectively, 0.425 day for MTT (mean transit time), and -0.00085 for gamma, which denotes the power of negative feedback component.

Conclusion: This work shows preliminary results for disease progression model of LYM during chemotherapy. Further analysis will include the analysis of PLT change, evaluation of potential covariates, and survival time analysis for these patients group.

209

Survival and toxicity in obese lymphoma patients receiving chemotherapy dosed on capped body surface area

Ms Geeta Sandhu[1,2], Dr Christine Carrington[1], Dr Sally Mapp[1], Dr Julia Korell[3]

[1]Division of Cancer Services, Princess Alexandra Hospital, Brisbane, Australia, [2]School of Pharmacy, The University of Queensland, Brisbane, Australia, [3]Model Answers Pty Ltd, Brisbane, Australia

Aims: To determine if obese non-Hodgkin lymphoma (NHL) patients receiving capped body surface area (BSA) dosing of Hyper-CVAD chemotherapy reduces treatment related neutropenia compared receiving full doses based on actual BSA. To determine if capped BSA dosing compromises progression free survival (PFS) compared to receiving full doses based on actual BSA.

Methods: A retrospective data collection was carried out on 108 adult patients with NHL receiving Hyper-CVAD B cycle (containing cytotoxic chemotherapy agents cytarabine and methotrexate) at a tertiary metropolitan hospital between 2002-2012. Two logistic regression models were built using NONMEM 7.3 to explore the relationship between physiological and dose exposure covariates and the likelihood of PFS and toxicity related events. In the PFS model, events were defined as death or disease relapse within two years post commencement of treatment, while events in the toxicity model were defined as prolonged neutropenia (neutrophils $<2x10^9$/L at 21 days after the start of a treatment cycle). Covariate-event relationships that resulted in a drop in objective function value of ≥3.84 ($P<0.05$) and reasonable standard errors with parameter estimates in the stepwise forward addition were included in the final model. Non-parametric bootstraps and visual predictive checks were used for model evaluation. Simulations for dosing based on actual BSA and over a range of capped BSAs (50-90% of actual BSA) using both models were used to analyse the differences in survival and toxicity for obese patients.

Results: PFS was influenced by dose exposure variables, total cumulative cytarabine dose (odds ratio (OR) 0.97 per 1000mg, 90% confidence interval (CI) 0.95-0.99) and relative dose intensity of methotrexate (OR 0.63 per 10%, 90% CI 0.41-0.81). As expected, the International Prognostic Index (IPI), a clinical tool which assigns patients to one of four prognostic categories, was negatively associated with PFS (OR 2.3, 90% CI 1.57-4.16). Simulations of actual BSA dosing versus capped BSA dosing revealed poorer PFS in obese patients in the worst prognostic category receiving capped dosing. In contrast, patients in better prognostic groups continued to have low relapse rates despite BSA dose capping.

Neutropenia was influenced by being male (OR 3.1, 90% CI 1.39-11.9) and baseline neutrophil count (OR 0.9 per $0.5x10^9$/L, 90% CI 0.69-0.98). Total cumulative cytarabine (OR 1.05 per 1000mg, 90% CI 1.04-1.09) also influenced the likelihood of prolonged neutropenia. Simulations demonstrated capped BSA dosing did reduce prolonged neutropenia in obese patients by 10-15% in patients with an average baseline neutrophil count of 6.18 x 10^9/L. However, dose capping only marginally reduced prolonged neutrophil toxicity for individuals with BSA >2.7 or baseline neutrophils <5 x 10^9/L.

Conclusion: Maintaining full Hyper-CVAD dose exposure appears to be important in reducing lymphoma relapse rates in obese patients, especially with a poorer IPI. The advantage of capped BSA dosing in reducing the risk of prolonged neutropenia cannot be discounted. However the significance of this reduction on infection rates and treatment delays requires further investigation.

210

Population pharmacokinetic analysis of Levetiracetam in adult Malaysian patients with epilepsy

Dr Li Ling Yeap[1], Professor Dr Chong Tin Tan[2], Associate Professor Dr Kheng Seang Lim[2], Dr Yoke LIn Lo[3]

[1]School of Pharmacy, Taylor's University Malaysia, Subang Jaya, Malaysia, [2]Department of Medicine, Faculty of Medicine, University of Malaya, Malaysia, Kuala Lumpur, Malaysia, [3]Department of Pharmacy, Faculty of Medicine, University of Malaya, Malaysia, Kuala Lumpur, Malaysia

Aims: To determine the pharmacokinetic parameters of levetiracetam (LEV), a third-generation antiepileptic drug, and its metabolite, etiracetam carboxylic acid (UCB L057) in adult Malaysian patients with epilepsy, and to identify any covariates predictive of the pharmacokinetic properties of LEV or UCB L057.

Methods: This study includes adult Malaysian patients with various types of epilepsy, receiving a stable oral LEV dose for at least 2 weeks. Demographic and clinical data, as well as serial blood samples, were collected prospectively on routine epilepsy clinic appointment days, at the University of Malaya Medical Centre. The plasma concentrations of LEV and UCB L057 were measured simultaneously by a locally developed and validated liquid chromatography-tandem mass spectrometry assay method(1). Pharmacokinetic analyses were performed using a nonlinear mixed-effects model approach. Population pharmacokinetic (PopPK) model of LEV was constructed using the plasma concentration-time data of LEV and UCB L057 simultaneously. Potential covariates for the popPK model were assessed using standard approach. The predictive performance of the population pharmacokinetic model was evaluated by visual predictive checks and nonparametric bootstrapping with replacement.

Results: Forty-eight adult patients who received LEV tablets as monotherapy or adjunctive therapy were enrolled in this study. Patients of Chinese descents made up 66.6% of the total number of study subjects, followed by an equal number of Malays and Indians. A one-compartment open model plus a gut compartment for oral LEV, and a metabolite compartment were fitted to 602 plasma concentrations-time points of LEV and UCB L057. The estimated total clearance of LEV is 3.24 L/h per 70 kg, while the population apparent clearance of LEV to UCB L057 (CL_{LU}) via hydrolysis reaction is 1.21 L/h per 70 kg. The value of CL_{LU} is influenced by body size and sex; with a multiplication factor of 1 for male, and 0.85 for female. The typical clearance of parent compound LEV via other routes besides hydrolysis reaction (CL_{LO}), for example via oxidative biotransformation pathway, is 2.03 L/h per 70 kg. Body weight, the presence of a metabolic enzyme inducer or inhibitor, and ethnicity, significantly influence the CL_{LO} value. The clearance of UCB L057 (CL_U) is estimated to be 11.7 L/h. The volume of distribution of LEV (V_L) is 34.2 L per 70 kg, and the absorption rate constant (k_a) of LEV is 1.46 per h.

Conclusion: The total clearance, the volume of distribution and the absorption rate constant of LEV in Malaysian patients are comparable to those of previously reported (2-5). The apparent clearance of metabolite UCB L057 that has not been previously estimated is 11.7 L/h. This study supports the hypothesis that concomitant antiepileptic agents that are cytochrome enzyme inducers could stimulate the oxidative biotransformation pathway but not the hydrolysis pathway of LEV, although the former accounts for less than 3% of the total LEV disposition in the absence of any cytochrome enzyme inducer or inhibitor (6).

References:

1. Yeap LL, Lo YL. Rapid and simultaneous quantification of levetiracetam and its carboxylic metabolite in human plasma by liquid chromatography tandem mass spectrometry. PLoS One. 2014;9(11):e111544.
2. Uges JWF, Van Huizen MD, Engelsman J, Wilms EB, Touw DJ, Peeters E, et al. Safety and pharmacokinetics of intravenous levetiracetam infusion as add-on in status epilepticus. Epilepsia. 2009;50(3):415-21.
3. Pigeolet E, Jacqmin P, Sargentini-Maier M-L, Stockis A. Population Pharmacokinetics of Levetiracetam in Japanese and Western Adults. Clinical Pharmacokinetics. 2012;46(6):503-12.
4. Patsalos PN. Clinical Pharmacokinetics of Levetiracetam. Clinical Pharmacokinetics. 2004;43(11):707-24.
5. Toublanc N, Okagaki T, Boyce M, Chan R, Mugitani A, Watanabe S, et al. Pharmacokinetics of the antiepileptic drug levetiracetam in healthy Japanese and Caucasian volunteers following intravenous administration. European Journal of Drug Metabolism and Pharmacokinetics. 2014;40(4):461-9.
6. Strolin Benedetti M, Whomsley R, Nicolas J-M, Young C, Baltes E. Pharmacokinetics and metabolism of 14C-levetiracetam, a new antiepileptic agent, in healthy volunteers. European Journal of Clinical Pharmacology. 2003;59(8):621-30.

211

A viral kinetic model for severe human cytomegalovirus infections in immunocompromised paediatric patients

Mr Ben Margetts[1,2,3], Professor Judith Breuer[2,3], Professor Nigel Klein[1,2,3], Dr Joseph Standing[1,2,3]

[1]UCL CoMPLEX, , United Kingdom , [2]UCL Institute of Child Health, , United Kingdom , [3]Great Ormond Street Hospital NHS Foundation Trust, , United Kingdom

Aims: To produce a viral kinetic (VK) model of Cytomegalovirus (CMV) that predicts changes in viral load within an individual as the infection responds to antiviral therapy and the immune response, based on data from an immunocompromised paediatric population.

Methods: Complete clinical datasets were taken from 335 bone marrow transplant (BMT) patients receiving care at Great Ormond Street Hospital (GOSH) between January 2010 and December 2014. 86 of these patients exhibited a serious active CMV infection following their BMT-associated immunosuppressive treatment regime. A total of 1,598 CMV viral load observations were included from these patients. For each of the patients studied, we had access to clinical history, treatment outcomes, and the results of all clinical tests undertaken. These tests include regular white cell counts, white cell subset counts, full blood counts, and a selection of viral load PCRs. Alongside this rich clinical data, we have access to full drug administration datasets for each patient during their stay at the hospital.

Viral load data was fitted to a viral growth model using NONMEM V7 3.0 [1], a growth inhibition term related to antiviral treatment was incorporated into the VK model alongside a growth limiting V MAX term that scales the rate of viral growth against the maximum amount of virus that is possible within an individual. Total lymphocyte count (TLC) was chosen to represent the efficacy of a patient's immune response against the virus due to the rich data available on this. From the 86 patients with active CMV infections, 13,933 TLCs were available from the course of their BMT recovery, and were utilised as a scalar on an immune kill parameter. Virions are also assumed to have a fast turnover rate, represented by a constant clearance parameter in the model. Viral load was used as the primary predictor of treatment outcome as high viral loads (>1 million copies/mL) are typically associated with higher levels of mortality.

Results: The viral kinetic model was shown to appropriately fit the data from the BMT patients, accurately estimating the viral growth and decay during key moments in the patient's disease progression cycle. Model parameter estimates generated during the estimation were appropriate, given the biological context, with viral doubling time agreeing with the faster ~1.4 day CMV doubling time previously shown in BMT patients with CMV infections [2]. Antiviral efficacy was estimated to be highly variable within the patient population, with the inclusion of immune parameters improving the fit, and accounting for large portions of the variation in viral growth. The model can provide realistic disease trajectory simulations that can be fitted to data from newly infected patients, as they present.

Conclusion: A dynamic VK model has now been developed for CMV. Future work will include the estimation of whole body CMV content, by scaling viral load up to match total predicted blood volume for each patient, and the inclusion of individual antiviral PK information. Following this, the use of rich CMV sequencing data currently being collected from BMT patients may allow us to monitor and predict the emergence of drug resistance, and model the relationship between it, estimated total viral load, and antiviral efficacy.

References:

1. Beal SL, Sheiner LB, Boeckmann AJ & Bauer RJ (Eds.) NONMEM Users Guides. 1989-2013. Icon Development Solutions, Ellicott City, Maryland, USA.
2. Mueller, Nicolas J. "Cytomegalovirus: Why Viral Dynamics Matter." *EBioMedicine* 2.7 (2015): 631.

212

Development of an interactive application to assist clinicians in the dose adjustment of voriconazole

Mr David McDougall[1,2], A/Prof Bruce Green[2]

[1]School of Pharmacy, University of Queensland, Woolloongabba, Australia, [2]Model Answers Pty Ltd, Brisbane, Australia

Aims: Voriconazole is a broad spectrum triazole antifungal used as first line therapy for invasive infections. Pharmacokinetic (PK) studies have indicated clearance (CL) is non-linear, with PK parameters such as CL and Vmax having large between-subject variability. Patient exposure is therefore highly variable, which has prompted the use of therapeutic drug monitoring (TDM) to optimise dosing [1] as there is a growing body of literature that relates exposure to both effectiveness and toxicity. Currently, no tools, guidelines, or nomograms exist to assist clinicians interpret individual voriconazole concentrations. The objective of this research was to develop an interactive application that allows clinicians to explore a range of likely exposures if doses are adjusted. The application was not designed to make specific dose recommendations.

Methods: The application (developed using the Shiny package in R) was constructed using a simulation approach. 100 stochastic simulations (each consisting of 2000 subjects from the NHANES database) were conducted using a previously published population PK model[2] under 60 different loading dose / maintenance dose scenarios. The user interface allows the clinician to input patient and sample specific data such as body weight, current dosing regimen, concentration achieved, and alternate doses to be explored. The application uses the inputted information to search the database of simulations to identify up to 30 "matched" subjects (and associated PK parameters) with similar weight, dosing history and plasma concentration. The application then predicts the likely exposure for the matched patients under alternative doses.

Results: A screenshot of the application is displayed in Figure 1. The user inputted information is on the left hand panel, and the results are in the main panel. The table on the top row displays the characteristics of the matched subjects and percentage of the simulations that fall within the therapeutic range under the alternate dose. The histograms on the top row display the distributions of the likely exposure (trough concentrations and area under the concentration time curve) under the new proposed dose. The concentration time plots in the middle row display four representative concentration time profiles from the matched subjects, while the histograms on the bottom row display the distribution of PK parameters for the matched subjects.

Conclusion: The application is a novel idea to assist clinicians to explore how alternate doses might impact exposure. Future prospective and retrospective validation of the application is planned.

Figure 1

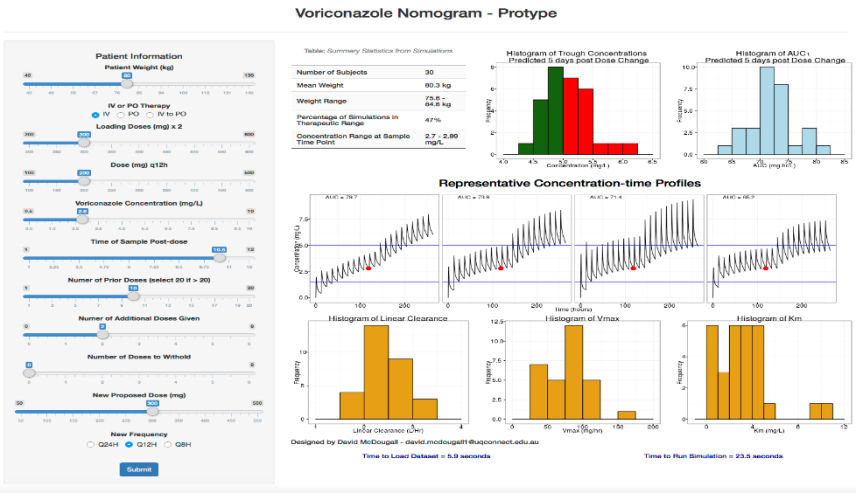

References:

1. Brüggemann RJM, Donnelly JP, Aarnoutse RE, Warris A, Blijlevens NMA, Mouton JW, et al. Therapeutic drug monitoring of voriconazole. Ther Drug Monit. 2008;30(4):403-11.46(4):225-34.
2. McDougall DA, Martin J, Playford EG, Green B. Determination of a suitable voriconazole pharmacokinetic model for personalised dosing. J Pharmacokinet Pharmacodyn. 2015

213

A PBPK model of phenytoin after intravenous administration of fosphenytoin sodium in Japanese pediatric patients

Mr Masayoshi Nakakuni[1], Dr Naohisa Yahagi[2], Miss Miki Akabane[3], Dr Hiroshi Terashima[4], Mr Yoichi Ishikawa[3]

[1]Department of Human Genetics, National Center For Child Health And Development, Tokyo, Japan, [2]Department of Data Management, National Center for Child Health and Development, Tokyo, Japan, [3]Department of Pharmacy, National Center for Child Health and Development, Tokyo, Japan, [4]Division of Neurology, National Center for Child Health and Development, Tokyo, Japan

Aim: To develop a physiology based pharmacokinetics (PBPK) model of phenytoin after intravenous administration of fosphenytoin sodium (FPHT) in Japanese pediatric patients.

Methods: The PBPK modeling was performed using Berkeley Madonna 8.3.18. We predicted ratios of tissue to plasma unbound concentration (kpu) of 9 organs and tissues based on the following equation: kpu (pediatric patients) = kpu (rat) x CF where CF is correction factor. Values of hepatic clearance (CLh) were adjusted using three different allometric scaling methods: body weight (BW), Body surface area (BSA), or 0.75 power of BW. Accuracy of the PBPK model was compared with those of one- and two-compartment pharmacokinetic models in three age groups (< 1 year old: n=26, 1-6 years old: n=20, 7-18 years old: n=15) by median absolute performance error (MAPE).

Results: We used the clinical data obtained from 61 patients treated with initial intravenous loading of FPHT. The CF in the < 1 year-old group showed the lowest values among 3 age groups. Regarding CLh, adjustment by BW was the lowest MAPE values in the < 1-year-old and the 1-6-years-old goups (13.7 % and 17.9 %, respectively). In the 7-18 years-old group, adjustment by BSA showed the lowest MAPE value (10.9%). The MAPE values of one- and two-compartment models were higher than the PBPK model (27.8% and 20.2%, respectively).

Conclusion: The PBPK model might predict serum phenytoin concentration after adiministration of FPHT more accurately than one- and two-compartment models.

Reference:

Macey, R., G. Oster, and T. Zahnley. Berkeley Madonna user's guide version 8.3. 18. University of California; 2010.

214

Clinical pharmacometrics for personalized dosing of teicoplanin

Mr Kazutaka Oda[1,2], Dr Hirofumi Jono[1,2], Dr Hideyuki Saito[1,2]

[1]Department of Pharmacy, Kumamoto University Hospital, Kumamoto, Japan, [2]Department of Clinical Pharmaceutical Sciences, Graduate School of Kumamoto University, Kumamoto, Japan

Aims: Pharmacometrics is a predicter for ideal dosing regimen by using population pharmacokinetic (PPK) model, pharmacodynamic information, and modeling and simulation (M&S)[1]. Teicoplanin (TEIC), a glycopeptide antimicrobial, plays essential role for treating various infectious diseases by methicillin resistant *staphylococcus aureus* (MRSA). However, personalized dosing regimen for teicoplanin (TEIC) has yet to be developed, and clinical PPK model for personalized dosing is not available. Moreover, MRSA has recently indicated reduced sensitivity against TEIC such as 2 mg/L of minimum inhibitory concentration (MIC). In this study, to take advantage of pharmacometrics in clinical settings (clinical pharmacometrics: CPMx) for personalized dosing, we evaluated usefulness of CPMx in TEIC treatment by determining personalized dosing regimen.

Methods: We conducted the retrospective CPMx-guided study with approval from institutional review board of Kumamoto University Hospital (the approval number was 955). We included the adult patients (over 18 years old) dosed TEIC. CPMx-guided study was performed as follows. 1, the clinical PPK was analyzed using NONMEM program. 2, Bacterial growth curve based on M&S was subsequently described for several dosing regimen with mutable MIC. We evaluated this clinical PPK model by comparing the predictive performance of blood TEIC level with current PPK model.

Results: We analyzed the clinical PPK in 79 eligible patients. We identified creatinine clearance (Ccr), serum albumin (ALB), and height (HT) to be the significant covariates for TEIC clearance (CL), by determining the final PPK model (table 1). The volume of distribution (Vss) was 1.22 L/kg. This clinical PPK model developed indicated improved predictive performance rather than current PPK model. Figure 1 shows bacterial growth curves (gray bold line) and blood TEIC concentration curves (black solid line). The required days for reduction of bacterial count to be 10^{-6} were between 4 days and 7 days in the case of MIC = 1.0 mg/L. Those were drastically elongated to be more than 9 days (underlined words in Figure 1A, B, and C) for the regimen with 400 mg of maintenance dose (resulted in 18.1 µg/mL for trough level) in the case of MIC = 2.0 mg/L (Figure 1A, B, and C). The regimen with 600 mg of maintenance dose (resulted in 28.0 µg/mL for trough level) showed improved bactericidal activity (Figure 1D and E). Further increased maintenance dose (800mg: Figure 1F) showed the unchanged required days.

Table 4

Final PPK model

$CL\ (L/hr) = \theta 1 * (Ccr/7.2)^{\theta 2} * (ALB/4)^{\theta 3} * (HT/170)^{\theta 4} * EXP(\eta 1)$

$Vss\ (L/kg) = \theta 5 * EXP(\eta 2)$

K12 (/hr) = 0.38, Fixed

K21 (/hr) = 0.0485, Fixed

Fixed effect parameter	value	shrinkage, %	Bootstrap estimation	
			Median	95 % CI
$\theta 1$	0.727		0.731	0.638 - 0.875
$\theta 2$	0.374		0.348	0.068 - 0.595
$\theta 3$	-0.609		-0.629	-0.888 - -0.169
$\theta 4$	3		3.08	0.720 - 5.736
$\theta 5$	1.22		1.22	0.934 - 1.540
ω_{CL}, %	18	27.6	16.9	5.2 - 28.7
ω_{Vss}, %	41.1	21.3	38.9	22.2 - 57.1
Residual variability, %	16.6	18.9	16.3	13.0 - 19.7

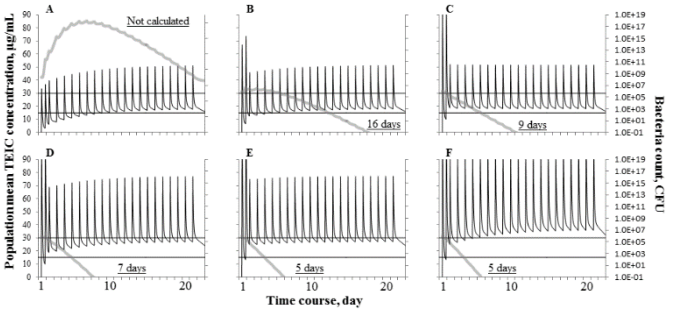

Figure 1

Conclusion: CPMx with clinical PPK and M&S in TEIC treatment may be useful for personal dosing. In this CPMx-guided study, we newly identified ALB and HT for the significant covariates for TEIC clearance through clinical PPK analysis. We speculate decreased ALB elevates TEIC clearance because of the elevated unbound TEIC fraction in plasma. The blood trough level (28 µg/mL) for TEIC was recommended, especially for MRSA with 2.0 mg/L of MIC.

References:

1. Barrett et al. Pharmacometrics: a multidisciplinary field to facilitate critical thinking in drug development and translational research settings. J. Clin. Pharmacol. 2008; 48: 632–649.
2. Neely et al. Practical, individualized dosing: 21st century therapeutics and the clinical pharmacometrician. J. Clin. Pharmacol. 2010; 50: 842–847.

215

Bayesian forecasting versus clinical practice for intravenous busulfan dose adjustment in paediatric stem cell transplantations

Mr Lachlan Paterson[1], Ms Rachael Lawson[2], Dr Stefanie Hennig[1]

[1]The University Of Queensland, Woolloongabba, Australia, [2]Lady Cilento Children's Hospital, South Brisbane, Australia

Aims: Haematopoietic stem cell transplantation (HSCT) is a vital therapy that is used to cure high-risk or relapsed malignant and nonmalignant conditions. Busulfan is an important chemotherapeutic agent used in HSCT, particularly in children with cancer. It has been demonstrated that optimal exposure over four days reduces the incidence of toxicities and decreases the risk of transplant failure. Current local clinical practice uses intensive sampling on each of the four days of dosing to calculate cumulative exposue over the dosing period. This study aimed to evaluate the predictive performance of two Bayesian forecasting programs under various sampling scenarios to estimate an individual's busulfan exposure to individulise doses and attain optimal busulfan exposure.

Methods: Pediatric oncology patients underwent repeated blood sampling seven times daily (samples taken at pre-dose trough, 3h after beginning infusion, 3:15h, 4h, 5h, 6h and 8h) to determine the patient's overall drug exposure throughout the conditoning regimen at the Lady Cilento Children's Hospital, Brisbane, Australia from 2012 to 2016. Patient characteristics, busulfan concentrations and sampling times were collected to estimate the daily area under the concentration-time curve (AUC) utilising two Bayesian forecasting programs (NextDose®, InsightRX®) and comparing these to the true measured AUC. Various sampling scenarios were tested using the programs including a full profile over all four days compared to reduced sampling strategies.

Results: Thirty-two children, median age 5.5 years, contributed 720 busulfan concentrations resulting in 93 true AUC calculations via the trapezoidal rule. The mean true daily AUC was 20.1 (8.83-41.81) mcg·hr·mL^{-1}. One child had a true AUC observation on day 1 only, seven children on the first 2 days, five children on days 1-3 and twelve children on all 4 days of the regimen. Of those remaining, one had a true AUC on day 3, four children had 2 days of true AUCs and two children had 3 days of true AUCs. The estimated AUC povided by the two Bayesian forecasting programs resulted overall in low impression and high accuracy compared to the true AUC under scenario 1-3 (see Table 1) over all 4 days of busulfan dosing.

Table 1: Predictive performance of two Bayesian forecasting programs estimating daily busulfan AUCs

Sampling scenario	Software	Mean absolute error [IQR] (mcg·hr·mL^{-1})	Relative mean prediction error [IQR] (%)	Root-mean-square error (%)
1. Full profile (4 days, 7 samples/day)	InsightRX	1.7, [-0.1, 4.3]	11.3 [- 0.3, 24.4]	24.5
	NextDose	-2.1, [-3.0, -0.2]	-9.3, [-15.7, -1.4]	17.1
2. Days 1-2 only (7 samples/day)	InsightRX	-0.1, [-1.1, 1.3]	2.8, [- 7.1, 8.7]	24.1
	NextDose	-4.0, [-4.6, -0.1]	-17.1, [-24. 7, -0.6]	37.6
3. Trough, 3h, 5h, 8h (4 days, 3 samples/day + C_0)	InsightRx	2.6, [0.2, 4.8]	16.1, [1.1, 26.2]	32.2
	NextDose	-2.0, [-2.8, -0.1]	-8.4, [-15.1, -0.5]	16.9
4. Trough, 3h, 5h (4 days, 2 samples/day + C_0)	InsightRX	2.6, [-0.3, 5.0]	16.2, [- 1.6, 25.0]	34.0
	NextDose	-4.6, [-6.6, -1.1]	-21.2, [-34.7, -5.5]	34.0

Conclusion: While Bayesian forecasting programs have been utilised in other countries, the Queensland paediatric HSCT unit has not yet adopted this practice. Balancing reduction in sampling and predictive ability of the Bayesian forecasting tools during further investigations may offer great potential for use of these programs in local clinical practice.

216

Population pharmacokinetic modeling of Atazanavir/r in Thai HIV-infected patients: an aid for optimal dose finding

Dr Baralee Punyawudho[1], Narukjaporn Thammajaruk[2], Dr Anchalee Avihingsanon[2,3]

[1]Department of Pharmaceutical Care, Faculty of Pharmacy, Chiang Mai University, Chiang Mai, Thailand, [2]HIV-NAT, Thai Red Cross AIDS Research Centre, Bangkok, Thailand, [3]Department of Medicine, Faculty of Medicine, Chulalongkorn University, Bangkok, Thailand

Aims: Ritonavir boosted atazanavir (ATV/r) is one of the most commonly used protease inhibitors (PI) in Thai HIV-infected patients. Previous studies found Thai patients may require a lower dose of ATV to achieve adequate ATV exposure. Therefore, this study aimed to develop the population pharmacokinetic model of ATV/r using nonlinear mixed-effects modeling approach. The developed model was further used to determine the optimal dose of ATV/r for Thai HIV-infected patients to achieve target concentration.

Methods: A cross-sectional study was performed at HIV Natherlands Australia Research Collaboration (HIV-NAT), Bangkok, Thailand. Patients aged 18 years and older, received ATV/r as part of the antiviral therapy for at least 2 weeks were included into the study. One random blood sample was collected at each clinic visit for ATV and RTV concentrations determination. Additionally, intensive data from 27 patients enrolled in previous studies were included (1, 2). The population pharmacokinetics of ATV was developed by NONMEM®. Monte Carlo Simulations were performed to assess ATV trough concentrations (C_{trough}) for patients receiving standard (300/100 mg/day of ATV/r) and lower dosage regimens (200/100 and 250/100 mg/day of ATV/r). The proportions of patients achieving target C_{trough} of ATV (0.15-0.85 mg/L) were calculated.

Results: A total of 127 patients with 627 ATV and RTV plasma concentrations were included in the analysis. The pharmacokinetics of ATV can be best described by a one-compartment model with first-order absorption with lag-time and first-order elimination. Gender was significant covariate for clearance (CL/F) and weight was significant covariate for volume of distribution (V/F) of ATV. The estimated CL/F of ATV was 4.93 L/hr in female with a 28.7% increase in male patients. The results from simulations showed a higher proportion of patients achieving target C_{trough} of ATV in a group of patients receiving ATV/r 200/100 mg/day compared with a group of 250/100 and 300/100 mg/day (65.5 vs 58.8 vs 51.7%). However, it was estimated that 17% of male patients would have subtherapeutic concentrations when 200/100 of ATV/r was given.

Conclusion: The population pharmacokinetics of ATV/r was successfully developed. Gender was significant covariate for CL/F whereas weight was significant covariate for V/F. The simulation results confirmed that the use of lower ATV/r dose can achieve target ATV concentration in this population.

References:

1. Avihingsanon A, van der Lugt J, Kerr SJ, Gorowara M, Chanmano S, Ohata P, et al. A low dose of ritonavir-boosted atazanavir provides adequate pharmacokinetic parameters in HIV-1-infected Thai adults. Clinical pharmacology and therapeutics. 2009;85(4):402-8.
2. Kerr SJ, Punyawudho B, Thammajaruk N, Colbers A, Chaiyahong P, Phonphithak S, et al. Factors associated with daily tenofovir exposure in Thai subjects taking combination antiretroviral therapy. AIDS Res Hum Retroviruses. 2015;31(4):368-74.

217

Modelling and simulation of fluconazole in critically ill adult patients

Dr Indy Sandaradura[1,2,3], A/Prof Ross Norris[1,2], Prof Debbie Marriott[1,2], Prof Ric Day[1,2], Dr Stephanie Reuter[4]

[1]St Vincent's Hospital, Sydney, Darlinghurst, Australia, [2]University of New South Wales, Sydney, Australia , [3]University of Notre Dame Australia, Western Australia, [4]University of South Australia, Adelaide, Australia,

Aims: The bis-triazole antifungal agent fluconazole was widely used as first-line treatment in patients with suspected and proven fungal infections (1) until a recent study found a higher mortality, even in patients with susceptible infections (2). It is postulated that patients with critical illness may be under-exposed with current fluconazole dosing, leading to poorer outcomes. A population pharmacokinetic approach was used to provide estimates of fluconazole pharmacokinetic parameters after intravenous administration in critically ill patients and to simulate the drug exposure from standard (400 mg/day) and alternative dosing.

Methods: Clinical and biochemical data including serum fluconazole concentrations were obtained from 30 adult patients treated in the intensive care unit. Population pharmacokinetic modelling was conducted using NONMEM VII.

Results: A one compartment model with first order elimination was found to adequately describe fluconazole concentration-time data. Introduction of covariates into the structural model identified a significant effect of weight on V and renal function and the use of continuous renal replacement therapy (CRRT) on CL. The population parameters were CL_{RENAL}= 0.70L/h; CL_{CRRT} = 1.90L/h and V = 45L. The final model was utilised to simulate the probability of target attainment based on dosing strategy, in light of the current European Committee on Antimicrobial Susceptibility Testing (EUCAST) breakpoint of 4 mg/L. Doses of up to and including 800 mg/day failed to achieve a free AUC:MIC >100 in over 50% of patients on CRRT. Doses of 400 mg/day failed to attain this target in over 25% of those who had higher renal function (>=120 ml/min)The current recommended loading dose (800mg) failed to achieve steady state in most patients at 72h.

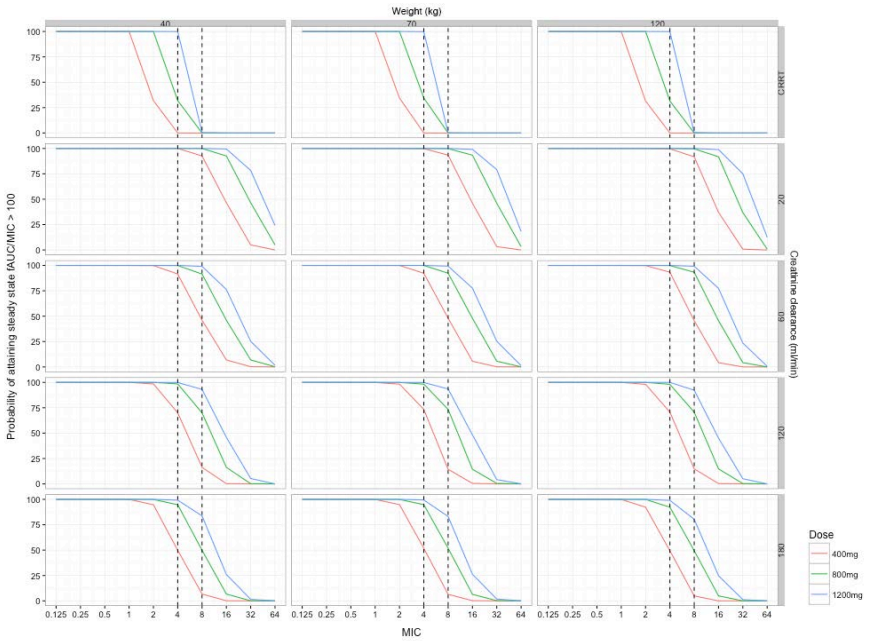

Figure 1. Probability of steady state target attainment

Conclusion: This population pharmacokinetic analysis strongly indicates that fluconazole dosage should be optimized in terms of CLcr and dialysis use in critically ill patients. Current loading doses are inadequate and maintenance dosing fails to attain targets in patients with higher renal clearance or undergoing CRRT.

References:

1. Pappas PG, Kauffman CA, Andes D, Benjamin DK, Jr., Calandra TF, Edwards JE, Jr., et al. Clinical Practice Guidelines for the Management of Candidiasis: 2009 Update by the Infectious Diseases Society of America. Clin Infect Dis. 2009;48(5):503-35.
2. Andes DR, Safdar N, Baddley JW, Playford G, Reboli AC, Rex JH, et al. Impact of treatment strategy on outcomes in patients with candidemia and other forms of invasive candidiasis: a patient-level quantitative review of randomized trials. Clin Infect Dis. 2012;54(8):1110-22.

218

Mechanistic model for calcium treatment effect in calcium-parathyroid hormone homeostasis after thyroidectomy in Koreans

MD Mijeong Son[1,2], MD Yukyung Kim[1,2], MD Dongwoo Chae[1,2], BS Jinju Guk[1,2], BS YuongA Heo[1,2], MD Yun Seob Jung[1,2], PhD, MD Kyungsoo Park[1]

[1]Department Of Pharmacology, Yonsei University College Of Medicine, Seoul, South Korea, [2]Brain Korea 21 Plus Project for Medical Science, Yonsei University, Seoul, South Korea

Aims: This study aims to develop a mechanism-based model of calcium treatment effect in calcium-parathyroid hormone (PTH) homeostasis after thyroidectomy in Koreans and evaluate the potential covariates influencing on the kinetics of calcium and PTH concentration.

Methods: A retrospective data set for 1142 patients who underwent thyroidectomy in 2013 at Severance hospital was collected from electric medical records (EMR) system. Post-thyroidectomy calcium concentrations and PTH levels obtained under the treatment of calcium and vitamin D supplements were analyzed as dependent variables, and demographics and operation conditions were tested as potential covariates. Calcium concentrations were described using a turn-over model and PTH concentration was described using a precursor-dependent indirect response model, where PTH is produced from PTH precursor (PP) through first order kinetics and PTH stimulation is modulated by a negative feedback system, with PTH stimulation increasing when occupancy decreases and vice versa. Population modeling approach was performed using NONMEM 7.3.

Results: The effect of thyroidectomy on calcium and PTH concentrations were best described by immediate drop in calcium and PTH levels at time of surgery and then exponentially increase up to maximum recovery level, with difference between baseline and maximum recovery levels corresponding to unrecovered calcium and PTH concentrations. Treatment effect by exogenous calcium was then modeled to stimulate calcium production rate in turnover model.

The parameter estimates were 9.19 mg/dl and 46.4 pg/ml for baseline calcium and PTH concentrations, 0.736/day and 0.626/day for recovery rate constants for calcium and PTH concentrations after thyroidectomy, 0.114 /day and 0.905 /day for fractional turn-over rates of calcium and PTH, 2180 L for volume of distribution of calcium compartment, and 0.26 mg/dL and 10.4 pg/ml for unrecovered calcium and PTH levels.

Conclusion: The developed model was adequately fitted to post-thyroidectomy calcium and PTH concentrations. Further studies will include evaluation of potential covariates on the kinetics of calcium and PTH.

References:

Abraham AK, Mager DE, Gao X, Li M, Healy DR, Maurer TS. J Pharmacol Exp Ther. 2009 Jul;330(1):169-78.

219

Operational characteristics of saemix, an R package implementing the SAEM algorithm

Ms Emmanuelle Comets[1,2], Ms Audrey Lavenu[1], Mr Marc Lavielle[3]

[1]Inserm CIC 1414, University Rennes 1, Rennes, France, [2]Inserm UMR 1137 IAME, University Paris Diderot, Paris, France, [3]INRIA Saclay, Popix, University Paris Sud, Orsay, France

Aims: The saemix package for R (1) provides an implementation of the SAEM (Stochastic Approximation Expectation Maximization) algorithm. In the present paper, we assess the operational characteristics of saemix in terms of performance and scalability, using simulated data.

Methods: The SAEM algorithm is used to obtain maximum likelihood estimates of the parameters of nonlinear mixed effects models without any linearisation of the model (2,3). The SAEM algorithm uses an EM algorithm, where the unknown individual parameters are treated as missing data, and replaces the usual E-step with a stochastic approximation step (3,4). The saemix package makes use of the S4 classes in R to provide a user-friendly functions for estimation, diagnostics and summary. We applied saemix on simulated data from Plan et al., who created it to compare the performance of various software (5). A sigmoid Emax model was fitted to dose-response data simulated with relatively large curvature (gamma=3), under a rich and a sparse design (respectively 4 and 2 points per subject). We compared the performance of saemix with results from nlme (6) and nlmer from lme4 (7). In parallel, we investigated the scalability of the algorithm by showing runtimes across models with varying numbers of parameters and across different designs.

Results: In the rich design, saemix was able to provide unbiased estimates of the population parameters, while both nlme and nlmer had trouble estimating ED50 and its variability. In the sparse design, the three algorithms exhibited bias but saemix showed the best performance. nlmer and to a lesser extent nlme exhibited convergence issues, especially for the sparse design. As expected due to the stochastic nature of the algorithm, runtimes for saemix increased as a function of the number of random effects in the model and of the number of subjects in the dataset. We also implemented an ODE model using the standard R solver (deSolve) but this proved extremely slow.

Conclusions: The saemix package provides the SAEM algorithm for R users, as an alternative to linearisation-based algorithms, implemented in nlme (6), or quadrature methods, implemented in glmmML or lme4 (7). Current development focuses on extending the capabilities of the package via new models, such as ODE systems or hidden Markov models (8), extended diagnostics, and automating covariate handling.

References:

1. R Development Core Team. R: A Language and Environment for Statistical Computing. R Foundation for Statistical Computing, Vienna, Austria, 2006.
1. Delyon B, Lavielle M, Moulines E. Convergence of a stochastic approximation version of the EM algorithm. Annals Stat 1999; 27:94-128.
2. Kühn E, Lavielle M. Maximum likelihood estimation in nonlinear mixed effects models. Comput Stat Data Anal 2005; 49:1020-38.
3. Lavielle M. Mixed Effects Models for the Population Approach - Models, Tasks, Methods and Tools. Chapman & Hall/CRC Biostatistics Series, CRC Press, Boca Raton, Florida, USA 2014.
4. Plan E, Maloney A, Mentré F, Karlsson M, Bertrand J. Performance Comparison of Various Maximum Likelihood Nonlinear Mixed-Effects Estimation Methods for Dose-Response Models. AAPS J 2012; 14:420-32.
5. Pinheiro J, Bates D, DebRoy S, Sarkar D, R Core team. nlme: Linear and Nonlinear Mixed Effects Models. R package version 3.1-96, 2009.
6. Bates D, Maechler M. lme4: Linear mixed-effects models using S4 classes. R package version 0.999375-34, 2010.
7. Delattre M (2010). Inference in mixed Hidden Markov models and applications to medical studies. J Soc Franc Stat 2010; 151:90-105.

220

nlmixr: an open-source package for pharmacometric modelling in R

Dr Rik Schoemaker[1], Dr Yuan Xiong[4], Dr Justin Wilkins[1], Dr Christian Laveille[3], Dr Wenping Wang[2]

[1]Occams, Amstelveen, The Netherlands, [2]Novartis Pharmaceuticals, East Hanover, USA, [3]SGS Exprimo NV, Mechelen, Belgium, [4]Certara Strategic Consulting, Princeton, United States

Aims: ***nlmixr*** is an open-source R package under development that builds on both RxODE[1], an R package for simulation of nonlinear mixed effect models using ordinary differential equations (ODEs), and the ***nlme***[2] package in R, for parameter estimation in nonlinear mixed effect models. ***nlmixr*** greatly expands the utility of ***nlme*** by providing an efficient and versatile way to specify pharmacometric models and dosing scenarios, with rapid execution due to compilation in C++. NONMEM®[3] with first-order conditional estimation with interaction was used as a comparator to test ***nlmixr***.

Methods: Richly sampled profiles were simulated for 4 different dose levels (10, 30, 60 and 120 mg) of 30 subjects each as single dose (over 72h), multiple dose (4 daily doses), single and multiple dose combined, and steady state dosing, for a range of test models: 1- and 2-compartment disposition, with and without 1st order absorption, with either linear or Michaelis-Menten (MM) clearance (MM without steady state dosing). This provided a total of 42 test cases. All inter-individual variabilities (IIVs) were set at 30%, residual error at 20% and overlapping PK parameters were the same for all models. A similar set of models was previously used to compare NONMEM and Monolix[4]. Estimates of population parameters, standard errors for fixed-effect parameters, and run times were compared both for closed form solutions and using ODEs.

Results: Parameter estimates were comparable across estimation methods; Figure 1 provides results for central volume of distribution (Vc) as illustration because it is the single parameter present in all models. In comparison to NONMEM, ***nlmixr*** was always faster for ODEs (MM-models) and comparable for closed form models. Standard error estimates were obtained for all ***nlmixr*** models, but not all NONMEM models. IIV estimates were regularly estimated close to 0% for ill-defined model parameters (e.g. for inter-compartmental clearance and peripheral volume), in ***nlmixr***, whereas NONMEM provided estimates closer to the original simulation values.

Figure 1. Fixed effects (top left) and IIV (bottom left) estimates for Vc, residual error (top right) and log run times (bottom right) comparing NONMEM (grey lines) and ***nlmixr*** (black lines). Horizontal black line: value used for simulation.

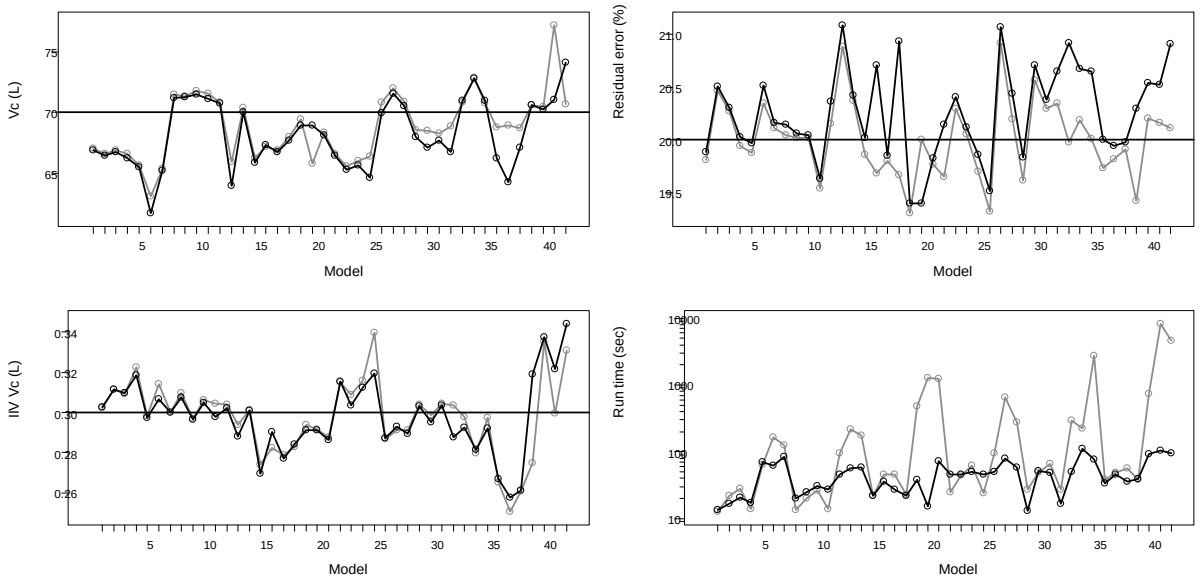

Conclusion: These findings suggest that ***nlmixr*** provides a viable open-source parameter estimation procedure for nonlinear mixed effects pharmacometric models within the R environment.

References:

1. Wang W *et al*. CPT:PSP (2016) 5, 3–10.
3. Pinheiro J *et al.* (2016). nlme: Linear and Nonlinear Mixed Effects Models. R package version 3.1-126,
4. Beal SL *et al*. 1989-2011. NONMEM Users Guides. Icon Development Solutions, Ellicott City, Maryland, USA.
5. Laveille C *et al* PAGE 17 (2008) Abstr 1356 [www.page-meeting.org/?abstract=1356]

221

Integrated population PK-PD model of pimobendan effects on the cardiovascular system in the dog

Dr David Foster[1], Dr Mariko Yata[2], Dr Niek Beijerink[2], Professor Andrew McLachlan[3], Dr Stephen Page[4]

[1]Australian Centre for Pharmacometrics, School of Pharmacy and Medical Sciences, University of South Australia, Adelaide, Australia, [2]Faculty of Veterinary Sciences, University of Sydney, Sydney, Australia, [3]Faculty of Pharmacy, University of Sydney, Sydney, Australia, [4]Luoda Pharma Pty Ltd, Caringbah, Australia

Aims: Using pooled data from 4 studies, the aims of the present study were to (i) develop a population PK-PD model for the effects of pimobendan on the cardiovascular (CV) system in dogs and (ii) identify major covariates which impact on the PK-PD with a focus on the impact of formulation type and food on oral administration.

Methods: In all studies a nominal dose of 0.25mg/kg was employed, and each animal only received a single dose of pimobendan. Pharmacokinetic data were available from 4 studies involving 29 healthy adult Beagles (16 female), providing a total of 278 plasma rac-pimobendan concentrations over up to 24h post-dose. For 10 dogs pimobendan was administered as the commercial Vetmedin® tablet, and the remainder as a novel oral solution with 3 dogs administered in the fed state. In one study (8 dogs administred pimobendan and 4 dogs administered placebo) mean arterial pressure (MAP) was also measured and echocardiography was employed to derive left ventricular fractional shortening (LVFS), stroke volume (SV), heart rate (HR) and cardiac output (CO) in triplicate at 11 time-points over 24h as well as ~1 day and 0.5h pre-dose in. All models were developed in a step-wise manner in NONMEM® 7.3 [1] using FOCE-I and the "YLO" method of handling BLQ data. Pharmacokinetics were allometrically scaled by default for a reference 18kg dog. The CV PD model was adapted from a published Frank-Starling baroreceptor model in the sheep [2]. Initially a "resting" CV model was developed using only pre-dose data and data from placebo treated dogs in conjunction with literature data. The PPP&D approach was used for PK-PD modelling with LVFS, HR, SV, MAP and CO as the independent variables fitted simultaneously, with pimobendan concentrations affecting LVFS.

Results: PK data were best described by a single Vd/F (212L/h/18kg) with linear CL/F (212L/h/18kg), with log-normal BSV on CL/F (64%CV) and V/F scaled via a shared eta (0.74), with additive (0.5ug/L) and proportional (25%) RUV. Absorption via 2 absorption transit compartments (5.86 /h), was highly variable between dogs (94% CV). Using log-likelihood profiling, bioavailability was found to be reduced to 20% of normal in the presence of a meal. Formulation type was not found to affect bioavailability or absorption rate. For the CV model, all structural paramters were fixed, but included correlated covariance between SV50, MAP set point, and systemic vascular resistance, and BSV (21%) and between occasion variability (9%) on LVFS. RUV on all independent variables was additive and estimated separately. The effect of pimobendan on LVFS was best described by an effect-delay half-life of 4h, via an Emax (42%) model additive to the "drug-free" baseline LVFS (32%), with an EC50 of 11ug/L. All PD parameters were estimated with an %RSE <10%. Simulations demonstrated that at a single 0.5mg/kg dose to a typical 18kg dog results in maximal changes in the cardiovascular system at approximately 2-3 hours, returning essentially to baseline by 12h. The most pronounced effects were for LVFS, SV and HR, with changes from 32%, 33mL and 100bpm, to 46%, 41mL and 87bpm, respectively. Changes from baseline for MAP (100mmHg), and CO (3.3L/min), were relatively minor (107 mmHg, and 3.6L/min, respectively). Compared to the single 0.5mg/kg dose, administering two 0.25mg/kg doses 12h apart (ie 0.5mg/kg/24h) resulted in much smaller changes in the CV system at 3-8h, substantially greater effects from approximately 15-20h (ie, 3-8h post second dose) but were similar at 12h and 24h.

Conclusion: The development of this model demonstrates a method for inter-species adaptation of a CV model and expansion to a population model. Importantly, the CV model provides a mechanistic understanding of the cardiovascular effects of pimobendan. Genrally drug effects can easily be included on other, or multiple, CV parameters. These features would be valuable in the design of clinical trials of CV agents.

References:

1. Beal S, Sheiner LB, Boeckmann A, Bauer RJ. NONMEM User's Guides, Part V. (1989-2009), Icon Development Solutions, Ellicott City, MD, USA. 2009.
2. Upton RN and Ludbrook GL. Pharmacokinetic-pharmacodynamic modelling of the cardiovascular effects of drugs – method development and application to magnesium in sheep. BMC Pharmacology (2005) 5:5.

222

Internal deterministic identifiability

Mr Vijay Kumar Siripuram[1], Dr Daniel F.B. Wright[1], Dr Murray L. Barclay[2], Dr Stephen B. Duffull[1]

[1]Otago Pharmacometrics Group, School of Pharmacy, University Of Otago, Dunedin, New Zealand, [2]Departments of Gastroenterology & Clinical Pharmacology, Christchurch Hospital , Christchurch , New Zealand

Aims: Identifiability is an important component of model development. An identifiability analysis can provide the basis for understanding the limits of model structure and parameterisation. There are two types of identifiability analysis, structural and deterministic. A structural identifiability analysis refers to the formal identifiability of model structure (see (1) for a description and expansion to a population PK model). Deterministic identifiability (DI) is concerned with the influence of study design on the precision of the parameter estimates in a structurally (at least locally) identifiable model given imperfect input-output data. We further classify DI into two sub-types external deterministic identifiability (EDI) and internal deterministic identifiability (IDI). EDI relates to the DI of models conditioned on the study design controlled by the investigator. In a simple case, a design where the number of unique observations (n) is less than the number of parameters (p) in the model will be deterministically unidentifiable despite being structurally identifiable. By contrast, IDI describes the situation in which a specific set of parameters yield unreasonably imprecise parameter estimates, despite the model being structurally identifiable and the design fulfilling the needs of EDI. Here EDI can be considered to be any unconstrained optimal design where unique (n) > p. In this setting a non-IDI situation is defined as one where , Where, is a vector of parameter values, is the vector of design variables from D-optimum design and represents the level of imprecision that is important to the investigator. For the purposes of this research, we define a relative standard error (RSE) 100 % to be upper limit of acceptable imprecision. The aim of this study is to investigate whether IDI can be identified in a common set of PK and PKPD models.

Methods: Three models were selected for the IDI analysis: 1) a first-order input and output PK model (FOIO), 2) a parent-metabolite (PM) model with iv-bolus input to the parent compartment (P), first-order metabolism of P to a metabolite (M) and first-order elimination of M. It is assumed that P is completely metabolised to M and that sampling occurs from both the P and M compartment. Finally, 3) a turnover model with iv-bolus input (IVBTO). The drug was assumed to reduce the rate of production of a hypothetical biomeasure of interest. An intensive, 78 sample, design was chosen for each response variable. For the FOIO and PM models the initial set of parameter values were arbitrary and for IVBTO the parameters were adapted from (2). Using boundaries on these selected initial sets of initial parameters, random variates were generated that cover a plausible profile of response. The sets of parameter values with high RSE values (above; 100%) were evaluated at their D-optimal design using POPT. This served the purpose of ruling out EDI. Any set of parameter values that retained RSE greater than 100% under the optimal design indicates that the respective model is not IDI.

Results: There was clear evidence that the FOIO model was not-IDI. It is seen in this trivial example that as the first-order rate constant of input (ka) approaches the value for output (k; CL/V) that the RSE values ka, V and their between-subject variance tends to infinity. Whereas for the PM-model, there is no such observation and the model was IDI. In case of the IVBTO model there existed several sets of parameter values that provided high RSE for the fixed and between-subject variance for IC50 for the optimal design.

Conclusion: From this work it is evident that sets of parameter values exist that can render our example models not identifiable. This occurs in models that are otherwise structurally identifiable as well as externally deterministically identifiable (i.e. under the optimal design). We have termed this as internal deterministic identifiability. This has been explored with three models. In the case of the FOIO, the presence of an IDI issue was explicable on the basis of the model structure. However for IVBTO this was not as obvious. There is a need to consider that IDI issues may be present during model development.

References:

1. Shivva V. An Approach for Identifiability of population pharmacokinetic–pharmacodynamic models. CPT: Pharmacometrics Syst Pharmacol. 2013; 2(e49):1-9.
2. Jusko W J. Characteristics of indirect pharmacokinetic models and applications to clinical drug responses. Br J Clin Pharmacol. 1998; 45:229-239.

223

Toxicokinetics of Endotoxin and its induction of pro-inflammatory cytokines tumor necrosis factor α and interleukin-6

Mr Anders Thorsted[1], Mr Salim Bouchene[1], Dr. Eva Tano[2], Dr. Markus Castegren[2], Dr. Miklos Lipcsey[2], Dr. Jan Sjölin[3], Dr. Mats Karlsson[1], Dr. Lena Friberg[1], Dr. Elisabet Nielsen[1]

[1]Department of Pharmaceutical Biosciences, Uppsala University, Uppsala, Sweden, [2]Department of Medical Sciences, Uppsala University, Uppsala, Sweden, [3]Department of Surgical Sciences, Uppsala University, Uppsala, Sweden

Aims: Infection with Gram-negative bacteria and the immune system's subsequent recognition of the potent membrane-bound activator, endotoxin (ETX), can lead to persistent immune activation. The purpose of the current work was to develop a model-based description of the toxicokinetics of ETX and its induction of the cytokines tumor necrosis factor α (TNF-α) and interleukin 6 (IL-6).

Methods: Based on data from experimental studies, a non-linear mixed effects model was developed in NONMEM 7.3. The modelled data arose from six experimental studies of varying length (6–30 h) in an anesthetized piglet model (n=116), with the aim of studying the inflammatory immune response and organ dysfunction following ETX exposure [1-6]. For the general study design, *E. coli* ETX was infused intravenously for different periods of time in rates ranging from 0.063 to 16.0 μg/kg/h across studies. Shortly, the studies set out to examine ETX tolerance development (dampened response upon second exposure) and differences in response following different infusion regimens, as well as establishing the ETX dose-response.

Results: The time-course of ETX could be described using a one-compartment model with linear elimination (with a half-life of 0.489 h). Observation of contamination in some early ETX measurements was handled by applying a mixture model (with two populations), and initializing the central compartment to an estimated parameter for the contaminated population. For cytokines, an indirect response model with ETX stimulated production (E_{max} model), delayed through a transit chain, was used to describe the shape of the observed cytokine profiles. To describe tolerance development in cytokine release following ETX exposure, a tolerance function was implemented in the parameter describing the potency of ETX to induce cytokine production (EC_{50}). Tolerance development was described using an E_{max} model which was driven by the final compartment in a transit chain, coupled to the compartment describing the time-course of ETX. Rapid tolerance development was identified with large increases in EC_{50}, and the developed model was able to describe both rapid development, and dampened responses upon a second exposure to a higher ETX load. In addition to the tolerance model described above previously published tolerance models were tested [7], but none were found to better describe the data.

Conclusion: A mathematical description was developed for the time-course of ETX following intravenous infusion, and linked to induction of the two immune response markers TNF-α and IL-6. This model-based approach is unique in its description of the three time-courses, and may later be expanded to better understand immune cell release in bacterial infections and sepsis-type pathophysiological changes in organ dysfunction.

References:

1. Lipcsey M, Larsson A, Eriksson MB, Sjölin J. Inflammatory, coagulatory and circulatory responses to logarithmic increases in the endotoxin dose in the anaesthetized pig. J Endotoxin Res. 2006;12(2):99-112
2. Carlsson M, Lipcsey M, Larsson A, Tano E, Rubertsson S, Eriksson M, Sjolin J. Inflammatory and circulatory effects of the reduction of endotoxin concentration in established porcine endotoxemic shock--a model of endotoxin elimination. Crit Care Med. 2009 Mar;37(3):1031-e4.
3. Lipcsey M, Larsson A, Eriksson MB, Sjölin J. Effect of the administration rate on the biological responses to a fixed dose of endotoxin in the anesthetized pig. Shock. 2008 Feb;29(2):173-80.
4. Castegren M, Skorup P, Lipcsey M, Larsson A, Sjolin J. Endotoxin tolerance variation over 24 h during porcine endotoxemia: association with changes in circulation and organ dysfunction. PLoS One. 2013;8(1):e53221.
5. Castegren M, Lipcsey M, Söderberg E, Skorup P, Eriksson M, Larsson A, Sjölin J. Differences in organ dysfunction in endotoxin-tolerant pigs under intensive care exposed to a second hit of endotoxin. Shock. 2012 May;37(5):501-10.
6. Goscinski G, Lipcsey M, Eriksson M, Larsson A, Tano E, Sjölin J. Endotoxin neutralization and anti-inflammatory effects of tobramycin and ceftazidime in porcine endotoxin shock. Crit Care. 2004 Feb;8(1):R35-41.
7. Gårdmark M, Brynne L, Hammarlund-Udenaes M, Karlsson MO. Interchangeability and predictive performance of empirical tolerance models. Clin Pharmacokinet. 1999 Feb;36(2):145-67.

224

A QSP model to predict the effects of different anticoagulants on the human coagulation network

Dr. Sonja Hartmann[1], Dr. Konstantinos Biliouris[1], Dr. Lawrence J Lesko[1], Prof. Dr. med. Ulrike Nowak-Göttl[2], Dr. Mirjam N Trame[1]

[1]University of Florida, Center for Pharmacometrics & Systems Pharmacology, Department of Pharmaceutics, Orlando, United States, [2]University of Schleswig-Holstein, Institute of Clinical Chemistry, Thrombosis & Hemostasis Treatment Center, Campus Kiel & Lübbeck, Germany

Aims: Warfarin is the anticoagulant of choice for venous thromboembolism treatment. However, its suppression of the endogenous clot dissolution components PC and PS, and consequently of the APC:PS complex, ultimately leads to longer time-to-clot dissolution profiles, resulting in an increased re-thrombotic risk.[1,2] Other anti-coagulants, such as enoxaparin or the direct oral anti-coagulants such as rivaroxaban, might constitute an alternative to warfarin as they act via different pathways, therefore hypothesized to not stimulate the suppression of the endogenous clot dissolution components. The objective was to develop a quantitative systems pharmacology (QSP) model describing the coagulation network to monitor coagulation factor levels under warfarin, enoxaparin, and rivaroxaban treatment.

Methods: Individual steady-state coagulation factor concentrations from therapeutic drug monitoring of 312 subjects on enoxaparin (dose levels: 40, 60, 80, 120 mg), rivaroxaban (dose levels: 15, 20, 30 mg) and warfarin/phenprocoumon (Vitamin K antagonists (VKA)) (dose levels: 2.5, 5, 7.5 mg) treatment (observed coagulation factor level concentrations for rivaroxaban: factor II (FII), FV, FVII, FIX, FX, FXI, FXII, FXIII, protein S (PS), protein C (PC); for VKA: PC, PS, plasminogen, for enoxaparin: PC, PS, plasminogen) were used to develop and to externally evaluate a QSP model of the coagulation network build in MATLAB® using Wajima *et al.*[3] as a starting point. Additional coagulation factor level concentrations of PC and PS were available from subjects (n=20) being switched from VKA to enoxaparin or rivaroxaban treatment. Parameter values for all factor rate constants (V_{max}, K_m) as well as production rates in the QSP model were estimated using global optimization. Inter-individual variability of ±20% was added on the production rates of FII, FV, FVII, FIX, FX, FXI, FXII, FXIII, PC, PS, plasminogen, and fibrinogen. Drug effects of rivaroxaban, enoxaparin and VKA were incorporated into the model via separate dosing compartments and pathways according to their specific mechanisms of action. Sobol sensitivity analysis[4] was performed to identify key parameters having the greatest impact on clot dissolution. External model evaluation using data not utilized for model development was performed using MatVPC[5].

Results: The developed QSP model allowed for estimation of the individual coagulation factor rate constants and production rates based on the available individual subject coagulation factor level concentrations. The coagulation factor activation reactions were computed using Michaelis-Menten kinetics. Predictions of individual coagulation factor time courses under steady-state VKA, enoxaparin, and rivaroxaban treatment were well described by the developed model and reflected the suppression of PC and PS under VKA treatment compared to rivaroxaban and enoxaparin. Treatment switch from VKA to either enoxaparin or rivaroxaban was simulated using the developed QSP model and evaluated by overlaying the simulations with the observed data. The simulations described the observed 50% increase in PC and PS factor levels adequately well after subjects were switched from VKA to rivaroxaban or enoxaparin treatment. Additionally, the model was able to estimate the duration of level recovery to be 9 and 11 days for PC and PS levels, respectively. Concordantly, treatment switch from enoxaparin to VKA lead to a 50% decrease in PC and PS factor levels and the estimated duration of level suppression was 8 and 10 days, respectively. Sobol sensitivity analysis[4] identified the production rate for vitamin K being the most influential parameter to stimulate clot-dissolution. External model evaluation using the Monte Carlo simulation tool in MatVPC[5], resulted in adequately well predictions of all coagulation factor level concentrations for dosing regimens and subjects not used during model development.

Conclusion: A QSP model was developed to describe the human coagulation network and time courses of several clotting factors under different treatment regimens. The model may be used as a tool during clinical practice or regulatory decision making to predict the effects of different anti-coagulant therapies on individual clotting factor time-courses to optimize anti-thrombotic therapy regimens.

References:

1. Haran MZ, et al. Unbalanced protein s deficiency due to warfarin treatment as a possible cause for thrombosis. *Br. J. Haematol.* **139,** 310–1 (2007)
2. Hackeng TM, et al. Protein s stimulates inhibition of the tissue factor pathway by tissue factor pathway inhibitor. *Proc. Natl. Acad. Sci. U. S. A.* **103,** 3106–11 (2006)
3. Wajima T, et al. A comprehensive model for the humoral coagulation network in humans. *Clin. Pharmacol. Ther.* 86, 290–8 (2009)
4. Zhang, X., et al. Sobol Sensitivity Analysis : A Tool to Guide the Development and Evaluation of Systems Pharmacology Models. *CPT Pharmacometrics Syst. Pharmacol.* 4, 1–4 (2015)
5. Biliouris K, et al. MatVPC: A user-friendly MATLAB-based tool for the simulation and evaluation of systems pharmacology models. *CPT Pharmacometrics Syst. Pharmacol.* 4, 547–557 (2015)

225

Population modelling of functional disability in early rheumatoid arthritis treated according to a treat-to-target strategy

Ms Jessica Wojciechowski[1], Mr Nasir Wabe[2], Associate Professor Michael D Wiese[2], Associate Professor Susanna M Proudman[3], Dr David J R Foster[1], Professor Richard N Upton[1]

[1]Australian Centre for Pharmacometrics, School of Pharmacy and Medical Sciences, University of South Australia, Adelaide, Australia, [2]School of Pharmacy and Medical Sciences, Sansom Institute for Health Research, University of South Australia, Adelaide, Australia, [3]Rheumatology Unit, Royal Adelaide Hospital & Discipline of Medicine, University of Adelaide, Adelaide, Australia

Aims: The treat-to-target approach in the management of rheumatoid arthritis (RA) involves frequent assessments of disease activity (measured by the 28-joint disease activity score [DAS28]) to guide drug dose and regimen adjustments until remission has been achieved. Previous work has shown that DAS28 progression with combination disease modifying anti-rheumatic drug (DMARD) therapy for RA follows a predictable population time-course, but between subject variability and residual error is large (1). Such that, the aim was to quantify and evaluate inter-individual differences in functional disability (as assessed by a modified version of the Health Assessment Questionnaire – Disability Index [mHAQ]), rather than disease activity, over 2-years for an early RA cohort treated with combination DMARD therapy according to a treat-to-target protocol using population (non-linear mixed effect) modelling.

Methods: Structural models comprised parameters that described the average maximum achievable change in mHAQ over time, the rate of change in mHAQ over time and the lag in onset to mHAQ change were tested using NONMEM® with respect to their ability to describe the average mHAQ trajectory since the initiation of therapy. Covariates and random effects were added to structural model parameters to quantify how, and by how much individuals in the study population varied from this average.

Results: The average mHAQ in the population (n = 241) had a baseline of 0.535 units and decreased by 0.450 units after 2-years of combination DMARD therapy, and 50% of the overall decrease in mHAQ was achieved by 14.4 weeks. The model sufficiently described both the overall population mHAQ trajectory and the mHAQ trajectory of each study participant. Higher baseline pain and baseline DAS28 were predictors of higher baseline mHAQ, and stringent compliance to the treat-to-target protocol was associated with improved 2-year mHAQ outcomes (Figure 1).

Figure 5

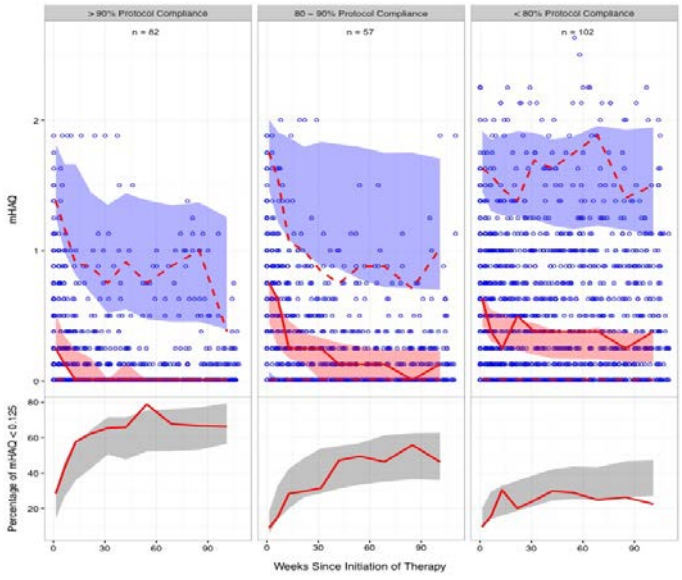

Conclusion: Population modelling accurately described and explained inter-individual differences in mHAQ within our cohort of early RA patients.

References:

1. Wojciechowski J, Wiese MD, Proudman SM, Foster DJ, Upton RN. A population model of early rheumatoid arthritis disease activity during treatment with methotrexate, sulfasalazine and hydroxychloroquine. British journal of clinical pharmacology. 2015;79(5):777-88.

226

Population of pharmacokinetics of tanezumab in pateints with chronic low back pain

Dr Rujia Xie[1], Dr Guangli Ma[1], Dr Scott Marshall[2], Dr Rosalin Arends[3]
[1]Pfizer Ltd, Shanghai, China, [2]Pfizer Ltd, Sandwich, UK, [3]Pfizer Inc, Groton, USA

Aims: Tanezumab is a monoclonal lgG antibody targeted against nerve growth factor (NGF). It is currently under clinical development for the treatment of chronic pain associated with osteoarthritis (OA), cancer and chronic low back pain (CLBP). A population pharmacokinetic (PK) analysis was conducted using pooled data from three CLBP studies. The purposes of this analysis were to i) characterize the PK of tanezumab after intravenous (IV) and subcutaneous (SC) administrations; ii) identify the factors that may impact the PK; iii) predict exposures for the PK/Pharmacodynamic (PKPD) analyses.

Methods: One Phase 2a study and one Phase 2b study with a long term open label extension were included in the analysis. In the former study, patients were treated with 1 dose of 200 μg/kg IV. In the latter study, 2 doses of either 5mg, 10mg or 20mg IV, 8 weeks apart, were administered, followed by entry into the long term safety extension study with up to 3 q8W IV doses, followed by up to 4 q8W SC doses, of either 10mg or 20mg. Plasma tanezumab concentrations over time were analyzed using nonlinear mixed effects modeling approach (NONMEM version 7.2). The estimation method was the first order conditional with interaction (FOCEI). Based on past experience [1,2] the potential covariates of interest were Dose, Age, SEX, baseline body weight (BWT), baseline creatinine clearance (BCRCL), and baseline albumin (BALB) on clearance (CL) and BWT and SEX on volume of distribution.

Results: In total 5332 observations from 1158 patients (536 males and 622 females) were included in the analysis, in which 17% of the patients followed SC dosing. The PK of tanezumab was best characterized by a two-compartment model with parallel linear and nonlinear elimination pathways with a first order absorption (K_a) after SC administration. Body weight was considered to be a structual covariate on CL, central volume (V_1) and peripheral volume (V_2). The other covariates identified were Dose, SEX, BCRCL and BALB on CL, and SEX on V_1. The parameter estimates for a typical female subject (BWT of 84.81 kg, BCRCL of 102.9 ml/min, BALB of 4.4 g/mL) receiving a 5mg IV dose were 0.133 L/day, 2.3 L, 2.07 L, 6.05 μg/day, and 22.6 μg/L for CL, V_1, V_2, maximum elimination capacity (V_m) and concentration at half of V_m (K_m), respectively. The absolute bioaviability (F) for SC and K_a were estimated to be 0.76 and 0.245 day^{-1}. Interindividual varibility (IIV expressed as %CV) on linear CL, V_1 and V_2, and V_m were estimated with a correlation between CL and V_1. BWT was the most influential covariate reducing IIV in CL from 29% to 23% and other covariates effects only accounted for ~ 2% reduction of IIV in CL. IIVs for CL, V_1, V_2 and V_m were 21%, 19%, 27% and 66%, respectively. Patients were assigned to one of two additive residual error terms using a previously described mixture model [1]. The probability of patients being assigned to the lower residual error term was estimated to be 84.3%. The impact of covariates on the parameters are presented in Table 1.

Table 1. The impact of covariates on the parameters

Covariate relationship	Parameter estimates (RSE%)	Impact
WT on CL	0.611 (7.61)	A 10% change in body weight leads a 6% change in CL
BCCL on CL	0.139 (20.65)	A 10% change in CRCL leads a 1% change in CL
Dose_10mg on CL	-0.0856 (9.91)	CL is 8.6% lower at dose of 10mg compared to 5mg
SEX on CL (male)	0.118 (16.1)	Males have a 11.8% higher CL than females
BALB on CL	-0.373 (25.09)	A 10% change in baseline albumin leads to a 4% change in CL
WT on V_1	0.417 (11.08)	A 10% change in body weight leads a 4% change in V_1
SEX on V_1 (male)	0.164 (13.66)	Males have 16.4% higher V1 than females
WT on V_2	0.374 (23.16)	A 10% change in body weight leads a 4% change in V_2

Conclusion: The parameter estimates and identified covariates describing the disposition of tanezumab are similar to a previous population PK analysis in an OA population, where the fast nonlinear pathway was considered to be related to target mediated clearance [1]. The rate and extent of absorption following SC administration was also characterized. The identified statistically significant covariates are not considered clinically relevant.

References:

1. Jonsson E.N. et al. Population pharmacokinetics of tanezumab in phase 3 clinical trials for osteoathritis pain. Br J Clin Pharmacol. 2016 April; 81(4):688-699.
2. Ordas I, et al. Anti-TNF monoclonal antibodies in inflammatory bowel disease: pharmacokinetics-based dosing paradigms. CPT 2012 Feb 22.

227

Understanding identifiability of random effects in mixed effects models

Prof Marc Lavielle[1,2], Prof Leon Aarons[1,2]

[1]Inria Saclay, Palaiseau, France , [2]University of Manchester, Manchester, United Kingdom

Aims: We discuss the question of model identifiability within the context of nonlinear mixed effects models and application to pharmacokinetic models.

Methods: Although there has been extensive research in the area of fixed effects models, much less attention has been paid to random effects models. In this context we distinguish between theoretical identifiability, in which different parameter values lead to non-identical probability distributions ,structural identifiability which concerns the algebraic properties of the structural model, and practical identifiability, whereby the model may be theoretically identifiable but the design of the experiment may make parameter estimation difficult and imprecise. We explore a number of pharmacokinetic models which are known to be non-identifiable at an individual level but can become identifiable at the population level if a number of specific assumptions on the probabilistic model hold.

Results: Essentially if the probabilistic models are different, even though the structural models are non-identifiable, then they will lead to different likelihoods. This requires strong assumptions about the probabilistic models which may be difficult to validate in practice. The findings are supported through simulations.

Conclusion: From a pharmacokinetic point of view it means that the differences between individuals can break the non-identifiability seen at the population level and this may allow better mechanistic understanding of the interindividual differences in pharmacokinetics. However, even if the models are identifiable at the individual level it may prove difficult to estimate the parameters of the model unless supported by good experimental design. A complete account of this research can be found in [1].

References:

1. Lavielle M, Aarons L. What do we mean by identifiability in mixed effects models? J Pharmacokinet Pharmacodyn DOI 10.1007/s10928-015-9459-4 (2016).

228

How pharmacometrics can improve the power of pharmacogenetic studies

Dr Julie Bertrand[1]

[1]*UMR1137 Inserm University Paris 7, Paris, France*

Aims: Pharmacogenetics (PG) studies the relationship between genetic variation and drug response with the aim of providing more precision to the development of personalized medicine. These last years, PG studies have for example identified the abacavir hypersensitivity syndrome association with the HLA-B*5701, HLA-DR7, and HLA-DQ3 variants (1) and the hepatitis C treatment response association with the rs12979860 variant, upstream of the IL28 gene (2). However the impact of PG studies in terms of treatment recommendations is still limited due to low power of studies and lack of precision in the estimation of the association effect size (3). Tessier et al. have shown how using nonlinear mixed effect modeling compared to non-compartmental analysis improved the power of PG tests in pharmacokinetic studies (4). The present work further develops how pharmacometrics can enhance the classic statistical approach in PG.

Methods: Data sets were simulated under the null and several alternative hypotheses. Genetic polymorphisms were simulated approximating the design of the DMET chip (5) with about 1200 genetic polymorphisms across the whole genome. Pharmacokinetic (PK) profiles were simulated using a two-compartment model. Both rich and sparse designs were investigated.

Genetic association was investigated through : i) a classic stepwise linear regression and two types of penalized regressions on the empirical Bayes estimates (EBEs) of the individual PK parameters with the hlasso program (6), ii) a classic stepwise covariate selection with saemix (7), iii) an integrated approach with a penalized regression embedded in the population parameters estimation step using saemix and hlasso and iv) Bayesian inference through informative prior distributions on the genetic effect sizes with Stan (8) and variable selection with JAGs (9).

Results: On EBEs all approaches show similar power, but penalized regression can be much less computationally demanding. Penalized regression should be preferred over stepwise procedures for PK analyses with a large panel of genetic covariates. In all scenarios, the integrated approach detected fewer false positives. A PK phase II study with 300 subjects lacks the power to detect genetic effects on PK using genetic arrays. The integrated approach can simultaneously analyse phase II and clinical routine data and identify when genetic variants affect multiple PK parameters.

Conclusion: Pharmacometrics allows statisticians to analyse together clinical data from multiple studies with different sampling designs. This is crucial as increasing the sample size is necessary to achieve sufficient power to detect realistic and clinically relevant PG effects.

References:

1. Mallal S. et al. Association between presence of HLA-B*5701, HLA-DR7, and HLA-DQ3 and hypersensitivity to HIV-1 reverse-transcriptase inhibitor abacavir. Lancet. 2002;359(9308):727-32.
1. Ge et al. Genetic variation in IL28B predicts hepatitis C treatment-induced viral clearance. Nature. 2009;461(7262):399-401.
2. Holmes et al. Fulfilling the promise of personalized medicine? Systematic review and field synopsis of pharmacogenetic studies. PloS One. 2009;4(12):e7960
3. Tessier A et al. Comparison of Nonlinear Mixed Effects Models and Noncompartmental Approaches in Detecting Pharmacogenetic Covariates. AAPS J. 2015;17(3):597-608
4. Daly TM et al. Multiplex assay for comprehensive genotyping of genes involved in drug metabolism, excretion, and transport. Clin Chem. 2007; 53:1222–1230.
5. Hoggart CJ et al. Simultaneous analysis of all SNPs in genome-wide and re-sequencing association studies. PLoS Genet 2008; 4:e1000130.
6. Comets E et al. SAEMIX, an R version of the SAEM algorithm. Athens, Greece: Population Approach Group in Europe; 2011.
7. Stan Development Team. 2016. The Stan C++ Library, Version 2.9.0.
8. Plummer M. 2003. JAGs: A program for analysis of Bayesian graphical models using Gibbs sampling.

229

Imputation methods to correct for overestimated shape parameter of Weibull hazard function in time-to-event modeling

Prof Dong-seok Yim[1]

[1]*The Catholic Univ Of Korea, Seoul, South Korea*

Aims: Hyper-acute, mass occurrence of events (e.g., at day 0~1) is not rare in biomedical data. If the event times are recorded on a daily basis in such situation, information loss occurs from discretization of events at day 1. However, the overestimation of maximum likelihood estimator (MLE) of the Weibull shape parameter at survival analysis of such data has been rather neglected so far. The problem of overestimated MLE was commonly observed at SAS, R and NONMEM. Thus, we performed a simulation study to explore its implication and present a method of using a hybrid dataset with its events at day 1 replaced with simulated events.

Methods: A 1,000 subject survival datasets per shape parameter (0.2, 0.4, 0.6, 0.8, 1.0, 1.5, 2.0; scale parameter fixed to 30) was simulated for the time range of 0 to 28 (days) using the Weibull function in the R. The simulated datasets were then discretized ("raw dataset" hereafter) so that the event time is recorded by the unit of day. The overestimation of the MLE of shape parameters of the raw datasets were assessed by comparing the K-M plots and biases. To correct the overestimation, we used the biased MLE of Weibull shape and scale parameters first: we simulated the events occurring within day 1 and replaced the discretized day 1 events in the "raw dataset" to build "hybrid dataset". The goodness of the hybrid dataset compared with the "raw dataset" was that the event time information within day 1 was alive usable. With the hybrid dataset, we obtained MLE of Weibull parameters (shape and scale) and tested its biases from the nominal parameters of the raw datasets with the Kolmogorov-Smirnov test comparing the similarity K-M plots from the raw dataset and hybrid dataset. We repeated the imputation process using the new MLEs of Weibull parameters iteratively until we arrive at satisfactory MLEs the pass the Kolmogorov-Smirnov test (p>0.999)

Fig 1. Iterative imputation process

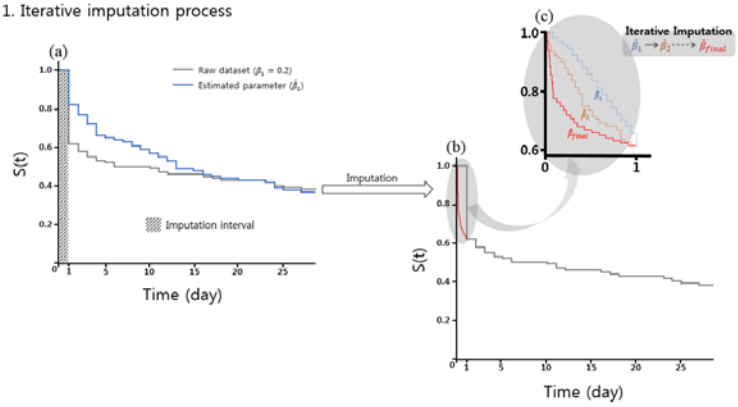

Results: When the nominal shape parameter was less than 0.6, the bias of MLE seemed evident. We arrived at satisfactory Weibull parameters with less than 5 iterative imputation steps.

Conclusion: The MLE of the shape parameter when its nominal true value was less than 0.6 not appropriate to model discrete time-to-event data with the Weibull base hazard. We suggest that our iterative imputation methods may be helpful when modeling time-to-event data with hyper-acute, mass occurrence of events at the very first recording interval (e.g., at day 0~1).

230

Application of Bayesian inference to a model of the dynamics of Plasmodium falciparum parasitaemia in severe malaria patients

Dr Sophie Zaloumis[1], A/Prof Julie Simpson[1], PKPD-IVARS Study Group

[1]*Centre for Epidemiology and Biostatistics, Melbourne School of Population and Global Health, University of Melbourne, Melbourne, Australia*

Aims: To illustrate how to use Bayesian inference for performing a pharmacokinetic-pharmacodynamic (PK-PD) analysis of the largest pooled dataset of drug concentration and parasite count data collected from severe malaria patients receiving intravenous artesunate (IV-ARS). This analysis will provide an example of how to adapt MCMC algorithms for complex nonlinear models, and of diagnostics to assess parameter identifiability.

Methods: The pooled dataset consists of 70 adults (age range 16 to 75 years) and 195 children (age range 6 months to 9 years) with severe malaria who were administered IV-ARS. There was a mixture of sparse and rich sampling designs over 12 hours with, on average, 6 parasite count measurements available per patient (range 1 to 14). The PD model is a mechanistic model relating antimalarial drug concentration to the clearance of parasites in the body over time, and incorporates the parasite life cycle (1 to 48 hours) within the red blood cell of an infected patient. Nonlinear mixed-effects (NLME) modelling was used to allow for between- and within-patient variability in the clearance of parasites over time. Bayesian inference and Markov chain Monte Carlo methods were implemented to derive point and interval estimates for the PD parameters of interest. The Metropolis algorithm was used to sample parameter values from the posterior distribution (joint distribution of the parameters conditional on the data). An adaptive candidate generating distribution (Robbins-Munro process[1]) was used to ensure efficient exploration of the posterior distribution. This algorithm was coded in the statistical software package R.

Results: Preliminary results (posterior median [95% credible interval]) indicate that the population average EC50 concentration for severe malaria patients (prior to emergence of artemisinin resistance) is 6.9 [2.72 – 28.0] ng/ml, and the population mean parasite age of the initial parasite load (IPL) before treatment is 32.7 [28.1 – 37.1] hours. The sampled population average EC50 values, however, struggled to achieve convergence suggesting that this parameter may not be identifiable given the parasite count data available from the clinical patients.

Conclusion: Current software for Bayesian inference is limited for mechanistic highly nonlinear models that are commonly used for PD models. The R code developed applies an adaptive Metropolis algorithm to complex PK-PD models, but requires the user to specify the mathematical form of the posterior distribution.

References:

1. Garthwaite PH, Fan Y, Sisson SA. Adaptive optimal scaling of Metropolis-Hastings algorithms using the Robbins-Monro process. Communications in Statistics-Theory and Methods [Internet]. Taylor & Francis; 2015; (just-accepted). Available from: http://www.tandfonline.com/doi/abs/10.1080/03610926.2014.936562.

231

Physiologically based pharmacokinetic models for trastuzumab using serial concentrations meausred by optical imaging in mouse

PhD Dong-Jun Bae[1], PhD Sang-Yeob Kim[1,2], Miss Ara Koh[3,4], Mr Kwan Cheol Pak[3,4], MD, PhD Hyeong-Seok Lim[3,4]

[1]ASAN Institute for Life Sciences, ASAN Medical Center, Seoul, South Korea, [2]Department of Convergence Medicine, University of Ulsan College of Medicine, Seoul, South Korea, [3]Asan Medical Center, Seoul, South Korea, [4]Ulsan University College of Medicine, Seoul, South Korea

Aims: Trastuzumab is a monoclonal antibody that is mainly used to treat breast cancer and exerts its therapeutic effect by inhibiting the HER2/neu receptor. The purposes of the present study were to measure the serial herceptin concentrations within each mouse after intravenous administration of trastuzumab by optical imaging, and construct physiologically based pharmacokinetic (PBPK) models for trastuzumab. By doing so, we tried to show the potential utility of nonlinear mixed effect modeling and optical imaging in pre-clinical PK evaluation.

Methods: Five serial trastuzumab concentrations (0.5, 2, 4, 6, 24 hour) in whole blood (30 μL in each) within each of 15 mouse were meaured using validated optical imaging after intravenous injection of trastuzumab, 334 μg (n=3) or 200 μg (n=12). At 24 hour after dosing, liver, lung, spleen, and kidney were enucleated and the concentrations were meaured using optical imaging. The blood and the other organ concentration data were analyzed by PBPK model implemented in NONMEM (version 7.3). In the PBPK model, volume of and blood flow to each organ were obtained from literature, and blood to organ partition coefficients were estimated. To examine the potential utility of nonlinear mixed effect PK modeling analysis using 5 serial concentration data within each animal which was possible by optical imaging, compared to conventional naïve pooled data analysis using only one concentration data within each animal, simulation study with 1,000 replicates was conducted using NONMEM.

Results: PBPK model were developed successfully from the blood and the other organ concentration data. Visual predictive check plots showed that the model predict the concentration reasonably well. In the simulation study, modeling analysis using 5 serial concentration data estimated better than that using 1 concentration. Especially, analysis using 5 data overwhelmed that using 1 datum in the reproducibility. Result of the current study suggests the potential utility of optical imaging which makes it possible to measure serial blood concentration within small, experimental animal such as mouse, in preclinical PK evaluation of drug under development in synergy with nonlinear mixed effect modeling analysis.

References:

1. ILSI. Physiological Parameter Values For PBPK Models. International Life Sciences Institute; 1994. p. 142.
2. Utturkar A, Paul B, Akkiraju H, Bonor J, Dhurjati P, Nohe A. Development of Physiologically Based Pharmacokinetic Model (PBPK) of BMP2 in Mice. Biol Syst Open Access. 2013.

232

Population plasma and urine pharmacokinetics of ivabradine and its active metabolite in Korean healthy volunteers

MD, PhD Hee Youn Choi[1], MD, PhD Kyun-Seop Bae[1], MD, PhD Sang-Heon Cho[2], MD, PhD Jong-Lyul Ghim[3], MD, PhD Sangmin Choe[4], MD, PhD Jin Ah Jung[3], MD, PhD Hyeong-Seok Lim[1]

[1]Department of Clinical Pharmacology and Therapeutics, Asan Medical Center, University of Ulsan College of Medicine, Seoul, South Korea, [2]Deparrtment of Clinical Pharmacology, Inha University Hospital, Inha University School of Medicine, Incheon, South Korea, [3]Department of Clinical Pharmacology, Busan Paik Hospital, Busan, South Korea, [4]Clinical Trials Center, Pusan National University, Busan, South Korea

Aims: Ivabradine, a selective inhibitor of the pacemaker current (If), is used for heart failure and coronary heart disease, and mainly metabolized to S18982 (1). The purpose of this study was to explore the pharmacokinetics (PK) of ivabradine and S18982 in healthy Korean volunteers.

Methods: Subjects in a phase I study were randomized to receive 2.5, 5, or 10 mg of ivabradine administered every 12 hours for 4.5 days, and serial plasma and urine concentrations of ivabradine and S18982 were measured using validated LC/MS-MS. Plasma and urine PK were analyzed by nonlinear mixed effect modeling implemented in NONMEM (version 7.3).

Results: The plasma PK of ivabradine was best described by a two-compartment model with mixed zero- and first-order absorption, linked to a two-compartment model for S18982. The final PK model described plasma concentration and cumulative amount excreted urine of ivabradine and S18982, reasonably well. The introduction of inter-occasional variabilities and period as covariate into absorption related parameters improved the model fit. Urine data have been applied to estimate renal and non-renal clearance, enabling a more detailed description of the elimination process.

Conclusion: We developed a population PK model describing the plasma and urine PK of ivabradine and S18982 in healthy Korean adult males. This model might be useful for predicting the plasma and urine PK of ivabradine, potentially helping to identify the optimal dosing regimens in various clinical situations.

References:

1. Ragueneau I, Laveille C, Jochemsen R, et al: Pharmacokinetic-pharmacodynamic modeling of the effects of ivabradine, a direct sinus node inhibitor, on heart rate in healthy volunteers. Clin Pharmacol Ther. 1998; 64(2):192-203.

233

Pharmacokinetic and pharmacodynamic analysis of GCC-4401C, a novel direct factor Xa inhibitor, in healthy volunteers

MD, PhD Hee Youn Choi[1,2], PhD Soongyu Choi[3], MD, PhD Yo Han Kim[1,2], MD, PhD Hyeong-Seok Lim[1,2]

[1]Asan Medical Center, Seoul, South Korea, [2]Ulsan University College of Medicine, Seoul, South Korea, [3]Research Center, Green Cross Corporation, Yongin, South Korea

Aims: GCC-4401C, an orally active direct factor Xa inhibitor which is similar to rivaroxaban, is currently under development for venous thromboembolic disease. The purpose of the present population analyses was to characterize the pharmacokinctics (PK)/pharmacodynamics (PD) of GCC-4401C and predict the proper dosage regimens in patients with venous thromboembolism, especially compared with rivaroxaban.

Methods: PK/PD data used in this analysis were from 94 healthy male subjects in two phase 1 studies, where 88 subjects received single or single (day 1) and multiple oral doses (day 3 through day 9) of placebo or GCC-4401C in fasting status in the range of 2.5 and 80 mg, and 6 received single and multiple oral dose of rivaroxaban, 20 mg in fed status. Most of the subjects were Caucasian (n=41) and African American (n=40). Plasma concentrations of GCC-4401C were measured using validated HPLC/MS-MS, and various PD endpoints were measured through the multiple assays such as PT, aPTT, coagulation factor X (CFX) assay, coagulation factor X chromogenic activity assay (FXCAA), ecarin-stimulated thrombin activity (ESTA), LMWH/anti-factor Xa (AFX) assay, and anti-thrombin III (AT III) activity assay. GCC-4401C (plasma and urine) and rivaroxaban (plasma) PK and PD were analyzed by nonlinear mixed effect modeling using NONMEM (version 7.2). Monte-Carlo simulations for plasma concentration and PD markers over time after various dosing regimens of GCC-4401C and rivaroxaban were performed based on the PK/PD models constructed in this study, and the respective median and 95% prediction intervals were visualized to compare the PK and PD characteristics between the two drugs.

Results: Plasma GCC-4401C concentrations over time were best described by a two compartment linear model. The plasma and urine PK modeling analysis results suggested that most GCC-4401C was eliminated by non-renal routes. All of the PD markers were described well with sigmoid, simple (inhibitory) E_{max}, or linear models, except for ESTA. For rivaroxaban, a two-compartment, linear model best described the plasma concentration over time for drug administration. Rough comparisons based on the simulation plots suggest that 20 and 40 mg of GCC-4401C are comparable to 10 and 20 mg of rivaroxaban in CFX assay, respectively. In other PD markers, the simulation showed that 10 mg of GCC-4401C under fasting status was comparable to 20 mg of rivaroxaban under fed status in AFX and 30-40 mg of rivaroxaban in FACAA and PT, whereas 20 mg of GCC-4401C was comparable to approximately 40 mg of rivaroxaban in AFX and PT, and 80 mg of rivaroxaban in FXCAA.

References:

1. Cohen, A.T. et al. Venous thromboembolism (VTE) in Europe. The number of VTE events and associated morbidity and mortality. Thrombosis and haemostasis 98, 756-764 (2007).
2. Naess, I.A., Christiansen, S.C., Romundstad, P., Cannegieter, S.C., Rosendaal, F.R. & Hammerstrom, J. Incidence and mortality of venous thrombosis: a population-based study. Journal of thrombosis and haemostasis 5, 692-699 (2007).
3. Heit, J.A., Silverstein, M.D., Mohr, D.N., Petterson, T.M., O'Fallon, W.M. & Melton, L.J. 3rd. Predictors of survival after deep vein thrombosis and pulmonary embolism: a population-based, cohort study. Archives of internal medicine 159, 445-453 (1999).
4. Andresen, M.S. et al. Mortality and recurrence after treatment of VTE: long term follow-up of patients with good life-expectancy. Thrombosis research 127. 540-546 (2011).
5. Heit, J.A., Mohr, D.N., Silverstein, M.D., Petterson, T.M., O'Fallon, W.M. & Melton, L.J. 3rd. Predictors of recurrence after deep vein thrombosis and pulmonary embolism: a population-based cohort study. Archives of internal medicine 160. 761-8 (2000).

234

Pharmacometric approaches to evaluate effect of weight and renal function on pharmacokinetics of lobeglitazone

Ms Hyang-Ki Choi[1], Mr Dong-Jin Kim[1], Dr Jong-Lyul Ghim[2], Dr Jin Ah Jung[1], Dr Jae-Gook Shin[1]

[1]Inje University College Of Medicine, Busan, South Korea, [2]Korea University College of Medicine, Seoul, South Korea

Aims: The aim of this study was to evaluate the population pharmacokinetics and to assess the influence of various covariates on lobeglitazone in Korean healthy and ESRD (end-stage renal disease) subjects.

Methods: Data were collected from two clinical trials, in which subejcts were administered 0.5 mg of lobeglitazone once or repeatedly. The pharmacokinetics of lobeglitazone was assessed in 9 ESRD patients and 34 healthy male subjects. Population pharmacokinetic analysis were performed using NONMEM software (version 7.3; Icon Development Solutions, Ellicott City, MD, USA).

Results: Forty-three (34 male and 9 female) healthy subjects ranged from 21 to 64 years were enrolled and completed the study. Two-compartment linear model with first order absorption and lag time best described the pharmacokinetics of lobeglitazone. The effect of sex was significant on apparent clearance and body weight was significant on volume of central compartment ($P < 0.05$ for all). When creatinine clearance and estimated glomerular filtration rate were screened for in the PK model, the objective function value of the model was not significantly decreased.

Table 1. Final estimates of pharmacokinetic parameters

Parameter (units)	Estimate	RSE	Bootstrap median (2.5, 97.5 percentile)[a]
CL1 (L/h), Apparent clearance for male	0.866	8.09%	0.860 (0.711, 1.003)
CL2 (L/h), Apparent clearance for female	0.505	7.78%	0.502 (0.428, 0.601)
V2 (L), Volume of central compartment V2 = estimate * body weight/65	8.62	5.71%	8.579 (7.680, 9.902)
Q2 (L/h), Inter-compartmental clearance	0.912	22.15%	0.935 (0.369, 1.357)
V3 (L), Volume of peripheral compartment	3.79	10.71%	3.904 (3.144, 5.151)
KA, Absorption rate constant of first-order absorption	3.35	15.58%	3.350 (2.521, 5.046)
ALAG1 (h), Lag time for absorption	0.254	4.61%	0.255 (0.227, 0.276)
Random variability (CV,%)			
ωCL1, Interindividual variability of CL_{male}	0.22	11.49%	0.213 (0.124, 0.340)
ωCL2, Interindividual variability of CL_{female}	0.051	10.58%	0.047 (0.001, 0.091)
ωV2, Interindividual variability of V2	0.068	7.62%	0.064 (0.032, 0.109)
ωV3, Interindividual variability of V3	0.255	16.71%	0.236 (0.001, 0.463)
ωKA, Interindividual variability of KA	0.534	18.88%	0.533 (0.263, 0.848)
ωALAG1, Interindividual variability of ALAG1	0.018	7.32%	0.017 (0.004, 0.053)
Residual variability (%)			
σPROP, Proportional error	0.15	14.07%	0.147 (0.112, 0.194)

Conclusion: The pharmacokinetics of lobeglitazone was well described by two-compartment model. Renal impairment and age were not significant covariates. The analysis suggested weight and sex were significant covariates, however, dose adjustment is not required based on weight and sex.

References:

1. Yin OQ., Population pharmacokinetic modeling and simulation for assessing renal impairment effect on the pharmacokinetics of mirogabalin, J Clin Pharmacol. 2016 Feb;56(2):203-12.

235

Evaluating methods using pharmacokinetic information to design dose-finding phase I studies in small populations

Dr Moreno Ursino[1], Dr Sarah Zohar[1], Dr Frederike Lentz[2], Dr Corinne Alberti[3], Dr Tim Friede[4], Dr Nigel Stallard[5], Dr Emmanuelle Comets[6,7]

[1]INSERM, UMRS 1138, team 22, CRC, University Paris 5, University Paris 6, Paris, France, [2]Federal Institute for Drugs and Medical Devices, Bonn, Germany, [3]INSERM, UMR 1123, Hospital Robert-Debré, APHP, University Paris 7, Paris, France, [4]Department of Medical Statistics, University Medical Center Goettingen, Goettingen, Germany, [5]Statistics and Epidemiology, Division of Health Sciences, Warwick Medical School, The University of Warwick, Warwick, France, [6]INSERM, CIC 1414, University Rennes-1, Rennes, France, [7]INSERM, IAME UMR 1137, University Paris Diderot, Paris, France

Aims: To highlight the benefits of conducting a sequential adaptive dose-finding clinical trial by adding information given by PK measurements. We looked at both the selection of the maximum tolerated dose (MTD) and the the ability of each method tested to estimate the dose-toxicity relationship.

Methods: In the context of phase I dose-finding studies in oncology, the objective is to determine the MTD while limiting the number of patients exposed to high toxicity. Two Bayesian ways to estimate probability of toxicity, that is toxicity versus dose or toxicity versus AUC coupled with AUC versus dose, were compared through simulations. In the second method the AUC, is present as covariate for a link function of probability of toxicity and as dependent variable in linear regression versus dose.

We assumed toxicity to be related to a PK measure of exposure, and consider 6 possible dose levels. We simulated trials based on a model for the TGF-β inhibitor LY2157299 in patients with glioma (1) and the PK model was reduced to a one-compartment model with first-order absorption as in (2). Toxicity was assumed to occur when the value of a function of AUC was above a given threshold, either in the presence or absence of inter-individual variability (IIV). For each scenario, 7 in total, we simulated 1000 trials with 30 patients, going up to 60 for checking the ability of each method to estimate the dose-toxicity relationship by considering the estimate of the probability of toxicity for each tested dose.

Results: The method which incorporates PK measurements had comparable performance to the other method in term of percentage of MTD selection. Regarding the ability to estimate the dose-toxicity relationship, the toxicity versus dose model is able to well estimate the probability of toxicity at MTD and nearer doses in each scenario; instead the model which includes PK is able to well estimate the probability associated to all the doses.

Conclusion: Incorporating PK values did not alter the efficiency of estimation of MTD but it increased the ability to estimate the entire dose-toxicity curve. This aspect is very important in case of data extrapolation for further clinical trials.

Acknowledgment: This research has received funding from the European Union's Framework Programme for research, technological development and demonstration under grant agreement no 602144. This work was part of the InSPiRe project but does not necessarily represent the view of all InSPiRe partners.

References:

1. Gueorguieva I, Cleverly AL, Stauber A, Pillay NS, Rodon JA, Miles CP, Yingling JM and Lahn MM. Defining a therapeutic window for the novel TGF-β inhibitor LY2157299 monohydrate based on a pharmacokinetic/pharmacodynamic model. Br J Clin Pharmacol 2014, 77: 796-807.
2. Lestini G, Dumont C, Mentré F. Influence of the size of cohorts in adaptive design for nonlinear mixed effects models: An evaluation by simulation for a pharmacokinetic and pharmacodynamic model for a biomarker in oncology. Pharm Res 2015; 32(10): 3159-69.

236

Tofacitinib pharmacokinetics in moderate-to-severe Crohn's Disease patients in phase 2 induction and maintenance studies

Dr Chenhui Deng[1], Rujia Xie[1], Steven Martin[2], Gary Chan[3], Michele Moscariello[4], Wojciech Niezychowski[4], Eric Maller[4], Arnab Mukherjee[4]

[1]Pfizer Inc, Shanghai, China, [2]Pfizer Inc, Cambridge, USA, [3]Pfizer Inc, Groton, USA, [4]Pfizer Inc, Collegeville, USA

Aims: Tofacitinib is an oral, small molecule Janus kinase inhibitor that is being investigated for inflammatory bowel disease. The aims of this analysis were to characterize the pharmacokinetics of tofacitinib in patients with moderate to severe Crohn's disease (CD) and to evaluate durability of exposures during the course of two randomized, double-blind, placebo-controlled, multi-center Phase 2b studies with tofacitinib 5 or 10 mg twice daily (BID).

Methods: Subjects in the 8-week induction study were randomized to placebo, tofacitinib 5 mg or 10 mg BID. Subjects meeting pre-defined efficacy criteria in the induction study were re-randomized to placebo, tofacitinib 5 mg BID, or 10 mg BID in the 26-week maintenance study. Plasma samples for the pharmacokinetic (PK) analysis were collected at baseline and Week 8 of the induction study, and Week 12 and 26 of the maintenance study. At each visit, 5 PK samples were collected from each subject. A population PK analysis was performed using NONMEM version 7.2 to describe the plasma concentration-time data and derive predicted exposure metrics, average concentration (C_{avg}) and trough concentration (C_{trough}). Covariates evaluated on model parameters included demographics (age, weight, gender, race), baseline creatinine clearance (BCCL), baseline CRP (BCRP), and baseline fecal calprotectin (BFCP).

Results: The PK analysis included 184 subjects from induction and 108 subjects from maintenance who received at least 1 dose of tofacitinib and had at least 1 measurable concentration. Plasma concentration-time data were described using a 1-compartment model with first order absorption, absorption lag time, and first order elimination. Parameter estimates for a typical subject (38-year old Caucasian male, body weight 68.6 kg, BCCL=112.4 mL/min, BCRP=5.9 mg/L, BFEC=360 mg/kg) were, oral clearance (CL/F)=23.8 L/hr and oral volume of distribution (V/F)=97.5 L. Inter-subject variability (coefficient of variation) in CL/F was 30.3%. V/F showed a significant positive correlation with body weight. CL/F was not influenced by any evaluated covariate, tofacitinib dose, or time on treatment, indicating that C_{avg} increased proportionately with dose and did not change over the duration of treatment. Individual, dose-normalized C_{avg} and C_{trough} values summarized over time (Figure 1) further supported the durability of tofacitinib exposure.

Figure 6

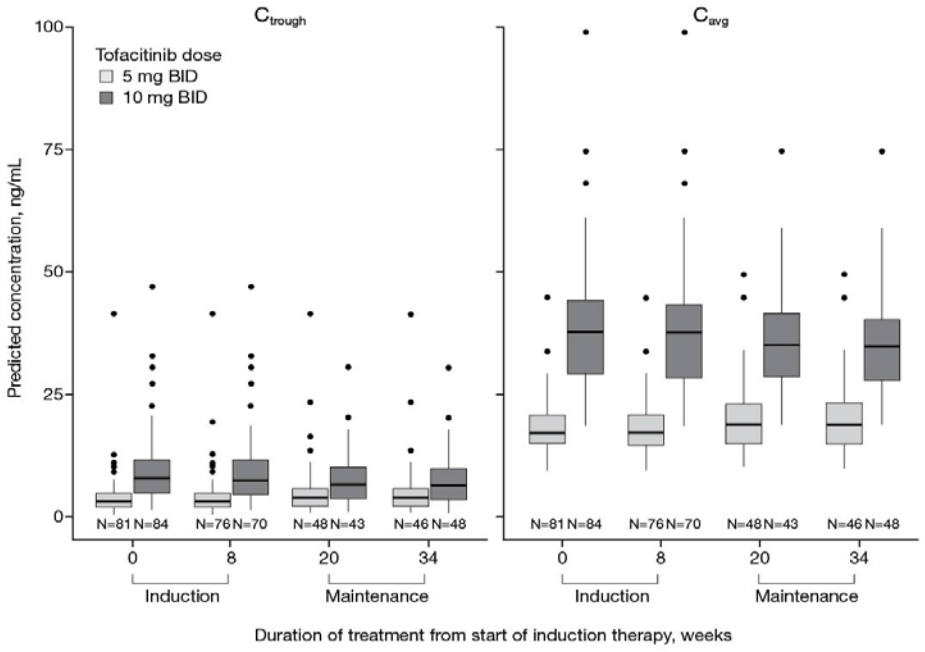

Conclusion: Tofacitinib PK characterization in CD patients indicated dose-proportional and durable exposure over the course of induction and maintenance therapy.

237

The pharmacokinetics of AT9283, a selective inhibitor of aurora kinases, in adults and children with solid tumours and leukemia

Dr Janna Duong[1], Melanie J Griffin[2], Darren Hargrave[3], Josef Vormoor[2], Raffaella Mangano[4], Alan V Boddy[1]

[1]Faculty of Pharmacy, The University of Sydney, Sydney, Australia; [2]Northern Institute for Cancer Research, Newcastle, United Kingdom; [3]Great Ormond Street Hospital for Children NHS Foundation Trust, London, United Kingdom; [4]Cancer Research UK, London, United Kingdom.

Introduction: AT9283 (Astex Pharmaceuticals, UK) is a multi-targeted kinase inhibitor and Phase I/II studies have reported anticancer activity in patients with solid tumours and leukemias. Like many anticancer drugs, AT9283 is dosed by body surface area (BSA) and is associated with a range of toxicities. The pharmacokinetics of AT9283 in children with leukemia is not known.

Aim: To investigate the pharmacokinetics of AT9283 in the adult and paediatric population.

Methods: A population pharmacokinetic (popPK) model was developed using data pooled from adults with solid tumours and leukemia (n=71), and children with solid tumours (n=32) and children with leukemia (n=7). AT9283 was administered as an IV infusion at dose levels from, 4 mg/m^2/72h to 486 mg/m^2/72h in adults and from 21 mg/m^2/72h to 69 mg/m^2/72h in children.

Results: The median age of the adults was 61 years (22–86 years, range) and median weight was 75 kg (40–160 kg). For the children (solid tumours and leukemia), the median age was 9 years (1–19 years), with a median weight of 28.5 kg (8.9 – 88.3 kg). The popPK model was built using 2119 observations from 110 individuals in NONMEM®. The best model was a 2-compartment model fitted to the log-transformed concentration data, with a different additive residual error model for adults and children. The estimated glomerular filtration rate (eGFR) was a significant covariate for the renal clearance (CL_R) and BSA was not a significant covariate for any of the parameters.

Discussion: A popPK model for AT9283 was developed and eGFR was a significant covariate for CL_R. The use of doses adjusted to body surface area did not appear to be appropriate for this drug and schedule.

238

Development of an interactive tool to explore paediatric doses and sample size for paediatric trials

Mr Michael Cheng[1], Mr David McDougall[1], Dr Julia Korell[1], Dr Bruce Green[1]

[1]*Model Answers Interactive, a division of Model Answers Pty Ltd, Brisbane, Australia*

Aims: The aim of this work was to develop an interactive tool that allows users to (1) explore paediatric dose levels that provide a similar exposure as predicted for an adult reference population, and (2) calculate the sample size required for a pharmacokinetic (PK) study in paediatrics based on FDA guidance [1,2].

Methods: A virtual demographic database of subjects aged ≥1 month to ≤65 years was created based on the Continuous NHANES database [3] and the WHO weight-for-age tables for paedaitrics aged ≤10 years [4]. To account for age-dependent maturation of elimination processes, maturation functions reported in the literature for common renal and hepatic elimination pathways were implemented in the tool [5-7]. Users are required to input a reference dose in adult subjects, together with typical estimates of clearance, volume of distribution and their variability. Users may also specify up to three age subgroups for the paediatric study, and select multiple elimination pathways.

Results: The typical exposure in adults and paediatrics is calculated based on the area under the plasma concentration-time curve (AUC) at steady state, approximated as: AUC=Dose/Clearance. Typical clearance values are simulated for the adult and paediatric populations based on demographics (age, sex, and bodyweight) randomly sampled from the virtual subject database, taking allometry and enzymatic and renal maturation into account. 500 subjects are randomly sampled in each age group. A bodyweight based paediatric dose range between 1-70 dose units/kg (e.g. mg/kg) with a step-size of 1 dose unit/kg is explored in the exposure simulations for the paediatrics, with paediatric doses capped at the adult reference dose. Using the simulated clearance values, AUCs are calculated at each dose level to approximate exposure in all age groups. For each paediatric age group, the bodyweight based dose level providing the best agreement with the exposure at the absolute reference dose in adults is determined. The percentage of paediatric subjects with typical exposures falling within the 95% prediction interval of the typical adult exposure is used as the decision criterion (Figure 1).

Figure 1

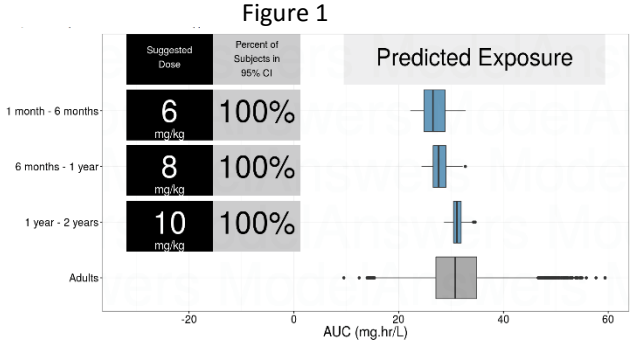

The sample size for a paediatric PK trial is determined based on the minimum number of paediatric subjects required to achieve "a 95% confidence interval within 60% and 140% of the geometric mean estimate of clearance and volume of distribution for the drug in each paediatric group with at least 80% power" [1]. Virtual paediatric PK trials with 5-30 subjects in each age group are generated at random by sampling paediatric subjects from the virtual database. Individual clearance and volume of distribution values are then simulated based on the sampled demographics (age, sex, and bodyweight) and the adult BSV estimates, taking allometry and, for clearance, maturation into account. By default, this process is repeated 500 times for each sample size, i.e. 500 trials are simulated. The power to fulfil the FDA requirement is explored for each sample size across all simulated trials, and the minimum number of subjects achieving at least 80% power in each age group is determined [2].

Conclusion: An interactive tool was developed to facilitate paediatric drug development.

References:

1. FDA. Guidance for Industry: Considerations for pediatric studies for drugs and biological products. December 2014.
2. Wang et al. J Clin Pharmacol. 2012;52:1601–1606.
3. National Center for Health Statistics (Center for Disease Control and Prevention). Continuous National Health and Nutrition Examination Survey. http://wwwn.cdc.gov/nchs/nhanes/search/nhanes_continuous.aspx.
4. World Health Organization. The WHO Child Growth Standards. http://www.who.int/childgrowth/en/.
5. Johnson et al. Clin Pharmacokinet. 2006;45(9):931-956.
6. Salem et al. Clin Pharmacokinet. 2014;53:625-636.
7. Rhodin et al. Pediatr Nephrol. 2009;24:67–76.

239

Exposure-response modeling of longitudinal Likert pain scores following treatment with Neublastin

Dr. Yaming Hang[1], Dr. Matt Hutmacher[2], Dr. Ivan Nestorov[1]

[1]Biogen Inc., Cambridge, United States, [2]Ann Arbor Pharmacometrics Group, Ann Arbor, United States

Aims: To develop a model to quantify the relationship between Neublastin concentration and patient-reported pain scores over time using a population approach and use the model to predict the pain reduction outcome for various untested dosing regimens.

Methods: PK and patient reported Likert pain score data were obtained from three studies (a phase 1 single ascending dose, a phase 1 multiple ascending dose and a phase 2a multiple dose dose-ranging study). The dose levels evaluated ranged between 0.3 and 1200 ug/kg, and drug was administered either IV or SC, in three different frequencies: single dose, once-every-week, or once every other day for 5 days. A Population PK model was constructed for serum Neublastin concentrations, which were measured with either an intensive sampling scheme or a sparse sampling scheme. Patient reported Likert pain scores were also recorded at various time points. A latent variable model was postulated to link Neublastin concentration with pain scores (range 0 – 10). Parameter estimation was performed by NONMEM 7.3. Diagnostics and VPC were used to evaluate model adequacy.

Results: Following IV administration, serum Neublastin concentrations demonstrated a quick distribution phase and an extended terminal elimination phase (terminal half-life ranged between 80-122 hours). A three compartment model characterized the serum Neublastin pharmacokinetics well across the different dose regimens. The exposure-response model for pain reduction included a term for placebo effect and a term for drug effect. The placebo effect was described by an exponential onset approaching a ceiling effect. The drug effect was best described by an indirect response model where the drug concentration reduced the rate constant Kin through an Emax relationship. Different baseline and maximum placebo effect parameters were needed for different studies. The estimated EC50 indicated that serum concentration levels were above EC50 for most of the time. The maximum drug effect on pain reduction was estimated to be around 0.9 units for the phase 1 studies but a much smaller magnitude was predicted for phase 2 study (0.15 units).

Conclusion: The relationship between serum Neublastin concentration and Likert pain scores measured longitudinally in multiple phase 1 and phase 2a studies were well described by an latent variable indirect response model. The model was used to predict untested longer-term treatment regimens to aid the dose selection of a subsequent Phase 2b study.

240

Dose selection for rifabutin in combination with HIV-protease inhibitors

Dr Stefanie Hennig[1], Ms Elin Svensson[2], Dr Roland Niebecker[2], Dr Bernard Fourie[3], Dr Marc Weiner[4], Dr Stefano Bonora[5], Charles A Peloquin[6], Keith Gallicano[7], Charles Flexner[8], Alex Pym[9], Peter Vis[10], Piero L Olliaro[11], Helen McIlleron[12], Mats O Karlsson[2]

[1]University of Queensland, Brisbane, Australia, [2]Department of Pharmaceutical Bioscience, Uppsala University, Uppsala, Sweden, [3]Department of Medical Microbiology, University of Pretoria, Pretoria, South Africa, [4]Department of Medicine, University of Texas Health Science Center and Veterans Administration Medical Center, San Antonio, USA, [5]Unit of Infectious Diseases, Department of Medical Sciences, University of Torino, Torino, Italy, [6]College of Pharmacy and Emerging Pathogens Institute, University of Florida, Gainesville, USA, [7]Novum Pharmaceutical Research Services, Murrieta, USA, [8]Johns Hopkins Adult AIDS Clinical Trials Unit, Division of Clinical Pharmacology, Baltimore, USA, [9]Tuberculosis Research Unit, Medical Research Council and KwaZulu-Natal Research Institute for Tuberculosis and HIV (K-RITH) , Durban, South Africa, [10]LAP&P Consultants BV, Leiden, The Netherlands, [11]Special Programme for Research and Training in Tropical Diseases (TDR), World Health Organization (WHO) , Geneva, Switzerland, [12]Division of Clinical Pharmacology, Department of Medicine, University of Cape Town, Cape Town, South Africa

Aims: Extensive but fragmented data from existing studies were used to describe the drug-drug interaction between rifabutin and HIV-protease inhibitors, and predict doses achieving recommended therapeutic exposure for rifabutin in patients with HIV-associated tuberculosis, with concurrently administered protease inhibitors.

Methods: Individual level data from 13 published studies were pooled, and a population analysis approach was used to develop a pharmacokinetic model for rifabutin, its main active metabolite 25-O-desacetyl rifabutin (des-rifabutin), and drug-drug interaction with protease inhibitors in healthy volunteers and patients who had HIV and tuberculosis (TB/HIV). Repeatedly significant covariates were tested collectively using a linearized stepwise covariate model (lin-SCM) building method implemented in the software PsN to reduce runtime and enable an extensive search for possible relations.(1) Final estimated model parameters were used to calculate the expected average steady-state concentrations (C_{av_ss}) for rifabutin and steady state peak concentration (C_{max_ss}) for rifabutin and des-rifabutin were predicted from the final model using Berkeley Madonna software to identify dosing regimens that provided an exposure >0.187 mg/L (C_{av_ss}) (2, 3), which previously was associated with acquired rifamycin resistance and dose-related toxicity (4, 5), respectively.

Results: Key parameters of rifabutin affected by drug-drug interaction in TB/HIV were clearance to routes other than des-rifabutin (reduced by 76%-100%), formation to the metabolite (increased by 224% in patients), volume of distribution (increased by 606%), and distribution to the peripheral compartment (reduced by 47%). For des-rifabutin, the clearance was reduced by 35% to 76% and volume of distribution increased by 67% to 240% in TB/HIV. These changes resulted in overall increased exposure to rifabutin in TB/HIV patients by 210% because of the effects of protease inhibitors and 280% with ritonavir-boosted protease inhibitors.

Conclusion: Given together with nonboosted or ritonavir-boosted protease inhibitors, rifabutin at 150 mg once daily results in similar or higher exposure compared with rifabutin at 300 mg once daily without concomitant protease inhibitors, and may achieve peak concentrations within acceptable therapeutic range. Although 300 mg rifabutin every three days with boosted protease inhibitor achieves an average equivalent exposure, intermittent doses of rifamycins are not supported by current guidelines.

References:

1. Khandelwal A, Harling K, Jonsson EN, et al. A fast method for testing covariates in population PK/PD Models. AAPS J. 2011;13(3):464-72.
2. Weiner M, Benator D, Peloquin CA, et al. Evaluation of the drug interaction between rifabutin and efavirenz in patients with HIV infection and tuberculosis. Clin Infect Dis. 2005;41(9):1343-9.
3. Weiner M, Benator D, Burman W, et al. Association between acquired rifamycin resistance and the pharmacokinetics of rifabutin and isoniazid among patients with HIV and tuberculosis. Clin Infect Dis. 2005;40(10):1481-91.
4. McGregor MM, Olliaro P, Wolmarans L, et al. Efficacy and safety of rifabutin in the treatment of patients with newly diagnosed pulmonary tuberculosis. Am J Respir Crit Care Med. 1996;154(5):1462-7.
5. Gonzalez-Montaner LJ, Natal S, Yongchaiyud P, et al. Rifabutin for the treatment of newly-diagnosed pulmonary tuberculosis: a multinational, randomized, comparative study versus Rifampicin. Rifabutin Study Group. Tuber Lung Dis. 1994;75(5):341-7.

241

Evaluation of intraocular penetration of levofloxacin after administration drop solution by high performance liquid chromatography and comparison with ciprofloxacin

Associate Professor Amir Heydari[1], Associate Professor Vafa Samarai[1], PhD Student Mahsa Hasanzadeh[1]
[1]*Urmia University of Medical Sciences, Urmia, Iran*

Introduction*:* Levofloxacin is used to treat a wide variety of bacterial infections. Levofloxacin belongs to a class of drugs called quinolone antibiotics. It works by stopping the growth of bacteria.

Fluoroquinolones are suitable for the treatment of ocular infections because of their excellent bactericidal activities and ocular penetration. Among different types of chromatographic methods, HPLC is found to be more effective to achieve separation, identification, purification and quantification of various compounds. Due to favorable pharmacodynamic and pharmacokinetic properties of levofloxacin, this study was evaluated the penetration of levofloxacin after administration of drop solutions. Intraocular penetration of levofloxacin was compared with ciprofloxacin. In this project, we studied the aqueous penetration of levofloxacin, in patients undergoing cataract surgery.

Methods: 33 volunteer patients received one drop of levofloxacin every six hours over three days before cataract surgery and on the day of surgery administration of drug was stopped one hour before surgery. Aliquot of Aqueous samples were stored at -20° C. The samples were thawed, mixed for one minute and centrifuged for 10 minute at 3000 g and 20 µl of the clear supernatant injected into the column of HPLC analysis to assay by reversed-phase HPLC method. The mobile phase consisted of a mixture of acetonitrile and aqueous solution. Levofloxacin concentration was evaluated by HPLC method with fluorescence detector. Peak area was selected as the best parameter for plotting calibration curves by an integration pack program.

Results: A simple, effective and sensitive HPLC assay for determination of levofloxacin in human ocular aqueous was validated. Linearity was shown for levofloxacin concentration over a wide range of 1.95×10^{-3}-1.50 µg/ml. The average level of the levofloxacin in the ocular aqueous was found to be higher than the MIC values that have been reported in the literature for a common bacterium. On the other hand, penetration of levofloxacin into aqueous humor in the patients who received eye drops of levefloxacin is much better than patients who received eye drops of ciprofloxacin. The result of experiments shows that, levofloxacin is a favorable antibiotic because of its ability to penetrate the surgical site with effective concentration.

Conclusions: Levofloxacin concentration was measured by HPLC proposed method that found to be less expensive, simple, rapid and sensitive. The results of experiments reveal that administration of levofloxacin as an eye drop can be more effective than ciprofloxacin because of its high concentration detected in human ocular aqueous rather than ciprofloxacin. In conclusion, this protocol is applicable for drug monitoring in patients undergoing prophylactic antibiotic therapy prior to surgery.

242

Population pharmacokinetic profile of zabofloxacin in Korean subjects

Ms Ji-Young Jeon[1], Prof Min-Gul Kim[1]

[1]Chonbuk National University Hospital, Biomedical Research Institute, Jeonju, South Korea

Aims: Zabofloxacin, a new fluoroquinolone, shows broad-spectrum antibacterial activity. This study aimed to evaluate the pharmacokinetic profile of zabofloxacin and the influence of covariates on the pharmacokinetic parameters of zabofloxacin.

Methods: A population pharmacokinetic analysis was conducted on 1828 zabofloxacin concentrations in 138 subjects who estimated pharmacokinetic of zabofloxacin during three phase I and one II clinical trials. The subjects administered single or multiple, oral doses of zabofloxacin ranging from 10 to 800 mg. The analysis was performed using nonlinear mixed-effect modeling as implemented in NONMEM (version 7.2). The effect of covariates, such as subject characteristics (age, sex, weight, and height) and renal function (serum creatinine, estimated glomerular filtration rate, and stage of renal function) was evaluated.

Results: The best basic model consisted of the two-compartment model with first-order absorption and fist-order elimination. In stepwise covariate modeling, apparent clearance showed a negative correlation with age and central volume showed a positive correlation with weight and a negative correlation with age. There were no obvious relationships among the covariates of renal function.

Conclusion: We developed a population pharmacokinetic model which identified covariate that account for zabofloxacin disposition in Korean subjects. The model can be provided optimization of individualized zabofloxacin dosing regimens.

243

Simulation analysis to explore the optimal combination of pregabalin and duloxetine

Ah Ra Koh[1,2], Kyun-Seop Bae[1,2], Seong Bok Jang[3], Woon Sook Na[3], Su Youn Nam[3], Hyeong Seok Lim[1,2]

[1]Department of Clinical Pharmacology and Therapeutics, Asan Medical Center, Seoul, South Korea, [2]University of Ulsan College of Medicine, Seoul, South Korea, [3]Yuhan Research Institute, Yuhan Corporation, 74, Noryangjin-ro, Dongjak-gu, Seoul 156-754, South Korea

Aims: Pregabalin, an anticonvulsant drug and duloxetine, a selective serotonin-norepinephrine reuptake inhibitor (SNRI) are used for pain relief. The purpose of this study was to explore the optimal combination of pregabalin and duloxetine based on reported modeling analyses.

Methods: Visual analogue scale (VAS) for pain over time were simulated as ordered categorical variables for pregabalin and duloxetine, respectively, based on the previously reported pharmacodynamic (PD) models, using NONMEM (version 7.2)(1, 2). In the Monte-Carlo simulation of 1,000 replicates, parameter uncertainties expressed as standard error of the parameter estimates in previous models for pregabalin and duloxetine were taken into account as well as inter-individual variability. The simulated VAS over time for duloxetine were added to those for pregabalin, assuming additive effect of pregabalin and duloxetine on pain control, and the results were visualized in 3-dimensional plots using R (version 3.0.1)(3).

Results: In the 3-dimensional plot for duloxetine and pregabalin dose per day, and VAS, the pain relief effect we could predict the optimal combinations of duloxetine and pregabalin, which will show the maximum pain relief effect (Figure 1). In monotherapy, 200 mg pregabalin and 50 mg duloxetine per day showed maximum effect. Although the time to maximum effect was reduced, the maximum effect increased no more with the increment of pregabalin and duloxetine, respectively (Figure 2,3).

Figure 7

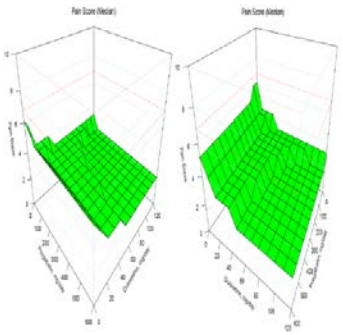

Figure 2

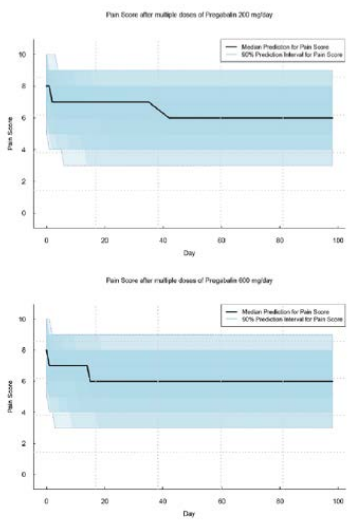

Figure 3

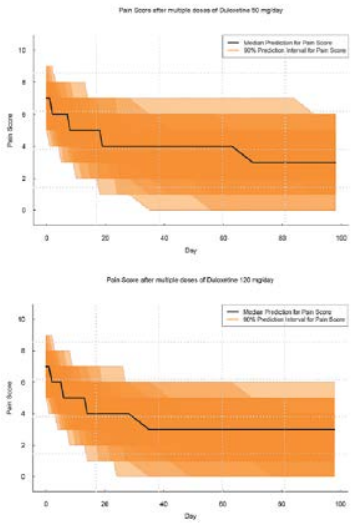

Conclusion: We predicted the optimal combinations of duloxetine and pregabalin with the smallest amount of duloxetine and pregabalin, each, where pain relief are expected to be maximized.

References:

1. Byon W, Ouellet D, Chew M, Ito K, Burger P, Pauer L, et al. Exposure-Response Analyses of the Effects of Pregabalin in Patients With Fibromyalgia Using Daily Pain Scores and Patient Global Impression of Change. *The Journal of Clinical Pharmacology*. 2010;50(7):803-15.
2. Yuen E, Gueorguieva I, Bueno-Burgos L, Iyengar S, Aarons L. Population pharmacokinetic/pharmacodynamic models for duloxetine in the treatment of diabetic peripheral neuropathic pain. *European Journal of Pain.* 2013;17(3):382-93.
3. Tesfaye S, Wilhelm S, Lledo A, Schacht A, Tölle T, Bouhassira D, et al. Duloxetine and pregabalin: high-dose monotherapy or their combination? The "COMBO-DN study"–a multinational, randomized, double-blind, parallel-group study in patients with diabetic peripheral neuropathic pain. *PAIN®*. 2013;154(12):2616-25.

244

Mechanism-based model to quantitatively characterise the impact of altered piperacillin pharmacokinetics on bacterial killing and resistance

Dr Phillip Bergen[1], A/Prof Jurgen Bulitta[3], Prof Carl Kirkpatrick[1], Ms Kate Rogers[1], Ms Megan McGregor[1], Dr Steven Wallis[2], Prof David Paterson[2], Prof Jeffrey Lipman[2], Prof Jason Roberts[2], Dr Cornelia Landersdorfer[1]

[1]Monash University, Parkville, Australia, [2]The University of Queensland, Brisbane, Australia, [3]University of Florida, Orlando, USA

Aims: Piperacillin is commonly used to treat serious infections caused by *Pseudomonas aeruginosa* in intensive care (ICU) patients. These patients often display substantially increased or impaired renal function, leading to a wide range of antibiotic exposures. We aimed to quantitatively characterise for the first time the impact of altered antibiotic pharmacokinetics (PK) on bacterial killing and regrowth *via* mechanism-based modelling (MBM) and the dynamic hollow fibre *in vitro* infection model (HFIM). The HFIM can mimic antibiotic concentration-time profiles as seen in patients and has been successfully used, in combination with MBM, to optimise dosing regimens for evaluation in clinical trials.[1]

Methods: Piperacillin concentration-time profiles for 3 dosing regimens (4g given over 30 min every 4h, 6h or 8h) were simulated in the HFIM over 7 days for ICU patients with augmented, normal and impaired renal function (creatinine clearance 250, 120 and 30 mL/min, piperacillin elimination half-life 0.8, 1.4 and 5.3 h, respectively) based on a population PK model[2] for unbound piperacillin in ICU patients. A piperacillin-susceptible ICU isolate of *P. aeruginosa* was utilised (initial inoculum ~10^7 colony forming units [cfu]/mL). Viable counts of total and less-susceptible bacteria and MICs were determined and piperacillin concentrations measured *via* LC-MS/MS. MBM was conducted using the importance sampling algorithm in S-ADAPT (version 1.57, pmethod=4) for simultaneous estimation of all parameters, facilitated by the SADAPT-TRAN tool. The model included 3 bacterial populations with different susceptibilities to piperacillin (susceptible, intermediate and resistant). The effect of piperacillin was described as both inhibition of the probability of successful bacterial replication and inhibition of bacterial growth.

Results: For augmented renal function all 3 regimens provided limited bacterial killing (≤~2 $\log_{10}$ cfu/mL) followed by rapid regrowth to 10^8-10^9 cfu/mL. Similar results were seen for the 8- and 6-hourly dosing in the context of normal renal function. The regimen of 4g every 4h for normal renal function and all regimens for impaired renal function prevented bacterial regrowth over 7 days. The mechanism-based model successfully quantified the time-course of bacterial growth, killing and regrowth, as demonstrated by visual predictive checks and a coefficient of correlation for the observed *vs.* individual fitted viable counts of 0.990. Maximum inhibition of the probability of successful bacterial replication was estimated at 100% for all populations, however a 55× higher piperacillin concentration was required for half-maximal inhibition of successful replication of the resistant ($IC50_{Rep,IR}$ = 45.8 mg/L) compared to the susceptible population ($IC50_{Rep,S}$ = 0.83 mg/L). The maximum extent of inhibition of bacterial growth was 2-3× higher for the susceptible and intermediate than the resistant population. The piperacillin concentration required for half-maximal inhibition of growth was estimated to span a 27-fold range between the susceptible ($IC50_{k12,S}$ = 0.88 mg/L) and the resistant ($IC50_{k12,R}$ = 23.7 mg/L) bacterial populations.

Conclusion: Piperacillin monotherapy in the context of augmented renal function, even at the maximum clinical dose, was not able to adequately inhibit the replication or growth of the less susceptible bacterial populations in the model. Only the maximum dose suppressed regrowth and resistance for normal renal function. As our model successfully described the time-course of bacterial growth, killing and regrowth over 7 days, it may be useful in simulations to predict bacterial responses to piperacillin dosing regimens for other than the studied renal functions and to individualise dosing regimens for ICU patients with altered PK. The combined experimental and modelling approach can be useful in antibiotic development to support the design of studies in patients.

References:

1. Tsuji et al. Clin Infect Dis 2011;52 Suppl 7:S513-9.
2. Udy et al. Crit Care 2015;19:28.

245

Utilisation of a pharmacokinetic model based approach to optimise paediatric dose selection and study design

Dr Fran Stringer[1], Dr Bruce Green[1]
[1]*Model Answers Pty Ltd, Brisbane, Australia*

Aims: Drug X is being developed to target a paediatric indication. A phase 1, double-blind, single and multiple ascending dose study in healthy adult male and female volunteers was recently completed (n=32). A population pharmacokinetic (PK) model was developed from the data collected during this study, which was then used to determine the dose and trial design for infants in an upcoming phase 1b study.

Methods: The population PK model was developed to describe the concentration-time profile in adults following single and multiple dosing for 7 days. Estimates of clearance (CL/F) and volume (V/F) were then scaled to the paediatric population using allometry with exponents on CL/F and V/F fixed to ¾ and 1, respectively. CL/F also included a maturation function describing the change in drug metabolising enzyme expression with age [1, 2]. Simulations were then performed across the age range (≥1 month to ≤24 months) to determine a dose that would reach a pre-defined target concentration based on non-clinical data.

Results: A one-compartment model that incorporated saturable dual-peak absorption based upon dose per kilogram was developed to describe the PK data in adults. Results from the simulations in paediatrics indicated cytochrome P450 (CYP) (CYP-3A4, CYP-2D6 and CYP-1A2) maturation had the greatest impact on drug exposure for subjects aged <6 months, with CL/F across the age range predicted to be only 10 to 22% of the adult value. As such, a conservative staggered dosing approach by age was implemented for the phase 1b study with the highest dose proposed for infants aged >6 months.

Conclusion: This approach demonstrates the utility of modelling and simulation in providing dosing recommendations to target exposure levels in paediatrics based on prior knowledge. Furthermore, the model will be subsequently utilised for exposure derivation to support adaptive dosing during the phase 1b study.

References:

1. Johnson et al. Prediction of the clearance of eleven drugs and associated variability in neonates, infants and children. Clin Pharmacokinet. 2006;45(9):931-956.
2. Salem et al. A re-evaluation and validation of ontogeny functions for cytochrome P450 1A2 and 3A4 based on in vivo data. Clin Pharmacokinet. 2014;53:625-636.

246

Optimal Ranirestat dose estimation in patients with diabetic sensorimotor polyneuropathy: non-linear population pharmacokinetic pharmacodynamic approach

Mr Takeshi Takagaki[1], Dr Yoshiko Tomita[1], Mrs Hisae Watanabe[1], Dr Hiroyoshi Kakuyama[1], Dr Yumi Sato[1]
[1]*Sumitomo Dainippon Pharma Co., Ltd., Chuo-ku, Tokyo, Japan*

Aims: Ranirestat, a novel aldose reductase (AR) inhibitor synthesized by Sumitomo Dainippon Pharma Co., Ltd., is now being developed as an agent to treat diabetic complications. In order to clarify Ranirestat pharmacokinetics and estimate a clinical optimal dose, population pharmacokinetic (Pop-PK) and pharmacokinetic and pharmacodynamic (PK/PD) analysis are conducted using Ranirestat concentration in plasma and sorbitol concentration in nerve tissue obtained from human clinical studies.

Method: Pop-PK model was developed with NONMEM based on 11 clinical studies and AR inhibition rate by Ranirestat was simulated. It is reported that damaged nerve function is improved when sorbitol accumulation in nerve tissue is reduced by more than 80% and this reduction is considered to be achieved with sufficient AR inhibition. PK/PD analysis was conducted for the evaluation of %reduction of sorbitol accumulation using plasma Ranirestat concentration and nerve tissue sorbitol concentration obtained from PIIa study. Then, clinical optimal dose in Japanese patients with diabetic sensorimotor polyneuropathy was evaluated.

Results: Two-compartment model with saturable specific binding site (supposed to be AR) in peripheral compartment was developed as a Ranirestat Pop-PK model (Figure 1). In peripheral compartment, saturable binding of Ranirestat was described by langmuir model with Bmax (maximum binding amount) and Kd (dissociation constant). CL/F, Vc/F, Kd/F, and Bmax/F were affected by body weight, and CL/F in patients was smaller than that in healthy volunteers. This model adequately described non-linear distribution characteristics of Ranirestat, and simulated mean AR inhibition rate obtained with this model was more than 90% in patients with diabetic sensorimotor polyneuropathy (50-100 kg of body weight) at the dose of 40 mg/day. PK/PD analysis revealed that at the same target patients and dose, mean %reduction of sorbitol accumulation (90%) was above the target reduction level (80%). Therefore, 40 mg/day of Ranirestat was estimated to be an optimal dose in patients with diabetic sensorimotor polyneuropathy.

Figure 1 Pop-PK model of Ranirestat

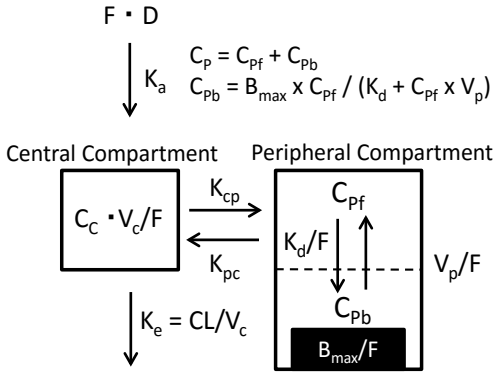

F: oral bioavailability
D: dose (mg)
Cc: total concentration of Ranirestat in central compartment (ng/mL)
Cpb: concentration of Ranirestat binding to specific binding site (ng/mL)
Cpf: concentration of Ranirestat non-binding to specific binding site (ng/mL)
Ka: absorption rate constant (1/h)
Ke: elimination rate constant (1/h)
Kcp, Kpc: rate constant between compartments (1/h)
CL/F: apparent total clearance (L/h/kg)
Vc/F: apparent central distribution volume (L/kg)
Vp/F: apparent peripheral distribution volume (L/kg)
Kd/F: apparent dissociation constant (mg/kg)
Bmax/F: apparent maximum binding amount (mg/kg)

Conclusion: Ranirestat Pop-PK model could describe non-linear distribution of Ranirestat. This model showed that Ranirestat inhibited AR by more than 90% at the dose of 40 mg/day and PK/PD analysis showed that Ranirestat was possible to inhibit 90% of sorbitol accumulation at the same dose in Japanese patients with diabetic sensorimotor polyneuropathy. Therefore, optimal dose of Ranirestat for Japanese patients could be estimated as 40 mg/day.

References:

Greene DA, Arezzo JC, Brown MB, Zenarestat Study Group. Effect of aldose reductase inhibition on nerve conduction and morphometry in diabetic neuropathy. Neurology. 1999;53:580-91.

247

Mechanism-based PK/PD modelling approach to optimise synergistic combinations against carbapenem- and aminoglycoside (AGS)-resistant clinical isolates of Pseudomonas aeruginosa (Pa)

Mr Rajbharan Yadav[1], Dr Jürgen Bulitta[2], Professor Roger Nation[1], Dr Cornelia Landersdorfer[1]
[1]Monash University, Parkville Campus, Melbourne, Australia, [2]University of Florida, Orlando, United State

Aims: Infections caused by carbapenem-resistant Pa are highly challenging clinically and effective early therapy is likely critical for treatment success. Synergistic combinations and optimised dosage regimens are promising to combat multidrug-resistant Pa. We hypothesised that a mechanistic understanding of bacterial killing and resistance will enable us to design innovative, clinically relevant antibiotic combination dosage regimens. Aminoglycosides yield synergistic killing without resistance in combinations with β-lactam antibiotics, since aminoglycosides disrupt the outer bacterial membrane and thereby increase the target site penetration of β-lactams. Aminoglycosides and β-lactams have different mechanisms of resistance. Therefore to test this hypothesis, we aimed to systematically evaluate synergistic killing and prevention of resistance of Pa by carbapenem plus AGS combinations and to rationally optimise combination dosage regimens *via* mechanism-based modelling (MBM).

Methods: We studied imipenem (IPM) in monotherapy & combination with tobramycin (TOB) or amikacin (AMK) vs. 3 carbapenem- and AGS-resistant clinical Pa isolates. Serial viable counts of total and resistant populations (at 3×MIC; minimum inhibitory concentration) were determined in 48h static concentration time-kill studies (inoculum $10^{7.5}$ CFU/mL). MBM characterised the time-course of bacterial killing & resistance. The importance sampling algorithm (S-ADAPT pmethod=4) was used for simultaneous estimation of all PD parameters in the parallelised S-ADAPT software (version 1.57) facilitated by the SADAPT-TRAN tool. Optimised clinically relevant combination dosage regimens vs. a Pa isolate representing the 98th percentile of the EUCAST MIC distributions for IPM (MIC 16 mg/L) and TOB (MIC 32 mg/L) were proposed *via* Monte Carlo simulations. These Monte Carlo simulations were based on the final MBM and population pharmacokinetics of imipenem and tobramycin in critically-ill patients. Between subject variability in the PK and between curve variability of the PD parameters were incorporated in the Monte Carlo simulations. The simulations were performed for 10,000 adult critically-ill patients with normal renal function using Berkeley Madonna (version 8.3.18).

Results: Monotherapies provided little bacterial killing, except for < 2 $\log_{10}$ killing at 1-3h by high (24 & 36 mg/L) IPM concentrations followed by extensive regrowth with resistance. Clinically relevant IPM + AGS concentrations achieved synergistic killing (>2 $\log_{10}$ vs. the most active monotherapy at 24h and 48h) and suppression of resistance for all isolates (MIC: IPM 16 to 32 mg/L & AGS 4 to 32 mg/L). For all three strains, synergistic killing without resistance was achieved by ≥0.88x MIC imipenem in combination with a median [range] of 0.53x [0.032–2.0] MIC tobramycin or 0.50x [0.25–0.50] MIC amikacin. MBM revealed that aminoglycosides significantly enhanced the imipenem target site concentration up to 3.1-fold; achieving half-maximal of this synergistic effect required an aminoglycoside concentration of 1.34 mg/L (if the aminoglycoside MIC was 4 mg/L) and 4.88 mg/L (for MIC 8-32 mg/L). An optimised combination regimen (IPM continuous infusion at 16.7 [9.63 - 29.1] mg/L (median [5th - 95th percentile]) + TOB 7 mg/kg body weight q24h) was predicted to achieve >2 $\log_{10}$ killing and prevent regrowth over 48h in 90.3% of simulated critically-ill patients vs. the double-resistant isolate.

Conclusion: The optimised imipenem plus tobramycin regimen is highly promising against Pa isolates resistant to both carbapenems and AGS. Future evaluation in dynamic infection models will provide guidance on effective early therapy vs. serious infections by these extremely difficult-to-treat Pa.

248

Exploring the effect of high-flux haemodialysis on oral amoxycillin/clavulanic acid using a semi-mechanistic model

Ms Katrina Hui[1], Dr David Kong[1], Ms Michelle Nalder[2], A/Prof Eugenie Pedagogos[2], A/Prof Craig Nelson[3,4], A/Prof Kirsty Buising[2,4], Prof Carl Kirkpatrick[1]

[1]Centre for Medicine Use and Safety, Monash University , Parkville, Australia, [2]Royal Melbourne Hospital, Parkville, Australia, [3]Western Health, Footscray, Australia, [4]University of Melbourne , Parkville, Australia

Aims: Oral amoxycillin/clavulanic acid combination therapy is commonly prescribed to patients receiving haemodialysis. Studies have reported that both molecules are removed during low-flux haemodialysis. However, there is a paucity of published data to guide the dosing of amoxycillin and clavulanic acid in high-flux haemodialysis, where more permeable dialysers are used. As such, the aim of this study was to develop a semi-mechanistic model to explore the effect of high-flux dialysers on the concentrations of amoxycillin and clavulanic acid with different dosage regimens and dialysis prescriptions and the potential impact on its therapeutic efficacy.

Methods: A semi-mechanistic model was developed based on a previously described model.(1) The model was developed using previously published parameters and was a one compartment model with first order input which included both non-renal and high-flux dialyser elimination pathways in Berkeley Madonna (version 8.3.13). For amoxycillin, the mean volume of distribution was 0.22L/kg and the mean non-renal clearance was 0.21ml/min/kg.(2) For clavulanic acid, the mean volume of distribution was 0.16L/kg and the mean non-renal clearance was 0.62ml/min/kg.(2) Haemodialysis was set to occur on the second day, either 2 hours or 8 hours after the morning amoxycillin/clavulanic acid dose was administered. Haemodialysis duration was limited to 2 to 4 hours and was influenced by the amount of fluid to be removed (mean of 2L) and the rate of fluid removal (mean 0.5L/hour). Dialyser specifications from Polyflux®210H were used where the dialyser surface area was 2.1m^2 and thickness was 50µm. Monte Carlo simulations of 1000 simulated patients were undertaken to evaluate the effect of high-flux haemodialysis on clinically prescribed doses of 875mg/125mg daily and 500mg/125mg twice daily of oral amoxycillin/clavulanic acid. Free drug concentrations were calculated from the simulations and linked to the following pharmacokinetic/pharmacodynamic targets to calculate the probability of target attainment (PTA). For amoxycillin, this was the time the free concentration was above the minimum inhibitory concentration for ≥50% of the dosing period. For clavulanic acid, the target was the time the free concentration was above 0.1mg/L for ≥45% of the dosing period.(3)

Results: Monte Carlo simulations predicted that the PTA was over 90% for amoxycillin for micro-organisms with an MIC ≤4mg/L with daily or twice daily dosing regardless of when high-flux haemodialysis occurred. For clavulanic acid, the PTA was over 90% with twice daily dosing. In contrast, with once daily dosing, the PTA for clavulanic acid was less than 60%. It was also noted that with once daily dosing, the PTA was considerably lower for clavulanic acid when high-flux haemodialysis occurred 2 hours after the morning dose was administered compared to haemodialysis occurring 8 hours after dose administration.

Conclusion: These results suggest that once daily oral amoxycillin/clavulanic acid in patients receiving high-flux haemodialysis may result in insufficient concentrations of clavulanic acid to have a synergistic effect with amoxycillin to treat infections. Clinical studies are required to verify and validate this model. Work to develop a more comprehensive dialyser model is in-progress.

References:

1. Dang L, Duffull S. Development of a semimechanistic model to describe the pharmacokinetics of gentamicin in patients receiving hemodialysis. J Clin Pharmacol. 2006;46(6):662-73.
2. Davies BE, Boon R, Horton R, Reubi FC, Descoeudres CE. Pharmacokinetics of amoxycillin and clavulanic acid in haemodialysis patients following intravenous administration of Augmentin. Br J Clin Pharmacol. 1988;26(4):385-90.
3. Lowdin E, Cars O, Odenholt I. Pharmacodynamics of amoxicillin/clavulanic acid against Haemophilus influenzae in an in vitro kinetic model: a comparison of different dosage regimens including a pharmacokinetically enhanced formulation. Clin Microbiol Infect. 2002;8(10):646-53.

249

Translation between two models: application with integrated glucose homeostasis models.

Moustafa Ibrahim[1], Anna Largajolli[1], Maria C Kjellsson[1], Mats O Karlsson[1]

[1]*Department of pharmaceutical biosciences, Uppsala University, Uppsala, Sweden*

Aims: Both the Integrated Glucose Insulin model (IGI) and the Integrated Minimal Model (IMM) have been proposed to characterize simultaneously glucose-insulin regulation system following intravenous glucose tolerance test (IVGTT) [1, 2]. Though with different structure, these models provide full simulation capabilities that allow their use as a platform to quantify disease status as well as analysis of treatment effects in clinical drug development. Here we investigated the translation of information between the two models in terms of parameters' identifiably and precision, as well as mapping two key parameters for clinical diagnosis, glucose effectiveness and insulin sensitivity available in IMM with parameters in the IGI model.

Methods: To investigate the parameter precision and ability of the model to simulate data mimicking real glucose homeostasis data, three sources of data were used: 1) a bootstrap (n=100) of real data, 2) 100 simulated datasets from point estimates of the IMM and 3) 100 simulated datasets from point estimates of the IGI model. Each source of data was analysed with the two models. The point estimates for each model used in the simulations and the bootstrap came from two previously published IVGTT studies performed in healthy subjects with one of the studies being insulin-modified [3, 4] with measurements of glucose and insulin plasma concentration. In total, for each of the models 300 sets of parameters were obtained. To map the clinically important parameters of the IMM with their corresponding parameter in the IGI, a large dataset was simulated using the IGI and analysed with the IMM. A generalized additive model (GAM) was used to evaluate differences between simulated and estimated individual parameters.

Results: Comparing the parameter precision of the three sources for the two models, unsurprisingly the precision is the highest when the same model is used for simulation and estimation. Additionally, the lowest precision is seen in the opposite situation, i.e. IMM generated data analysed with the IGI model and vice versa. When data was generated by the IGI model, bias was observed in 26% of the IMM parameters ranging from 10.9% to 30.6%, while data generated by the IMM, resulted in 75% of the IGI model parameters being biased, ranging from 13% to 4859 For the GAM, the strongest parameter correlations across models were found for: insulin dependent glucose clearance (IGI) – insulin sensitivity (IMM); insulin independent glucose clearance (IGI) – glucose effectiveness (IMM); and rate constant related to insulin effect on glucose clearance (IGI) – insulin action (IMM).

Conclusion: The results of this translation between two models of glucose homeostasis indicate that when analyzed with the IMM, real data and data simulated with the IGI model gave similar results. When analyzed with the IGI model, real data and data simulated from the IMM gave different results. The poor estimation of the rate constant related to suppression of endogenous glucose production indicate that the reason could be a model misspecification in the implicit description of hepatic glucose production. The clinically important parameters in the IMM were successfully mapped to the expected IGI model parameters.

References:

1. Silber HE, Jauslin PM, Frey N, Gieschke R, Simonsson US, Karlsson MO. An integrated model for glucose and insulin regulation in healthy volunteers and type 2 diabetic patients following intravenous glucose provocations. Journal of clinical pharmacology 2007, 47(9): 1159-1171.
2. Largajolli A., Bertoldo A.,Cobelli C., and Denti P., An integrated glucose-insulin minimal model for IVGTT, PAGE 22 (2013) Abstr 2762 [www.page-meeting.org/?abstract=2762]
3. Vicini P, Caumo A, Cobelli C. The hot IVGTT two-compartment minimal model: indexes of glucose effectiveness and insulin sensitivity.Am J Physiol. 1997; 273:E1024-E1032.
4. Vicini P, Zachwieja JJ, Yarasheski KE, Bier DM, Caumo A, Cobelli C. Glucose production during an IVGTT by deconvolution: validation with the tracer-to-tracee clamp technique. Am JPhysiol. 1999; 276:E285-E294.

250

Evaluation of covariate effect size based on parameter variability

Dr Takayuki Katsube[1], Dr Toru Ishibashi[1], Dr Toshihiro Wajima[1]
[1]*Shionogi & Co., Ltd., Osaka, Japan*

Aims: Parameter variability in a model can be described as an explained parameter variability with covariates (EPV) and unexplained parameter variability (UPV) [1,2]. The differences in EPV (dEPV) and UPV (dUPV) between models are indices to assess an impact of covariate effect [2]. In covariate modeling based on the difference in the objective function value (dOFV), dEPV and dUPV can be alternates of dOFV, however, there is no report quantifying impacts of dEPV and dUPV on covariate modeling. The aim of this study was to evaluate how much dEPV or dUPV had an impact on covariate modeling with evaluation of covariate effect size.

Methods: The simulation study was performed using an exponential covariate model given by $TVCL_i = \theta_1 \cdot \exp(\theta_2 \cdot COVR_i)$, where $TVCL_i$ is a typical clearance value for the i^{th} subject and $COVR1_i$ is a normaly-distributed continuos covariate assumed by N(0, variance(COVR)). The individual clearance for i^{th} subject (CL_i) was given by $CL_i = TVCL_i \cdot \exp(\eta_{CLi})$, where η_{CLi} is normally distributed with $N(0, \omega_{CL}^2)$. For the log-transformed CL_i, dEPV between the covariate model and the base mdoel (i.e., the model with no covariate) can be described by variance(log($TVCL_i$)), and dUPV can be described by a difference in ω_{CL}^2 between the base model and the covariate model. As the crucial part of this study, we used the ratio of 95^{th} percentile for $TVCL_i$ relative to 50^{th} percentile as the "inferential index" to be the covariate effect size, where the inferential index of less than 1.25 was considered to describe a slight effect size. As the simulation condition, variance(COVR) of 0.09 and the coefficients for covariate effect (i.e., θ_2) of 0.1, 0.5, and 1 were used. The simulation conditions to result in low to high η shrinkage were also considered. Simulations using a power covariate model with a log-normal-distributed covariate were also tested. The stochastic simulation and estimation approach was performed to evaluate the relationship between the inferential index and dEPV or dUPV. NONMEM ver. 7.3 [3] and Perl-speaks NONMEM [4] were used for the evaluation.

Results: dEPV and dUPV were typically consistent with the expected value calculated from each simulation condition for both types of covariate model (exponential model and power model). The relationship between the inferential index and dEPV or dUPV was described with the theoretical equation under the normality for log-trabsformed $TVCL_i$, which was given by exp[qnorm(0.95)·sqrt(dEPV or dUPV)]. Based on the theoretical equation, dEPV or dUPV was 0.0184, 0.0608 and 0.178 when the inferential index of 1.25, 1.5 and 2, respectively, suggesting less than 0.0184 of dEPV or dUPV idicate slight covariate effect size. In case of the high-η-shrinkage condition, dUPV was smaller than the expected value, whereas dEPV was typically consistent with the expected value.

Conclusion: dEPV and dUPV described the covariate effect size in the theoretical manner. Less than 0.0184 of dEPV or dUPV would indicate slight covariate effect size (inferential index < 1.25) on the covariate modeling. dEPV can be used for evaluating the covariate effect size in case of high η shrinkage.

References:

1. Lagishetty CV, Vajjah P, Duffull SB. A reduction in between subject variability is not mandatory for selecting a new covariate. J Pharmacokinet Pharmacodyn. 2012;39:383-92.
2. Hennig S, Karlsson MO. Concordance between criteria for covariate model building. J Pharmacokinet Pharmacodyn. 2014;41:109-25.
3. Beal SL, Sheiner LB, Boeckmann AJ 1989-2006. NONMEM users guide. Icon Development Solutions, Ellicott City, MD.
4. Lindbom L, Pihlgren P, Jonsson EN. PsN-Toolkit--a collection of computer intensive statistical methods for non-linear mixed effect modeling using NONMEM. Comput. Methods Programs Biomed. 2005;79:241-57.

251

A simulation study to evaluate treatment effect of tamoxifen by CYP2D6 genotypes compared with AIs

Mr Kwan Cheol Pak[1,2], Miss Ara Koh[1,2], MD, PhD Kyun-Seop Bae[1,2], MD, PhD Hyeong-Seok Lim[1,2]
[1]Asan Medical Center, Seoul, South Korea, [2]University of Ulsan College of Medicine, Seoul, South Korea

Aims: Tamoxifen is a prodrug, and active metabolites including endoxifen are known to exert its therapeutic effect of tamoxifen. Tamoxifen is converted to endoxifen mainly by CYP2D6 enzymes. The CYP2D6 enzyme activity is known to be associated with *CYP2D6* genotypes. Although the role of *CYP2D6* genotyping in the prediction of patient outcomes of tamoxifen therapy remains to be controversial, some studies reported the association between *CYP2D6* genotypes and therapeutic effect of tamoxifen in patients with breast cancer. 3rd generation aromatase inhibitors (AI) such as letrozole and anastrozole has been replacing tamoxifen since mid-2000s because some studies had showed superior results of AI over tamoxifen (disease-free survival (DFS) $HR_{AI/TAM}$=0.86 in ATAC trial, $HR_{AI/TAM}$=0.81 in BIG 1-98 trial). However, studies showing therapeutic superiority of AI over tamoxifen, such as ATAC and BIG 1-98 trial, did not take loss of heterozygosity (LOH) into account, which occurs when genotyping using tumor tissue. Therefore, the objective of this study was to evaluate treatment effect of tamoxifen by *CYP2D6* genotypes considering to LOH in comparison with aromatase inhibitors.

Methods: Using the reported result of ATAC and BIG1-98 trials ($HR_{AI/TAM}$=0.86, 0.81 for DFS), $HR_{PM,IM/EM}$ calculated from the meta-analysis, and the *CYP2D6* genotype frequencies in Caucasian populations, which were intended to represent the all the possible scenarios of *CYP2D6* genotype frequencies in the subjects enrolled in ATAC and BIG1-98 trials, hazard ratio between AI and tamoxifen in patients with *CYP2D6* genotypes associated with EM ($HR_{AI/TAM\ EM}$), and that in patients with *CYP2D6* genotypes associated with IM or PM ($HR_{AI/TAM\ IM/PM}$) were estimated separately in each replicate of the simulation. From the simulation study conducted using NONMEM (version 7.3) and R (version 3.12), median and 95% prediction interval (PI) of $HR_{AI/TAM\ EM}$ and $HR_{AI/TAM\ IM/PM}$ were estimated and compared between *CYP2D6* genotypes.

Results: The median $HR_{AI/TAM\ IM/PM}$ (95% PI) was 0.43 (0.23-0.79) in the simulation for ATAC trial and was 0.40 (0.22-0.73) for BIG 1-98 trial. However, the median $HR_{AI/TAM\ EM}$ (95% PI) was 0.97 (0.84-1.11) in the simulation for ATAC trial and was 0.91 (0.77-1.08) for BIG 1-98 trial. These results suggest that the treatment effect of tamoxifen for postoperative breast cancer patients carrying *CYP2D6* genotypes representing extensive metabolizer (EM) is comparable to letrozole or anastrozole (Table1).

Table 8. Predicted Hazard ratio of aromatase inhibitor versus tamoxifen by *CYP2D6* genotypes from the simulation studies based median estimated *CYP2D6* genotype frequencies

Arimidex, Tamoxifen, Alone or in Combination (ATAC) trial					
Study Population	Genotype Frequency	Hazard Ratio			
		Anastrozole versus Tamoxifen (EM)		Anastrozole versus Tamoxifen (IM, PM)	
Anastrozole: 3,094,	0.86 versus 0.14	Median	95% PI	Median	95% PI
Tamoxifen: 3,092		0.97	0.84–1.11	0.43	0.23–0.79
The Breast International Group (BIG) 1-98 study					
Study Population	Genotype Frequency	Hazard Ratio			
		Letrozole versus Tamoxifen (EM)		Letrozole versus Tamoxifen (IM, PM)	
Letrozole: 4,003	0.86 versus 0.14	Median	95% PI	Median	95% PI
Tamoxifen: 4,007		0.91	0.77–1.08	0.40	0.22–0.73

Conclusion: In this simulation study, the treatment effect of tamoxifen in patients with *CYP2D6* genotypes representing EM was comparable to the 3rd generation AI of letrozole and anastrozole. Based on these results, tamoxifen could be a good therapeutic alternative to patients experiencing severe side effects from the 3rd generation AI.

252

Mechanism-based modelling to assess suppression of bacterial resistance by high intensity, short duration tobramycin exposure

Miss Vanessa Rees[1], Ass Porf Jürgen Bulitta[2], Dr Antonio Oliver[3], Prof Dr Fritz Sörgel[4,5], Ass Prof Brian Tsuji[6], Dr Craig Rayner[1,7], Prof Roger Nation[1], Dr Cornelia Landersdorfer[1,6]

[1]Monash University, Melbourne, Australia, [2]University of Florida, Orlando, USA, [3]Hospital University Son Espases, Palma de Mallorca, Spain, [4]IBMP, Nürnberg-Heroldsberg, Germany, [5]University of Duisburg-Essen, Essen, Germany, [6]SUNY Buffalo, Buffalo, USA, [7]d3 Medicine LLC, Parsippany, USA

Aims: Infections involving hypermutable *Pseudomonas aeruginosa* (Pa) are highly problematic due to their enhanced resistance emergence. For aminoglycosides such as tobramycin (TOB), the area under the unbound concentration-time curve divided by the MIC (*f*AUC/MIC) is used to predict bacterial killing and clinical success. We hypothesized that delivering the same *f*AUC over short vs. long durations of exposure would provide better killing and minimize TOB resistance in both hypermutable and non-hypermutable Pa. To test this hypothesis, we aimed to quantitatively characterise bacterial killing and emergence of resistance of Pa for different concentration-time profiles with the same overall TOB exposure using *in vitro* time-kill experiments and mechanism-based modelling (MBM).

Methods: *P. aeruginosa* PAO1 (wild-type) and PAOΔ*mutS* (hypermutable) were studied in 24 h *in vitro* static concentration time-kill experiments with TOB (MIC=0.5 mg/L for both strains). This was carried out at *f*AUC/MIC of 36, 72 and 168 with initial inocula of 10^4 and 10^6 colony forming units (cfu)/mL, in duplicate. Antibiotic concentrations were calculated by the exposure durations and targeted *f*AUC/MIC. TOB was added at 0 h and removed at 1, 4, 10 or 24 h *via* multiple centrifugation and re-suspension of bacteria in antibiotic-free broth. The time-courses of bacterial killing and resistance were determined through viable counts of the total and resistant populations and then characterized by novel MBM (80 profiles). The importance sampling algorithm (S-ADAPT pmethod=4) was used in parallelised S-ADAPT (version 1.57), facilitated by SADAPT-TRAN. The model included 3 bacterial populations to represent the different susceptibilities (TOB susceptible, TOB intermediate and TOB resistant). The bacterial killing by TOB was described by direct killing functions with a post antibiotic effect (PAE). The emergence of TOB resistance was included in the model as amplification of pre-existing resistant mutants and adaptive resistance.

Results: For both PAO1 and PAOΔ*mutS* at the same *f*AUC/MIC more rapid and extensive killing was observed with high concentrations over 1 and 4 h durations of exposure (4 to 6 $\log_{10}$) compared to 10 and 24 h exposures (<4 $\log_{10}$). Regrowth at the 24 h time point was extensive (up to 9 $\log_{10}$) after 1 and 4 h duration of exposures, but bacteria which regrew remained TOB susceptible with unchanged mutation frequencies compared to the untreated control. While there was less pronounced regrowth (0 to 6 $\log_{10}$) for the 24 and 10 h exposure durations, susceptible bacteria had been completely replaced by TOB resistant bacteria at 24 h for the 10^6 cfu/mL inoculum. The hypermutable PAOΔ*mutS* revealed higher MF at 0 and 24 h in comparison to PAO1. The killing rate constant (K_{max}) was estimated to be over 3 times higher for the susceptible compared to resistant populations, with the KC_{50} being over 28 times higher in the resistant populations. Incorporation of functions for both pre-existing and adaptive resistance in the model was required. The MBM well described the time-courses of the total and resistant bacterial populations simultaneously (r=0.97).

Conclusion: The concentration-time profile shape was important to prevent resistance emergence. Short durations of TOB exposure yielded extensive killing with resistance prevention, whereas emergence of resistance was substantial for 24 and 10 h durations. Therefore, high intensity, short durations of TOB exposure are highly promising for use in innovative combination dosage regimens where the second antibiotic would combat the TOB-susceptible regrowth. MBM allowed us to quantitatively characterise the time-course of TOB resistance emergence. Simulations using this model will aid the optimisation of future combination dosage regimens that allow resistance prevention.

253

Warfarin maintenance dose prediction models do not work for patients who would benefit the most

Mr Shamin Saffian[1], Professor Stephen Duffull[1], Dr Daniel Wright[1]

[1]*Otago Pharmacometrics Group, School Of Pharmacy, University of Otago, Dunedin Central, New Zealand*

Background: The warfarin maintenance dose required to achieve therapeutic anticoagulation is known to differ by upwards of 15 fold between patients [1]. A large number of dose prediction tools have been developed to aid dosing in the clinic. Arguably, these tools are of most value for those patients who differ significantly from the average population in terms of their dose requirements. A recent *post-hoc* analysis by our group suggested that some published warfarin dosing tools may under-predict the maintenance dose for patients who require the upper quartile of dose requirements (≥7 mg/day), the upper quartile of warfarin doses [2].

Aim: We conducted a meta-analysis to determine if warfarin dosing tools produce unbiased dose predictions in patients who require ≥7mg/day.

Methods: We searched MEDLINE and EMBASE for studies that evaluated the predictive performance of warfarin dosing tools. We included studies that; 1) provided a scatterplot of the observed versus predicted maintenance doses and 2) the scatterplot included observed doses from a validation (external) dataset. We excluded scatterplots that had; 1) insufficient resolution to count the data points, and, 2) less than 5 patients requiring doses ≥7mg/day. We counted the data points for patients requiring ≥7mg/day and quantified the proportion of over- and under-predicted doses. A null proportion of 0.5 was used, assuming that there is an equal probability of the predicted dose lying on either side of the line of identity when no bias is present. A meta-analysis was conducted on the pooled proportion of over- or under-predicted doses across algorithms using MedCalc v15.10 (MedCalc Software, Ostend, Belgium).

Results: We identified 32 studies that met the inclusion criteria, representing 21 different dosing tools. Nine algorithms were evaluated in multiple publications these were treated as a repeated measures in a 3rd stage of the hierarchical meta-analytical model. Overall, 42 scatterplots were included in the meta-analysis. The meta-analysis included data from 1082 patients who required ≥7mg/day. We found that there was a significant proportion of under-predicted doses produced by the dosing tools (Proportion 0.93, 95% CI 0.90 to 0.95, random effects model).

Conclusion: Published warfarin dosing algorithms cannot be relied upon to accurately predict maintenance doses in those patients who require doses in the upper quartile of the dose requirements. At therapy initiation, dose requirements are not known, so the use a warfarin dosing tool to predict the maintenance doses for these patients may result in under–prediction. This will put the patients at risk of thromboembolism in the absence of parenteral anticoagulant cover and result in a protracted period of under-anticoagulation.

References:

1. Klein T et al. Estimation of the warfarin dose with clinical and pharmacogenetic data. N Engl J Med 2009; 360(8): 753-64.
2. Saffian SM et al. Methods for Predicting Warfarin Dose Requirements. Ther Drug Monit 2015; 37(4): 531-8.

254

Influence of body composition on disposition of highly fat distributed compound analyzed by PBPK modeling

Mr. Akihiko Goto[1], Dr. Yoshihiko Tagawa[1], Dr. Yuu Moriya[1], Dr. Sho Sato[1], Mr. Yoshiyuki Furukawa[2], Dr. Takeshi Wakabayashi[3], Dr. Tetsuya Tsukamoto[3], Dr. Joost DeJongh[4], Dr. Tamara van Steeg[4], Dr. Toshiya Moriwaki[1], Dr. Satoru Asahi[1]

[1]Drug Metabolism and Pharmacokinetics Research Laboratories, Takeda Pharmaceutical Company, Fujisawa, Japan, [2]Drug Safety Research Laboratories, Takeda Pharmaceutical Company, Fujisawa, Japan, [3]Central Nervous System Drug Discovery Unit, Takeda Pharmaceutical Company, Fujisawa, Japan, [4]Leiden Advanced Pharmacokinetics & Pharmacodynamics (LAP&P) Consultants, Leiden, The Netherlands

Aims: TAK-357 is an extremely lipophilic compund and has shown high distribution into fat tissues in animals. In a dog toxicokinetic study, an increase of the plasma TAK-357 concentration was observed over 2-weeks after termination of a 2-week repeated dosing in one dog. This dog also showed an acute and severe body weight loss. The present study investigates the cause of the unusual PK. Additionaly, the possible influence of body composition on the disposition of TAK-357 was investigated.

Methods: Physiologically-based PK (PBPK) modeling and simulation was applied on single and multiple dose rats and dogs PK data of TAK-357. The basic PBPK model enabled evaluation of the relationship between PK and bodyweight and was developed using the PK data in obese Wistar fatty rats and Wistar lean rats having approximately 45% and 13% body fat, respectively.

Results: A relevant PBPK model structure was constructed and the drug-specific parameter values were estimated on the basis of comprehensive PK data. PBPK model-derived simulation suggested that redistribution from adipose tissues to plasma due to loss of body fat caused the observed concentration increase of TAK-357 in dog plasma. The expected effects of an elevated fat mass in Wistar fatty rats on plasma concentrations appeared to be partly compensated for by other physiological differences between the two rat strains. A decrease in tissue to blood partition coefficients under obese conditions was identified as a factor contributing to the overall difference in PK. A higher lipid content of plasma in obese animals may result in relatively lower tissue to blood partition coefficients. PBPK-based simulations after a repeated dosage scenario indicate that plasma concentrations of lipophilic compounds under obese condition can differ up-to two-times at steady-state. This confirms that only a small impact of body composition change on the PK of highly lipophilic drugs.

Conclusion: The analysis demonstrates that the disposition of a highly lipophilic and fat-distributed compound is affected by acute changes in adipose tissue mass. However, the need for therapeutic dose adjustments may be limited at the steady state during repeated dosing, if the physiological (e.g. blood flow rate) and/or pharmacokinetic factors (e.g. metabolic activity) other than body composition were comparable.

255

Effect of developmental growth and FcRn expression on the pharmacokinetics of monoclonal antibodies in mice

Wararat Limothai[1], Prof Bernd Meibohm[1]

[1]*University Of Tennessee Health Science Center, Memphis, United States*

Aims: To determine the effect of developmental growth and FcRn expression on the pharmacokinetics of monoclonal antibodies in mice.

Methods: Total protein was extracted from various organs (skin, liver, kidneys, lungs, spleen) of C57BL/6J mice with postnatal age 2, 10, 21, 42, and 70 days. The levels of FcRn expression were subsequently examined by Western blot analysis with quantification relative to GAPDH expression. Average relative expression of FcRn in each organ was compared among each age group by analysis of variance with Bonferoni correction. The pharmacokinetics of a fully human investigational monoclonal antibody (mAb) with no cross-reactivity to murine ligands were characterized after a subcutaneous injection of 50 mg/kg in different age groups (2, 10, 21, 42, and 70 days old) of C57BL/6J mice. The plasma concentration-time profile of the mAb was monitored at six time points over 3 weeks. At least three mice were sacrificed at each blood collection time point. mAb concentrations in plasma were quantified by a validated ELISA assay and analyzed by non-compartmental pharmacokinetic analysis. A nonlinear mixed effects modeling approach using NONMEM was applied to characterize the disposition of the mAb and identify potential covariates. To delineate the effects of FcRn expression on the pharmacokinetics of the mAb in different age groups of C57BL/6J mice, the effect of body size was first evaluated by an allometric scaling approach. Due to the large relative changes of body weight throughout the sampling period, a growth model based on published growth curves was integrated into the structural model to account for the incremental changes in mouse body weight during development. Thereafter, the effect of age and FcRn expression in each organ were evaluated. The precision and stability of the final model estimates were evaluated by nonparametric bootstrap analysis, and the ability of the final population pharmacokinetic model to adequately describe the observed data was determined by visual predictive check.

Results: The relative quantification of FcRn expression in 2, 10, 21, 42, and 70 day old C57BL/6J mice showed no difference across all age groups in skin and spleen. However, the relative FcRn protein expression exhibited organ-specific ontogenic patterns in liver, lungs, and kidneys. Two-fold increases in FcRn expression were observed in liver and lungs of 10 day old mice, whereas FcRn expression in kidneys showed two-fold increases in 10 and 42 day old mice. This ontogeny of FcRn expression, however, was not correlated with the AUC or half-life of the mAb. The negligible influence of the ontogeny of FcRn expression on the pharmacokinetics of the mAb in various age groups of mice was confirmed by the nonlinear mixed effects modeling. The analysis revealed that after the effect of body weight was adjusted by allometric scaling, only age and FcRn expression in skin were the additional factors that influenced the pharmacokinetics of the mAb in the different age groups of mice. Volume of distribution was negatively correlated with age, which is likely a reflection of the age-associated decrease in relative tissue water content in juvenile animals. Between-animal variability in clearance could be partially explained by a negative correlation with the expression of FcRn in skin, one of the putative major elimination organs for immunoglobulin G molecules, even though FcRn expression in skin did not show any ontogeny.

Conclusion: Similar expression levels of FcRn from birth through day 70 were observed in skin and spleen of C57BL/6J mice, whereas age-associated expression was observed in liver, lungs, and kidneys. However, the ontogeny of FcRn expression in either of these organs did not affect the disposition of the studied mAb. The nonlinear mixed effects modeling revealed three factors that influence the pharmacokinetics of the mAb in mice: body weight, age, and FcRn expression in skin. Among these factors, at least body weight as the most prominent factor should be taken into consideration during dosage regimen design for monoclonal antibodies in pediatric patients.

256

Amikacin pharmacokinetics in pediatric patients with burn injuries compared to those with oncology conditions

Di Xiaoxi Liu[1], Dr Anne Smits[2,3], Dr Tian Yu[1], Dr Stephanie Wead[4], Dr Alice Neely[5], Dr Richard Kagan[5,6], Dr Daniel Healy[5,7], Dr Karel Allegaert[8,9], Dr Catherine Sherwin[1]

[1]Depart of Pediatrics, University Of Utah School of Medicine, Salt Lake City, United States, [2]Neonatal Intensive Care Unit, University Hospitals , Leuven, Belgium, [3]Depart of Pediatrics, University Hospital , Leuven, Belgium, [4]Wayne Healthcare, Greenville, United States, [5]The Shriners Hospitals for Children®, Cincinnati, United States, [6]Depart of Surgery, University of Cincinnati College of Medicine, Cincinnati, United States, [7]James L. Winkle College of Pharmacy, University of Cincinnati, Cincinnati, United States, [8]Intensive Care and Department of Surgery, Erasmus MC-Sophia Children's Hospital, Rotterdam, The Netherlands, [9]Depart of Development and Regeneration, KU Leuven, Leuven, Belgium

Aims: Physiologic changes due to disease status can lead to highly variable pharmacokinetics (PK) of amikacin in children. Therefore, considerations should be given when determining optimal amikacin dose for patients with specific diseases. Improved understanding of factors influencing PK can allow for the optimizing of dosage regimens to reduce adverse effects. The aim of the study was to undertake a comparative pharmacometric analysis of amikacin use in pediatric patients with burn injuries verses those with oncology conditions.

Methods: Population PK modeling was performed in NONMEM® version 7.3 (ICON Development Solutions, Ellicott City, MD, USA) for pediatric patients < 18 years of age with burn injuries (group 1) and with oncology conditions (group 2) who received > 1 dose of amikacin for the empirical treatment of gram-negative bacterial infections between Jan 2007 to Dec 2009 and Jan 2006 to Dec 2011, respectively. The covariates examined included sex, body weight (WT), age (AGE), height, serum creatinine (SCR), C-reactive protein, and serum albumin levels. Both studies used the enzymatic method to measure SCR. The Schwartz equation was used to calculate creatinine clearance for both groups. The available shared covariates between the two subpopulations were separately checked in individual models. A binary covariate TYPE was created to denote the two different patient groups (burn 0, oncology 1). Patients with burn injuries received amikacin at 10-20 mg/kg/day as part of early empiric treatment of presumed burn-related sepsis. Pediatric oncology patients received 20 mg/kg of amikacin intravenously for treatment of febrile neutropenia. Patients were treated once daily and concentrations were collected immediately before and 1 hour after the second dose. A population PK model was developed to describe the observed amikacin concentration over time in both subpopulations.

Results: Data from pediatric patients (0.83 – 15 years) with burn injuries (n=72) and pediatric patients (0.8 – 16.4 years) with oncology conditions (n=111) were pooled for model development. The characteristics between the two groups was very similar with no statistical differences. In the burn injury group and the oncology group, SCR had a median (range) of 0.4 (0.2 – 1) and 0.32 (0.15 – 0.68) mg/dL, respectively. In addition the median of creatinine clearance (CRCL) was 170.5 and 195.4 mL/min/1.73m2, respectively. However, the overall range was lower in the burn injury patient group, 81.1 – 327.5 mL/min/1.73m2. The data were best described by a two-compartmental PK model with a proportional error model. Stepwise covariate search (forward addition $p<0.05$, backward elimination $p<0.01$) returned WT, subpopulation type (TYPE), AGE and CRCL as significant covariates. Allometric scaling was initially tested during model development but was abandoned after systematic covariate analysis. The final population PK covariate model is outlined in Table 1.

Table. 1 Summary of PK parameters

	Parameters	Descriptions	Base Model		Final Model	
			Estimates	95% CI	Estimates	95% CI
	CL (L/h)	Clearance	2.79	2.47 - 3.11	2.36	2.04 - 2.68
	V1 (L)	Central volume of distribution	1.73	1.26 - 2.2	5.62	4.46 - 6.78
	Q (L/h)	Distribution CL	1.3	1.05 - 1.55	0.93	0.624 - 1.24
	V2 (L)	Peripheral volume of distribution	9.07	7.32 - 10.8	5.54	3.40 - 7.68
α	CL-WT	Weight influence on CL	-	-	0.201	0.087 - 0.315
	V1-WT	Weight influence on V1	-	-	0.146	0.029 - 0.263
	CL-AGE	Age influence on CL	-	-	0.269	0.098 - 0.44
	V1-AGE	Age influence on V1	-	-	0.313	0.07 - 0.556
	V2-AGE	Age influence on V2	-	-	0.579	0.363 - 0.795
	CL-CRCL	Creatinine clearance on CL	-	-	0.245	0.117 - 0.373
	V2-CRCL	Creatinine clearance on V2	-	-	0.548	0.213 - 0.883
β	CL-TYPE (L/h)	Subpopulation influence on CL	-	-	0.648	0.401 - 0.895
	V1-TYPE (L)	Subpopulation influence on V1	-	-	0.42	0.261 - 0.579
	ω^2CL	Variance of CL BSV	0.154	0.116 - 0.192	0.051	0.036 - 0.066
	ω^2V1	Variance of V1 BSV	-	-	0.055	0.018 - 0.092
	ω^2Q	Variance of Q BSV	0.0956	0.007 - 0.185	-	-
	σ^2	Variance of proportional residual error	0.0972	0.074 - 0.120	0.053	0.035 - 0.071

Conclusion: The results of the current study suggest that besides patient-specific characteristics (current WT, AGE and CRCL) also disease-related characteristics should be considered when dosing amikacin in critically ill pediatric patients, in order to optimize therapeutic concentration targeting.

257

Predicting the pharmacokinetic changes in fluoxetine during pregnancy

Dr Manoranjenni Chetty[1], Dr Felix Stader[1], Dr Krishna Machavaram[1], Dr Masoud Jamei[1], Prof Amin Rostami-Hodjegan[1,2]

[1]Simcyp (a Certara company), Sheffield, United Kingdom , [2]Manchester Pharmacy School, Manchester University, Manchester, United Kingdom

Aims: The aim of this project was to construct a PBPK model to predict the changes in fluoxetine pharmacokinetics (PK) associated with the changes in the body composition, physiology and biochemistry that occur during pregnancy. Mood changes during pregnancy may necessitate the use of drugs such as fluoxetine, although little is known about the appropriate doses. One clinical study on 11 mothers showed that plasma concentrations of fluoxetine were on average 35% lower during the third trimester of pregnancy, following a daily dose of 20 mg or 40 mg of the drug.[1] Models to predict such changes will be useful since ethical constraints prevent adequate clinical testing.

Methods: The pregnancy model available in the Simcyp population-based simulator (V15) was used in this study. The model incorporates anatomical, physiological and metabolic changes associated with gestational age[2]. Metabolic changes include an increased activity of of CYP3A4 and CYP2D6 but reduced activity of CYP1A2. The fluoxetine model included first order absorption, distribution characterised by a full PBPK model and elimination based on enzyme kinetics. CYP2D6 has a major role in the elimination of this drug, with minor contributions from CYP3A4, CYP3A5, CYP2C9, CYP2C19, CYP1A2 and CYP2B6. In addition, fluoxetine is a competitive inhibitor of CYP2D6. The PK concentration-time profiles and parameters were simulated in 10 trials of 10 females following administration of a 40mg dose of fluoxetine for 5 days in the third trimester of pregnancy as well as in the nonpregnant healthy volunteer. The concentration-time profile, maximum plasma concentrations (Cmax) and area under the curve (AUC_{0-24}) for the last dose were compared in the two groups.

Results: The concentration-time profile for fluoxetine in the third trimester of pregnancy (dashed line) and in non pregnant females (solid line) are presented in figure 1. The mean Cmax and AUC in pregnancy were 75% and 76% of those in nonpregnant women. These values are marginally higher than the 65% reported in the clinical study.

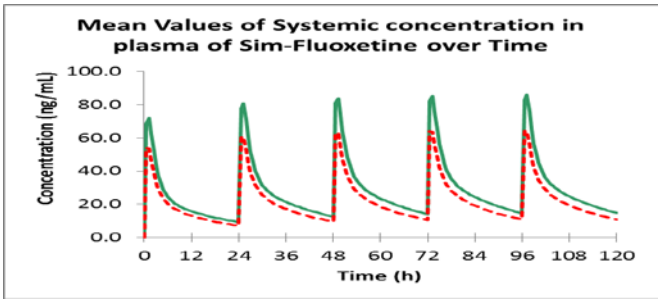

Figure 1

Conclusion: The predictions of PK changes of fluoxetine during pregnancy using the PBPK model were acceptable. Further refinement of the model to include the active metabolite would be an advantage. In general, PBPK modelling may be a useful tool in predicting PK changes of drugs resulting from differences in body composition, physiology and metabolism.

References:

1. Heikkinen T. et al. Pharmacokinetics of fluoxetine and norfluoxetine in pregnancy and lactation. Clin Pharmacol Ther 2003;73:330-337.
2. Abuljalil K. et al. Anatomical, Physiological and Metabolic Changes with Gestational Age during Normal Pregnancy. Clin Pharmacokinet 2012; 51:365-396.

258

A PBPK/PD model to describe the impact of CYP2C19 polymorphisms on the response to clopidogrel

Dr Manoranjenni Chetty[1], Dr Khaled Abduljalil[1], Dr Maurice Dickins[1], Dr Masoud Jamei[1], Prof Amin Rostami-Hodjegan[1,2]

[1]Simcyp (a Certara company), Sheffield, United Kingdom , [2]Manchester Pharmacy School, Manchester University, Manchester, United Kingdom

Aims: The aim of this study was to develop a PBPK/PD model to simulate the impact of CYP2C19 polymorphisms on the pharmacokinetics (PK) and pharmacodynamics (PD) of clopidogrel. CYP2C19 is a key enzyme that converts the prodrug clopidogrel to its active metabolite (Clopi-H4), while esterases hydrolyse clopidogrel to an inactive carboxylic acid metabolite. Significant differences in PK and response to clopidogrel have been observed in patient groups with differing CYP2C19 activity. The development of a reliable PBPK/PD model will be useful to explore the impact of various scenarios that may influence CYP2C19 activity and clopidogrel response, such as different population groups, comedications and disease states.

Methods: The Simcyp simulator (V15) was used to construct a previously described PBPK model[1] with clopidogrel and its primary (intermediate) and secondary (active) metabolites. A first order absorption model was used for the absorption of clopidogrel, which was converted to its intermediate metabolite (2-oxo-clopidogrel) by CYP2C19 as well as a minor contribution from CYP2B6 and CYP1A2. 2-oxo-clopidogrel was converted to Clopi-H4 by CYP2C19, with some contribution from CYP2C9, CYP3A4 and CYP2B6. Esterase enzymes converted clopidogrel to the inactive form. The model was verified by comparing simulations with clinical observations. Differences in PK profiles and PK parameters of clopidogrel and Clopi-H4 with extensive (EM), intermediate (IM) and poor (PM) metabolisers of CYP2C19 were simulated, using a clopidogrel loading dose of 300mg followed by 75mg QD for 5 days. The PBPK model was then linked to a PD model, with unbound plasma concentrations of clopi-H4 used as input. A modification of the indirect response turnover model[2,3], with maximum platelet aggregation (MPA%) as the response marker, was used with the custom lua scripting feature within Simcyp to model PD. Model predictions of the impact of CYP2C19 EMs, IMs and PMs on response were then compared with clinical observations.

Results: Comparison of the predicted concentration-time profiles of clopidogrel and clopi-H4 in EMs, IMs and PMs with clinical observations were well matched. In addition, predicted $AUC_{0\text{-}24}$ for the last dose was within 2-fold of the observed values, with the exception of AUC of clopidogrel in PMs and IMs, where the predicted:observed ratios were 2.5 and 3 respectively. The high inter-individual variability within these groups may account for this. The PBPK/PD model recovered the observed diffences in MPA% between EMs, IMs and PMs, and supported a dosage adjustment in PMs to achieve optimal therapeutic effect.

Conclusion: The PBPK/PD model for clopidogrel recovered the clinically observed differences in PK and response acceptably. This model will be useful to explore PK changes and potential dosage adjustments for clopidogrel when used in the presence of variables that may impact on CYP2C19 activity.

References:

1. Djebli N. et al. Physiologically Based Pharmacokinetic Modeling for Sequential Metabolism: Effect of CYP2C19 Genetic Polymorphism on Clopidogrel and Clopidogrel Active Metabolite Pharmacokinetics Computer-aided long-term anitcoagulation therapy. Drug Metab Dispos 2015; 43:510–522.
2. Dayneka N.I. et al. Comparison of four basic models of indirect pharmacodynamic responses. J. Pharmacokinet. Biopharm 1998; 21: 457–478.
3. Jiang X-L. et al. Development of a physiology-directed population pharmacokinetic and pharmacodynamic model for characterizing the impact of genetic and demographic factors on clopidogrel response in healthy adults. Eur J Pharm Sci 2016; 82: 64–78.

259

Nonlinear pharmacokinetic modeling of rheumatoid arthritis biologics after intravenous and subcutaneous administration in rats

Prof. In-hwan Baek[1]

[1]*College Of Pharmacy, Kyungsung University, Busan, South Korea*

Aims: Etanercept was approved as a biologic agent for the treatment of rheumatoid arthritis (RA) by the Food and Drug Administration (FDA) in 2010 (Enbrel 2004). Etanercept is a dimeric fusion protein, which consists of the extracellular ligand-binding protein of the human 75-kDa (p75) tumor necrosis factor (TNF) receptor linked to the Fc portion of human immunoglobulin G1 (IgG1. Etanercept competitively inhibits the interaction of TNF with cell-surface receptors, and thus, prevents TNF-mediated cellular responses and modulates the activity of other proinflammatory cytokines that are regulated by TNF. In this study, we investigated the pharmacokinetic properties of etanercept after intravenous and subcutaneous injection in rats. In addition, we explained the nonlinear elimination kinetics using Michaelis–Menten equations. The aim of study was to investigate the bioavailability of etanercept administered subcutaneously and to develop a pharmacokinetic model to explain the nonlinear elimination kinetics

Methods: Animal experiments were performed according to the institutional guidelines for the care and the use of laboratory animals, and the protocol was approved by the animal ethics committee of Kyungsung University. Ten SD rats were randomly divided into two groups. Rats in group A (n = 5) were administered etanercept 2 mg/kg (Enbrel®; Wyeth, Cambridge, MA, USA) intravenously by tail vein injection. Rats in group B (n = 5) were administered etanercept 2 mg/kg subcutaneously by injection into the scruff of the neck. Blood samples (300 µL) were collected from the retroorbital plexus of rats into microfuge tubes containing heparin as an anticoagulant at 1, 2, 4, 8, 12, 24, 48 (2 days), 96 (4 days), 144 (6 days), and 312 h (13 days) after administration. The blood samples were centrifuged at 10,000 rpm (13,416×*g*) for 2 min, and the plasma was collected and stored at 70°C until enzyme-linked immunosorbent assay (ELISA). The plasma concentration of etanercept was determined using horseradish peroxidase (HRP)-coupled goat anti-human IgG (gahIgG-HRP) with the HRP substrate kit. The absorbance values of the solutions in each well were recorded by using an ELISA plate reader at 405 nm. Non-compartmental pharmacokinetic analyses and compartment analyses were performed using the WinNonlin Standard Edition software and ADAPT program.

Results: The plasma concentration versus time profiles of etanercept after intravenous and subcutaneous administration in rats were fitted to a two-compartment model using Michaelis–Menten elimination kinetics (V_{max} and K_m; Fig. 1). Intravenous and subcutaneous administration of 2 mg/kg of etanercept to rats showed that etanercept was slowly absorbed (time to reach the peak drug concentration [T_{max}] = 1.60 days, bioavailability [F] = 47.18%) and slowly eliminated (half-life [$t_{1/2}$], 2.33 days after intravenous administration and 3.31 days after subcutaneous administration). The area under the curve values on day 13 (AUC_{13day}) were 121.25 ± 14.37 and 48.56 ± 6.78 µg·day/mL after intravenous and subcutaneous administration, respectively. A two-compartment model with Michaelis–Menten elimination kinetics (V_{max} = 94.28 µg/day; K_m = 10.88 µg/mL) was used to describe the pharmacokinetic profile of etanercept.

Figure 9

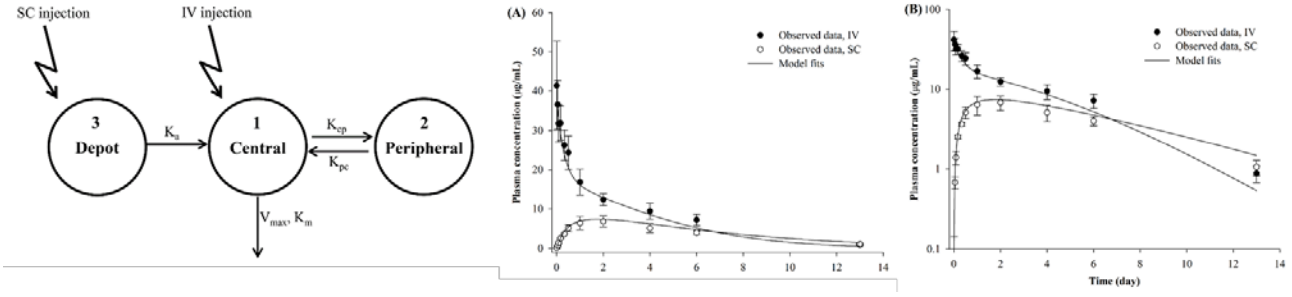

Conclusion: In this study, we investigated the pharmacokinetics of etanercept was after intravenous and subcutaneous administration in rats. Etanercept was slowly and moderately well absorbed (T_{max} = 1.60 days, F = 47.18%) and slowly eliminated ($t_{1/2}$ = 2.33 and 3.31 days after intravenous and subcutaneous administration) in rats. The two-compartment model with Michaelis–Menten elimination kinetics described the pharmacokinetic profile after intravenous and subcutaneous administration of 2 mg/kg etanercept in rats. Michaelis–Menten kinetics was sufficient to explain the nonlinear elimination process of etanercept. This study provides a detailed pharmacokinetic profile of etanercept, and our results could be used for the development of etanercept biosimilars.

260

Model-based meta-analysis on the efficacy of pharmacological treatments for idiopathic pulmonary fibrosis

Ms Phyllis Chan[1], Mr Leon Bax[2], Mr Chunlin Chen[1], Ms. Nancy Zhang[2], Mr Shu-Pang Huang[1], Ms Holly Soares[1], Mr Glenn Rosen[1], Mr Malaz AbuTarif[1]

[1]Bristol-Myers Squibb, Lawrenceville, United States, [2]Quantitative Solutions, Menlo Park, United States

Aims: Recently the FDA approved the first two drugs (pirfenidone and nintedanib) indicated for the treatment of idiopathic pulmonary fibrosis (IPF), a therapeutic area that has highly variable placebo effects across clinical trials but more consistent treatment effects within trials[1]. The purpose of this analysis was to leverage publically available data to understand and quantify comparative efficacy in order to support future trial designs and decision making as part of model-informed drug development in IPF.

Methods: An augmented database with efficacy and safety endpoints was developed using published data from PubMed literature, FDA summaries, and clinicaltrials.gov reports that includes 40 citations from 32 trials. A model-based meta-analysis (MBMA) with a longitudinal profile of placebo-corrected change from baseline (mean difference) of percent predicted forced vital capacity (%predicted FVC) was characterized by a regression model using maximum likelihood estimation as implemented in R. Multiple levels of heterogeneity were described as mixed-effect variability terms. Covariates of population characteristics were imputed for trial arms with missing values, and standard deviations were modeled and predicted. Treatment effects, time courses, and potential dose-response relationships were estimated, and covariate effects on treatment effects were investigated.

Results: The analysis dataset is composed of %predicted FVC summary-level data of 5090 subjects from 45 arms in 20 trials, 17 of which were double blinded and placebo controlled. The trial durations ranged from 8 to 470 weeks. A non-parametric placebo model was used to fit the longitudinal %predicted FVC data. Treatment effects were estimated for all 14 active treatments in the analysis dataset, and the dose-response of pirfenidone was characterized using a step-function (low vs. high dose). The final model includes a time course of the drug effect that is described by an increasing form of the exponential decay function: 1-exp(-lambda*time), where lambda determines the steepness of the curve. Covariates investigated for their potential to influence treatment effects included baseline %predicted FVC, disease duration, age, gender, race, and smoking status. The covariate distribution ranges were narrow, and ultimately baseline %predicted FVC was the only covariate included in the final model. Model diagnostic plots showed that the model predictions adequately fit the observed data. Pirfenidone and nintedanib were the only drugs identified to have significant estimated positive treatment effects, with 95% confidence intervals not overlapping zero. Model simulations were performed to further evaluate the treatment and covariate effects on longitudinal change from baseline %predicted FVC.

Conclusion: A mixed-effect model was developed using publically available data to describe the treatment and covariate effects on longitudinal profiles of change from baseline %predicted FVC. The results from this MBMA approach allow quantification of treatment profiles and estimation of relative efficacy between treatments that have not been directly evaluated in the same trial, which is essential for drug development in a therapeutic area such as IPF. Additionally, clinical trial simulations using the final model developed from the MBMA will be used to inform future trial designs.

References:

1. FDA Clinical Pharmacology and Biopharmaceutics Review(s) for Pirfenidone, 2014.

261

Population pharmacokinetics of RedituxTM, a biosimilar Rituximab, in Diffuse Large B Cell Lymphoma

Dr Vikram Gota[1], Dr. Ashwin Karanam[1], Dr. Prashant Tembhare[2], Dr. PG Subramanian[2], Dr. Hari Menon[3]
[1]Department of Clinical Pharmacology, ACTREC, Tata Memorial Centre, Navi Mumbai, India, [2]Department of Pathology, Tata Memorial Hoospital, Mumbai, India, [3]Department of Medical Oncology, Tata Memorial Hospital, Mumbai, India

Aims: Rituximab (MabThera™, Roche) is a chimeric IgG1 monoclonal antibody targeting the CD20 surface antigen on normal and neoplastic B-cells. It revolutionized the treatment of Diffused Large B-Cell Lymphoma (DLBCL) but its prohibitively high cost makes it inaccessible to majority of patients in developing countries. Reditux™ (Dr Reddy's Laboratories, India), a biosimilar was introduced in India in 2007 at nearly half the price of the innovator. A retrospective analysis from our centre showed no significant difference between Reditux™ and MabThera™ with respect to toxicity, response rates, progression free survival (PFS) and overall survival (OS) (1). However, there is dearth of data regarding the pharmacokinetics of Reditux™ and hence its equivalence to MabThera™ is uncertain.

Methods: Twenty one patients of DLBCL on rituximab regimen were enrolled for the study. Reditux™ was administered as a slow i.v. infusion at a dose of 375 mg/m^2 on day 1 of a 21-day cycle. PK sampling was performed at predose, post infusion, 24, 48 hours, 7 and 21 days. Rituximab levels were estimated by ELISA. Population pharmacokinetics was performed using NONMEM. Covariate effects were added to the model by forward addition followed by backward deletion using PsN toolkit on Pirana GUI. B-cell count on day 3 and day 21 was used as an efficacy measure. All patients were followed-up and OS was estimated using Kaplan-Meier analysis.

Results: An open two compartment linear pharmacokinetic model using ADVAN 3, TRANS 4 subroutines was used which could describe the observed concentrations adequately. The Vd of central compartment and clearance of Reditux™ were estimated at 0.95L and 5.98 mL/hr respectively. No covariate effects were seen. Diagnostic plots demonstrating goodness of fit is shown in figure 1. B-cell count was completely depleted by day 3 and remained so on day 21. OS at 36 months was found to be 84.6% which is comparable with Mabthera™.

Conclusion: PK profile of Reditux™ is comparable to that reported for MabThera™ (2). B-cell response and OS are also comparable, suggesting the biosimilar may be equivalent to MabThera™ in treating DLBCL.

References:

1. Roy PS, John S, Karankal S, et al. Comparison of the efficacy and safety of Rituximab (Mabthera) and its biosimilar (Reditux) in diffuse large B-cell lymphoma patients treated with chemo-immunotherapy: A retrospective analysis. Indian J Med Paediatr Oncol. 2013;34(4):292-298.
2. Blasco H, Chatelut E, de Bretagne IB, et al. Pharmacokinetics of rituximab associated with CHOP chemotherapy in B-cell non-Hodgkin lymphoma. Fundam Clin Pharmacol. 2009;23(5):601-8.

262

Pharmacokinetic study of Boswellic acids formulated as solid lipid Boswellia serrata particiles in healthy volunteers

Mrs Preeti Kulkarni[1], Dr. Neena Damle[2], Dr. Vikram Gota[3]

[1]Gahlot Institute Of Pharmacy, Navi Mumbai, India, [2]DY Patil University, School of Ayurveda, Navi Mumbai, India, [3]ACTREC, Tata Memorial Centre, Navi Mumbai, India

Aims: Osteoarthritis is one of the leading causes of disability and impaired quality of life among elderly people. NSAIDS and steroids are associated with intolerable side effects on long term use. There is a need to find out safe and effective alternative treatment for such inflammatory conditions. Extracts of Boswellia serrata (BSE), a herb used in traditional Indian medicine, has become very popular worldwide for its anti-inflammatory activity. Boswellic acids (BA) including 3-O-acetyl-11-keto-beta-boswellic acid (AKBA) and 11-Keto-Boswellic acid (KBA) are the major constituents of BSE with anti-inflammatory properties. A major limitation of BAs is their poor oral bioavailability limiting their use. BAs are steroidal (lipophilic) in nature and do not solubilize in the intestinal fluid. Complexing of phospholipids with standardized botanical extracts has provided dramatic enhancement of bioavailability and faster and improved absorption in the intestinal tract. In an effort to enhance bioavailability of BAs, a solid lipid particles of boswellia serrata extract (SLBSP) have been developed. The pharmacokinetic profile of these BAs following oral administration of 333mg of SLBSP to healthy human subjects is described here.

Methods: Each 333mg capsule of SLBSP is equivalent to 100mg of BSE containing 6.5 mg of KBA and 1.5 mg of AKBA. Baseline evaluation comprising of complete blood counts (CBC), Liver function test (LFT), renal function test (RFT), ECG and Urine analysis were done before administration of medicine. Eligible healthy volunteers were administered one SLPSP capsule orally and blood samples were collected at pre-dose, 0.5, 1, 1.5, 2, 2.5, 3, 4, 5, 6, 8 and 12 hrs after dosing. KBA and AKBS concentrations were measured using a validated LC-MS/MS method. Pharmacokinetics parameters were estimated by non-linear regression fitting of the data using Pheonix WinNonlin (Build 6.4.0.768) software for both KBA and AKBA.

Results: Ten healthy male volunteers completed the study. The median age of the subjects was 25.5 years (Range 23 - 32 Years). The median weight of the subjects was 65.8(53 – 76) kg. KBA was found to fit into one-compartment model, while AKBA was found to follow two-compartment pharmacokinetic model. Better fit was observed with use of lag time and weighting of 1/(Yhat*Yhat) for both. A representative model fit and residual plot is shown in the figure. For AKBA, t_{max} was observed at 1.5 hours and the C_{max} was 8.04±1.67 ng/mL. Absorption rate constant was 4.57±2.26 hr^{-1}(K01) with absorption half life of 0.54±0.17 ($t_{1/2}$ a), and the elimination rate constant was 0.28±0.09 (K10) with elimination half life 6.8±2.97 ($t_{1/2}$e). Volume of distribution was found to be 78.80±11.82 L (V1) and 530.93±173 L (V2). Clearance was found to be 26.25±7.86 L/hr/kg. For KBA, t_{max} was observed at 2.3 hours and the C_{max} was 29.83±4.41 ng/mL. Absorption rate constant was 2.42±0.93 hr^{-1}(K01) with absorption half life of 0.72±0.0.20 ($t_{1/2}$ a), and the elimination rate constant was 0.32±0.05 (K10) with elimination half life 2.45±0.31 ($t_{1/2}$e). Volume of distribution was found to be 164±21 L and clearance was found to be 50.2±7.28 L/hr/kg.

Conclusion: The SLBSP formulation of BSE showed improved oral bioabailability of KBA aand AKBA making it a potentially good candidate for further clinical evaluation and development.

263

Population pharmacokinetic analysis of Daclatasvir, Asunaprevir and Beclabuvir in HCV-infected non-Japanese and Japanese subjects

Mayu Osawa[1], Takayo Ueno[1], Tomomi Shiozaki[1], Hiroki Ishikawa[1], Li Hanbin[2], Phyllis Chan[3], Tushar Garimella[3], Frank LaCreta[3], Brenda Cirincione[3]

[1]Bristol-Myers Squibb K.K., Tokyo, Japan, [2]Quantitative Solutions,US, [3]Bristol-Myers Squibb, , US

Aims: The combination regimen of Daclatasvir (DCV), Asunaprevir (ASV) and Beclabuvir (BCV) is being developed for the treatment of HCV infection in Japan. The objectives of these analyses were to develop population pharmacokinetic (PPK) models for DCV, ASV and BCV to estimate the effects of demographic, pathophysiologic, and disease-related covariates for non-Japanese and Japanese HCV patients and to provide individual patient PK parameter estimates for subsequent exposure-response (E-R) analyses.

Methods: The PPK analysis for the components of the combination regimen was conducted in two phases. An original PPK model was developed using data from one Phase2 study and two Phase3 studies in non-Japanese HCV-infected subjects. The model was subsequently updated using data from a Phase 3 study in Japanese HCV-infected subjects. The impact of baseline covariates was evaluated using a univariate screening method, and significant covariates ($p < 0.05$) were incorporated into the full model. For covariates that were highly correlated, only one of the correlated covariates was included in the full model. The final model was derived by eliminating each covariate one by one until all covariates retained were significant ($p < 0.001$) by likelihood ratio test. The robustness and predictive performance of the final PPK model was evaluated through evaluation of key diagnostic plots and prediction-corrected visual predictive check (pcVPC), respectively. Bayesian post-hoc PK parameters of individual subjects were obtained from the PPK models for E-R assessment. All PPK models were developed with FOCE-I in NONMEM V7.2.0.

Results: DCV PK was described by a one-compartment model with linear elimination. The absorption of DCV was described by zero-order drug release followed by first-order absorption into the central compartment. Female had ~25% greater DCV exposures than male. The other statistically significant covariates had < 20% effect on DCV exposure relative to typical values. ASV PK was described by a two-compartmental model with linear elimination. The absorption of ASV was described with zero-order drug release followed by first-order absorption into the central compartment. A step-wise increase in clearance was used to describe ASV auto-induction. Cirrhosis, baseline and time-varying ALT were significant covariates on ASV CL/F. ASV exposure increased to 65.8% and 35.2% in subjects with cirrhosis and high baseline ALT (167 U/L) value, respectively. Asians (primarily Japanese: 292 of 303) had 59.4% greater ASV exposure than White subjects in the updated analysis. BCV PK was described by a one-compartment linear elimination model, with first-order absorption and a lag time. Step-wise factors on clearance and bioavailability were used to model BCV auto-induction. Asians (primarily Japanese: 217 of 228) had 44.3% greater BCV exposure than White subjects. The diagnostic plots and pcVPC indicated that all final models adequately described the PK profile of DCV, ASV and BCV in non-Japanese and Japanese subjects with HCV infection.

Conclusion: The effects of covariates on DCV PK were modest and not considered clinically significant. With the exception of Asian race on ASV and BCV PK, no other parameters for DCV, ASV and BCV PPK models were meaningfully impacted during the refinement with Phase 3 data from Japanese subjects. ASV CL/F decreased with cirrhosis and with increasing ALT value indicating an association between hepatic markers and ASV CL/F. The DCV and ASV results here were comparable to those results from the previous DCV and ASV PPK analyses[1,2,3].

References:

1. Li et el.,5th ACoP; October 12-15, 2014; Las Vegas, Nevada, USA. Poster T-001.
2. Chan et el.,5th ACoP; October 12-15, 2014; Las Vegas, Nevada, USA. Poster T-002.
3. Osawa et al., PAGE, June 2-5, 2015, Hersonissos, Crete, Greece. Poster IV-19.

264

Application of QSP model to evaluate xCT inhibition as target for central nervous system diseases

Dr Mike Reed[1], Dr Christina Friedrich[1], CM Witt[1], MM Pryor[1], T Rooney[2], A Genevois-Borella[2], MC Obinu[2], A Guerreiro[2], J Konop[2], Z Bocskei[2]

[1]Rosa & Co., San Carlos, United States, [2]Sanofi Research and Development, Chilly-Mazarin, France

Aims: Neuronal excitotoxicity, often mediated by glutamate, has been implicated as a factor in a number of central nervous system (CNS) diseases. In order to improve the understanding of the role of the cysteine-glutamate transporter (xCT) in excitotoxicity and CNS diseases and the potential utility of xCT inhibitors, Sanofi and Rosa collaborated in the development of a CNS PhysioPD™ Research Platform, a QSP model that supported hypothesis generation and testing. The objectives of the project were to evaluate the degree of xCT inhibition required to reduce CNS glutamate levels below neurotoxic levels and retain normal microglial phagocytic function, and to provide guidance on the CNS indications most likely to respond to this mechanism of action.

Methods: The ordinary differential equations based Platform represented 1./ cell dynamics of microglia activation, neuronal stress and death 2./ synthesis/expression and metabolism of mediators and surface markers 3./ xCT function (amino acid transport) and dysfunction processes associated with multiple sclerosis (MS) and Alzheimer's disease and 4./ GSH metabolism in healthy white and gray matter) 5./ effects of treatment by xCT inhibitors.

Results: The developed Virtual Patients represent an initial extrapolation step toward in vivo representation to gain initial insights on the chances of maintaining healthy microglial function and reducing neurotoxicity by altering glutamate and cystine concentrations via inhibition of the xCT antiporter. Results from simulated xCT inhibition in the Platform supported the prioritization of MS as the lead therapeutic indication. Additionally, simulation research and insights led to focused recommendations for in vitro experiments to resolve material uncertainties in the understanding of xCT function and xCT inhibition and to reduce risk in the development program.

Conclusion: The Platform is a useful illustration of the key role that QSP modeling can play in providing quantitative integration of internal and external knowledge, mechanistic insight and support decisions already in early stage drug discovery.

265

The application of continous-time Markov exposure-response model to sIGA – the case study of nemolizumab

Dr Tomohisa Saito[1], Dr Satofumi Iida[1], Kimio Terao[1]
[1]*Chugai Pharmaceutical. Co., Ltd., Tokyo, Japan*

Aims: It is usually more difficult to build a PK-PD model with discrete symptomatic disease endpoints than a PK-PD model with continuous biomarkers because a symptomatic endpoint has often discrete scores with unbalanced scales. A static Investigator's Global Assessment (sIGA) is one of the primary efficacy endpoint of atopic dermatitis evaluation and a basis for FDA approval of atopic dermatitis evaluation in clinical study. It has a discrete score (0, 1, 2, 3, 4 or 5) and had a difficulty to apply the model for continuous values like indirect turnover model. A continuous-time Markov exposure-response model has been published by Lacroix et. al. in 2014 to model ACR20, 50 and 70 which are the discrete efficacy endpoints in rheumatoid arthritis area simultaneously (1). The model includes Markov element and it enables to consider individual time course of discrete scores. We hypothesized that the sIGA could be described with kind of continuous-time Markov exposure-response model and has developed the model for future clinical study design optimization based on simulated longitudinal sIGA scores.

Methods: A population PK-PD (sIGA) model was implemented to the data from the patients with atopic dermatitis in randomized double blind phase 2 study (ClinicalTraials.gov Identifier: NCT01986933) which included 5 arms (0.1, 0.5, 2 mg/kg Q4W, 2 mg/kg Q8W and placebo) up to 84 days after the first administration using a first-order conditional estimation method in NONMEM version 7.3.0. Modified continuous-time Markov exposure-response model was applied to sIGA with above 5 categories. Emax model was used to link the relationship between observed serum nemolizumab concentration and sIGA. Visual predictive check was performed to confirm a predictability of the model and bootstrapping method was utilized to estimate median and 90% confidence interval of the estimated parameters.

Results: The data of 1488 sIGA observations from 264 patients with severe to moderate atopic dermatitis was applied to the continuous-time Markov exposure-response model. The run has been converged successfully. The sIGA score showed improvement with the nemolizumab treatment and the rates of the patients who were in each category were calculated and compared to the simulated outputs as visual predictive check. The model described the observed data well. Population mean (90% bootstrapped range) of Emax on transfer rate constant of disease improvement, that of disease progression and EC50 were 121% (53.9% to 217%), -32.3% (-66.5% to -4.66%) and 1830 (749 to 5490) ng/mL, respectively. The mean serum nemolizumab trough concentration in 2 mg/kg arm was 8110 ng/mL and it was suggested that almost maximum effect was obtained between 0.5 and 2 mg/kg dose.

Conclusion: The sIGA scores were well described by the continuous-time Markov exposure-response model. The model had a longitudinal predictability of the sIGA scores with any dose regimen of nemolizumab. Continuous-time Markov exposure-response model is relatively accessible to implement and one of the recommended option to fit a symptomatic and categorical endpoint with discrete scores.

References:

1. Lacroix BD, Karlsson MO, Friberg LE. Simultaneous exposure-response modeling of ACR20, ACR50, and ACR70 improveement scores in rheumatoid arthritis patients treated with certolizumab pegol. CPT Pharmacometrics Syst. Pharmacol. 2014 Oct 29;3:e143.

266

Population pharmacokinetic-pharmacodynamic model of prednisolone in lupus nephritis patients

Ms Azrin N Abd Rahman[1,2], Prof Susan E. Tett[1], Dr Abdul Halim Abdul Gafor[3], Mr Brett C. McWhinney[4], Dr Christine E. Staatz[1]

[1]University of Queensland, Brisbane, Australia, [2]International Islamic University Malaysia, Kuantan, Malaysia, [3]Universiti Kebangsaan Malaysia Medical Centre, Cheras, Malaysia, [4]Royal Brisbane and Women's Hospital, Brisbane, Australia

Aim: The aim of this study was to develop a population pharmacokinetic-pharmacodynamic (PK-PD) model of unbound prednisolone in patients with lupus nephritis, taking into account: its non-linear protein binding and competition for binding sites with cortisol; the cortisol circadian rhythm; and the inhibitory effect of prednisolone on cortisol production.

Methods: Unbound and total prednisolone and cortisol concentration-time profiles, serum albumin and transcortin levels from 25 patients receiving doses of oral prednisolone ranging from 10 to 30 mg/day were included in the analysis. Samples were collected pre-dose and at 1, 2, 4, 6 and 8 hours post-dose on one or two occasions, with median (range) time between occasions of 59 (33 – 70) days. Population modelling was performed using NONMEM® software.

Results: Unbound prednisolone concentration-time profiles were adequately described by a two-compartment model with first-order absorption and elimination processes (See Figure 1). Cortisol and prednisolone protein binding were described using the sum of a Langmuir and linear type binding model. Endogenous cortisol production which follows a circadian rhythm was described using a dual linear release model. The PD characteristics of prednisolone were estimated by incorporating its inhibitory effect on cortisol production using an indirect response model. Apparent clearance and central volume of distribution of unbound prednisolone were estimated as 44.3 L/h/70 kg and 168 L/70kg with corresponding between subject variability (BSV) of 34.6% and 7.1%, respectively. CL_{CR} was found to have a significant influence on . The maximum cortisol production rate (R_{max}) had a median value of 0.683 µmol/h with BSV and between occasion variability (BOV) of 13.3% and 36.1%, respectively. BOV was also associated with bioavailability of unbound prednisolone (). Prednisolone nearly completely inhibits cortisol synthesis with an estimated maximum inhibitory effect (I_{max}) of 98.8% and a concentration causing 50% of maximum inhibition (IC_{50}) of 0.0001 µmol/L. Based on simulations from the final model at a prednisolone dose of 10 mg/day, greater than 2-fold increase in exposure to unbound prednisolone was noted in patients with a CL_{CR} of 10 mL/min compared to 90 mL/min suggesting that prednisolone dose reduction may be necessary in individuals with very poor renal function.

Conclusion: An integrated PK-PD model of prednisolone has been developed in Malaysian adults with lupus nephritis. The present model provides a greater understanding of the disposition of prednisolone and factors that influence unbound prednisolone concentrations in plasma.

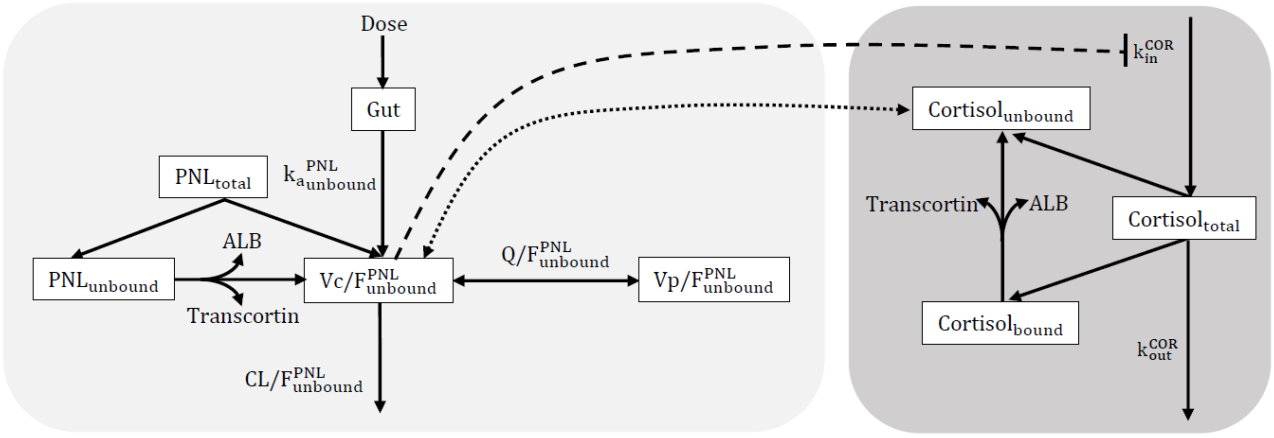

Figure 1: Graphical representation of the final structural model to describe the PK-PD of prednisolone.
The light grey block represents the PK model for prednisolone and the dark grey block represents the PD model of cortisol production. The dotted line represents the competitive binding of unbound prednisolone and unbound cortisol to transcortin. The dashed line represents the inhibition of cortisol production by prednisolone.

267

Quantitative review and meta-models of gastrointestinal pH to help inform mechanistic oral absorption models

Mr Ahmad Abuhelwa[1], Dr David Foster[1], Dr Richard Upton[1]

[1]*Australian Centre for Pharmacometrics, University Of South Australia, Adelaide, Australia*

Aims: The oral bioavailability of drugs is influenced by a many factors including the regional gastrointestinal (GI) pH. Small changes in the GI pH profile may have a great influence on the dissolution and absorption of drugs that exhibit pH-dependent dissolution and absorption. The aims of this study were to conduct a quantitative meta-analysis for the values of, and variability in, gastrointestinal (GI) pH in the different GI segments, characterize the effect of food on the values and variability in these parameters, and present quantitative meta-models of the distributions of GI pH to inform models of oral drug absorption.

Methods: The literature was systemically reviewed for the values of, and the variability in, GI pH under fed and fasted conditions in healthy subjects. The GI tract was categorised into 10 distinct regions: stomach (proximal, mid-distal), duodenum (bulb, mid-distal), jejunum & ileum (proximal jejunum, mid small intestine, and distal small intestine), and colon (ascending, transverse, and descending colon). Search engines of Web of Science, PubMed, and Google Scholar were used to screen for potential articles. The key words used in the search were “gastric pH”, “small intestinal pH”, “gastrointestinal pH”, “colonic pH”, AND “healthy subjects”. References in primary articles of GI pH were reviewed and relevant studies were included in the analysis. Meta-analyses of the means and SDs of GI pH were conducted using the “metafor” package (1) of the R language. Modelling the time-course of postprandial stomach pH was performed in NONMEM (2). The effect of various categorical and continuous moderators on GI pH were investigated including method of pH measurement, study origin, caloric content of administered food, age, and time since last meal.

Results: The final number of studies included in the meta-analysis of GI pH was 23 with a total number of 89 mean and SD values for the pH in the different GI locations. The fed status was the only moderator that significantly affected the meta mean pH of the stomach (p-value < 0.001) but had no significant influence on small intestinal and colonic pH (Table I). The time-course of postprandial gastric pH was described using an exponential model. Increased meal caloric content increased the extent and duration of postprandial gastric pH buffering. The different parts of the small intestine had significantly different pH while colonic pH was not significantly different between ascending, transverse and descending colon. Meta-models of the respective GI region were presented based on the results of meta-analysis.

Table X. Estimated meta-mean and meta-standard deviation of gastrointestinal pH

GI Location	Meta-mean	se-mean	95% CI	Meta-SD	se-SD	95% CI
Proximal stomach-fasted	2.01	0.29	1.42-2.61	0.41	0.12	0.16-0.66
Mid/distal stomach-fasted	1.68	0.19	1.30-2.06	0.39	0.08	0.23-0.54
Proximal stomach-Fed	4.47	0.29	3.875.07	0.46	0.12	0.20-0.71
Mid/distal stomach-Fed	4.14	0.28	3.58-4.71	0.43	0.12	0.19-0.68
Stomach pH-fasted	1.76	0.17	1.41-2.11	0.39	0.07	0.25-0.53
Stomach pH-fed	4.29	0.24	3.80-4.78	0.44	0.10	0.24-0.64
Whole Duodenum	6.12	0.12	5.86-6.34	0.43	0.09	0.24-0.63
Duodenum SD-duodenal bulb	-	-	-	0.70	0.14	0.40-0.99
Duodenum SD-mid/distal	-	-	-	0.28	0.08	0.09-0.46
Proximal jejunum	6.49	0.09	6.29-6.68	0.35	0.05	0.25-0.44
Mid small intestine	6.96	0.12	6.72-7.21	0.33	0.06	0.21-0.45
Distal small intestine	7.42	0.09	7.22-7.61	0.29	0.05	0.20-0.38
Ascending colon	6.32	0.15	6.00-6.64	0.37	0.07	0.22-0.52
Transverse colon	6.20	0.31	5.53-6.87	0.50	0.14	0.19-0.80
Descending colon	6.78	0.20	6.34-7.21	0.43	0.10	0.23-0.64

CI: confidence interval; se: standard error, SD: standard deviation.

Conclusion: Knowledge of GI pH is important for the formulation of pH-dependent dosage forms and in understanding the dissolution and absorption of orally administered drugs. The meta-models of GI pH could be used as part of semi-physiological pharmacokinetic models to characterize the effect of GI pH on the *in vivo* drug release and pharmacokinetics.

References:

1. Viechtbauer W. metafor: Meta-Analysis Package for R. R package version. 2010;2010:1-0.
2. Beal S, Sheiner LB, Boeckmann A, Bauer RJ. NONMEM User's Guides, Part V. (1989-2009), Icon Development Solutions, Ellicott City, MD, USA. 2009.

268

Faster ADVAN-style analytical solutions for simulations from common pharmacokinetic models

Mr Ahmad Abuhelwa[1], Dr David Foster[1], Dr Richard Upton[1]

[1]*Australian Centre for Pharmacometrics, University Of South Australia, Adelaide, Australia*

Aims: ADVAN-style analytical solutions for 1, 2, 3 compartment linear pharmacokinetic models of intravenous bolus, infusion, and first-order absorption have been derived and published by Abuhelwa et al., 2015 (1). The analytical solutions are used to simulate the time-course of drug amounts in the compartments of a pharmacokinetic models and they "advance" the solution of the model from one time point to the next, allowing for any dose or covariate factors to be accounted for. The ADVAN-style analytical solutions were coded in the R programming language (2) and have been shown to have speed advantages over solutions using differential equation solvers (1). The aims of this study were to enhance the performance and increase the computational speed for the ADVAN-style analytical solutions through coding the ADVAN-style analytical functions in a hybrid R/C++ programming languages and to present them in an Rpackage to make them available for the wider audience to be utilized for various applications.

Methods: ADVAN-style analytical solutions were written in the C++ programming language and were integrated in R using the Rcpp package attributes (3). The integrated R/C++ ADVAN-style analytical solutions were then made into an open-source R package ("PKADVAN") using RStudio. To assess computational speed, simulations for 1000 subjects using three compartment IV bolus, infusion, and first-order absorption models were performed and compared to relative computational speed of the equivalent compiled/uncompiled R-coded functions published by Abuhelwa et al. (1). For each subject, two doses were simulated with the evaluations performed at 1 hour time intervals for 2 days.

Results: Simulations using the integrated R/C++ ADVAN-style analytical solutions performed substantially faster than the equivalent R-coded functions. The integrated R/C++ functions simulated data for 1000 subjects in ~1 second, which was 2326 times faster than the equivalent R-coded functions. The relative speed of the integrated R/C++ functions was greater with the more complex models and with more extensive sample time evaluations. For example, simulations from the 3 compartment IV infusion model using the integrated R/C++ function were ~46 times faster than the R-coded function when the same dosing regimen simulations were extended for 5 days. The integrated R/C++ functions for 1, 2, 3 compartment IV bolus, infusion, and first-order absorption models are presented in the "PKADVAN" package which can be downloaded from GitHub.

Conclusion: A main application for the integrated R/C++ functions is for simulation from stochastic population pharmacokinetic models coded in R and incorporated into reactive Shiny Web applications (4). The speed of the integrated R/C++ analytical solutions is important here as they allow for simulating larger populations (e.g. 1000 subjects) without compromising the speed and the reactivity benefits of the Shiny application. The integrated R/C++ functions could be incorporated into an open-source mixed-effect modelling framework to estimate population parameters where speed is always desirable. With their capacity to handle complex dosing regimens and covariate structures, the "PKADVAN" package is expected to facilitate the investigation of useful open-source software for modelling and simulating pharmacokinetic data.

References:

1. Abuhelwa AY, Foster DJ, Upton RN. 2015. ADVAN-style analytical solutions for common pharmacokinetic models. J Pharmacol Toxicol Methods 73:42-48.
2. R Core Team. 2014. R: A Language and Environment for Statistical Computing R Foundation for Statistical Computing, Vienna, Austria
3. Eddelbuettel D, François R, Allaire J, Chambers J, Bates D, Ushey K. 2011. Rcpp: Seamless R and C++ integration. Journal of Statistical Software 40:1-18.
4. Wojciechowski J, Hopkins A, Upton R. 2015. Interactive Pharmacometric Applications Using R and the Shiny Package. CPT: Pharmacometrics & Systems Pharmacology 4.

269

Quantitative review and meta-models of gastrointestinal transit times to help inform mechanistic oral absorption models

Mr Ahmad Abuhelwa[1], Dr David Foster[1], Dr Richard Upton[1]

[1]*Australian Centre for Pharmacometrics, University Of South Australia, Adelaide, Australia*

Aims: The *in vivo* performance of single-unit ("tablet/capsule") and multiple-units ("pellets, multi-tablets") dosage forms may sometime be markedly influenced by their transits through the gastrointestinal tract (1). The aims of this study were to conduct a quantitative meta-analysis for the values of, and variability in, gastrointestinal (GI) transit times of single-unit and multiple-units solid dosage forms, characterize the effect of food on the values and variability in these parameters, and to present quantitative meta-models of the distributions of GI transit times in the respective GI regions to help inform models of oral drug absorption.

Methods: The literature was systemically reviewed for the values of, and the variability in, gastric, small intestinal, and colonic transit times under fed and fasted conditions in healthy subjects. Search engines of Web of Science, PubMed, and Google Scholar were used to screen for potential articles. The key words used for search were "gastric emptying", "small intestinal transit", "colonic transit", AND "non-disintegrating tablets" OR "pellets", AND "healthy subjects". References located in primary articles of GI transit times were reviewed and relevant studies were included in the analysis. Meta-analyses of the means and SDs of GI transit times were conducted using the "metafor" package (2) of the R language. Meta-models of GI transit were assumed to be log-normally distributed between the studied populations.

Results: Twenty nine studies including 125 reported means and standard deviations were used in the meta-analysis. Caloric content of administered food increased variability and delayed the gastric transit of both pellets and tablets (Table I). Small intestinal transit time (SITT) was significantly enhanced with increased food caloric content. The variability in the SITT of pellets was higher than tablets, regardless of the fed status. Food had no significant effect on the transit time through the colon; however, less is known about the transit of dosage forms through colon.

Table I. Estimated meta-mean and meta-standard deviation of Gastrointestinal Transit time (hours)

Calories	Meta-mean	se-mean	95% CI	Meta-SD	se-SD	95% CI
Gastric Transit time						
0-Fasted	1.39	0.16	1.07-1.71	0.67	0.08	0.51-0.83
100	1.69	0.14	1.42-1.96	0.71	0.07	0.58-0.85
300	2.28	0.12	2.05-2.52	0.81	0.06	0.68-0.93
700	3.47	0.21	3.06-3.87	0.99	0.11	0.77-1.21
1000	4.36	0.31	3.75-4.96	1.13	0.17	0.80-1.45
Small intestinal transit						
0-Fasted	3.61	0.14	3.34-3.89	1.19[a] (pellets)	0.11	0.96-1.41
100	3.51	0.12	3.28-3.74	0.89[a] (Tablet)	0.07	0.74-1.03
300	3.29	0.10	3.10-3.48			
700	2.86	0.15	2.57-3.16			
1000	2.54	0.23	2.09-3.00			
Colonic transit time	21.97	3.10	12.09-31.85	13.03	1.80	7.31-18.75
Whole gut transit time	29.81	1.90	23.78-35.85	14.52	1.10	11.01-18.03

CI: confidence interval; se: standard error, SD: standard deviation. Transit times are in hours.

[a] Formulation was the only significant moderator on standard deviation. Standard deviation was not significantly different between fasted and the different fed conditions.

Conclusion: GI transit times may influence the dissolution and absorption of orally administered drugs. The meta-values of GI transit times could be used as part of semi-physiological absorption models to characterize the influence of transit time on the dissolution, absorption and in vivo pharmacokinetic profiles of oral drugs.

References:

1. Connor A. Location, location, location: gastrointestinal delivery site and its impact on absorption. Therapeutic delivery. 2012;3(5):575.
2. Viechtbauer W. metafor: Meta-Analysis Package for R. R package version. 2010;2010:1-0.

270

Population pharmacokinetics of OZ439 in patients with falciparum and vivax malaria

Dr Piyanan Assawasuwannakit[1], Dr Aung Pyae Phyo[1,2,3], Dr Podjanee Jittamala[4], Prof François Nosten[1,2,3], Prof Sasithon Pukrittayakamee[5], Dr Mallika Imwong[6], Prof Nicholas White[1,3], Dr Stephan Duparc[7], Dr Fiona Macintyre[7], Dr Mark Baker[7], Dr Jörg Möhrle[7], Assoc Prof Joel Tarning[1,3]

[1]Mahidol-Oxford Tropical Medicine Research Unit, Faculty of Tropical Medicine, Mahidol University, Bangkok, Thailand, [2]Shoklo Malaria Research Unit, Mahidol-Oxford Tropical Medicine Research Unit, Faculty of Tropical Medicine, Mahidol University, Tak, Thailand, [3]Centre for Tropical Medicine, Nuffield Department of Clinical Medicine, University of Oxford, Oxford, UK, [4]Department of Tropical Hygiene, Faculty of Tropical Medicine, Mahidol University, Bangkok, Thailand, [5]Department of Clinical Tropical Medicine, Faculty of Tropical Medicine, Mahidol University, Bangkok, Thailand, [6]Department of Molecular Tropical Medicine and Genetics, Faculty of Tropical Medicine, Mahidol University, Bangkok, Thailand, [7]Medicines for Malaria Venture, Geneva, Switzerland

Aims: Artemisinin-based combination therapies are the recommended first-line treatment for *falciparum* malaria. Artemisinin derivatives, containing the peroxide pharmacophore, are the most potent and rapidly acting antimalarial drugs available. OZ439 is a novel synthetic trioxolane with a similar pharmacophore but with improved pharmacokinetic (PK) properties of prolonged elimination half-life and therefore prolonged antimalarial activity [1]. The aim of this work was to characterise the population PK properties of OZ439 in patients with *falciparum* and *vivax* malaria in Thailand.

Methods: Data were obtained from a phase 2a exploratory, open-label trial in 81 adult patients with acute, uncomplicated *falciparum* or *vivax* malaria. Patients were assigned to receive OZ439 as a single oral dose of 200 mg (n=20), 400 mg (n=20), 800 mg (n=20) or 1200 mg (n=21). Blood samples of OZ439 and its metabolites were collected at baseline and at 0.5, 1, 2, 3, 4, 6, 8, 12, 18, 24, 36, 48, 72, 96 and 168 hours post-dose. A population analysis was performed using NONMEM v.7.3. Concentrations measured to be below the lower limit of quantification were accounted for using the M3-method. One-, two- and three-compartment disposition models were evaluated. Zero-order, first-order with and without lag time and transit compartments were explored as absorption models. Covariates tested included total body weight, lean body weight, age, sex, dose and infection (*falciparum* vs *vivax*). Model evaluation was performed using likelihood ratio testing (OFV) and visual predictive checks (VPCs).

Results: The PK properties of OZ439 were best described by three transit compartments in the absorption phase followed by two distribution compartments with first-order elimination. Total body weight was a significant covariate on clearance and volume of distribution parameters. Dose was found to be a significant covariate resulting in a decreased mean transit time with increasing doses.

Conclusion: The PK properties of OZ439 were well described by the developed population PK model. Final PK parameter estimates had high precision and the final model showed a high predicitve performance, suggesting it to be suitable for further optimal trial design simulations. This will be a crucial tool in the further development of the antimalarial drug OZ439. Also, the developed model will be expanded to include all measured OZ439 metabolites.

References:

1. Phyo P *et al.* Antimalarial activity of artefenomel (OZ439), a novel synthetic antimalarial endoperoxide, in patients with *Plasmodium falciparum* and *Plasmodium vivax* malaria: an open-label phase 2 trial. Lancet Infect Dis. 2016;16(1):61-9.

271

A population dose-response analysis of lurasidone in treatment of major depressive disorder with mixed features

Dr. Yu-Yuan Chiu[1], Dr. Sunny Chapel[2], Dr. Jongtae Lee[2], Dr. Felix Agbo[1], Dr. Anthony Loebel[1]
[1]Sunovion Pharmaceuticals Inc., Fort Lee, United States, [2]Ann Arbor Pharmacometrics Group Inc., Ann Arbor, United States

Aims: Major depressive disorder (MDD) with mixed features is newly recognized by DSM-5 as a variant of MDD that is associated with subthreshold hypomanic symptoms. A recently completed placebo-controlled trial investigated the efficacy of lurasidone in this patient population. The objective of this pharmacometric analysis was to characterize the dose-response profile of lurasidone in patients with MDD with mixed features.

Methods: Population PK/PD modeling was performed based on data derived from a randomized, 6-week, double-blind, placebo-controlled, flexible-dose study (20–60 mg/day of lurasidone) in patients with MDD with mixed features (1). Pooled data included 1405 Montgomery-Åsberg Depression Rating Scale (MADRS) observations from 208 patients who had received lurasidone or placebo treatments. Potential covariates that might influence response to lurasidone were evaluated. Simulations were performed to reconcile the underlying linear dose-response relationship and the apparent flexible dose design-induced flat dose-response relationship. To incorporate the non-random nature of dose escalation in the current flexible dose design, the observed pattern of dose escalation depending on the weekly MADRS score improvement was stochastically accounted for.

Results: The placebo effect on the MADRS was adequately described by an exponential asymptotic placebo model. A linear dose-response model best described the effect of lurasidone across the dose range of 20–60 mg/day. Concomitant medication on drug effect slope is the only significant covariate thus no dose adjustment on the basis of demographic covariates is likely to be necessary. The study observed placebo-adjusted mean reductions in MADRS at Week 6 were 7.20, 7.75, and 7.45 for modal doses of 20, 40, and 60 mg/day, respectively. However, the model-based, placebo-adjusted mean reductions in MADRS at Week 6 were estimated to be 7.1, 8.6, and 10.6 for doses of 20, 40, and 60 mg/day, respectively. This difference was reconciled by simulations incorporating the non-random nature of the dose-escalation (ie, patients with less improvement tended to have dose escalation). The flexible-dose study simulation with an underlying linear dose-response relationship resulted in 8.6, 9.2, and 9.3 placebo-adjusted mean MADRS score reductions for doses of 20, 40, and 60 mg/day, respectively, which were generally consistent with the observed values.

Conclusion: A dose-response relationship for lurasidone in the treatment of MDD patients with mixed features was identified based on the current pharmacometric analysis. These findings suggested that higher lurasidone doses in the 20-60 mg/day range may be associated with larger treatment effects. Current results are consistent with a previous lurasidone dose-response analysis in patients with bipolar depression (2).

References:

1. Suppes T, Silva R, Cucchiaro J, et al. Lurasidone for the Treatment of Major Depressive Disorder With Mixed Features: A Randomized, Double-Blind, Placebo-Controlled Study. Am J Psychiatry. 2015 Nov 10. [Epub ahead of print].
2. Chapel S, Chiu YY, Hsu J, et al. Lurasidone Dose Response in Bipolar Depression: A Population Dose-Response Analysis. Clin Ther (2016)38 (1): 4-15.

272

Population pharmacokinetic analysis of 2'-benzoyloxycinnamaldehyde and its metabolites

Dr Sangmin Choe[1]

[1]*Pusan National University Hosptal, Busan, South Korea*

Aims: To build single dose population pharmacokinetic (PK) models for 2'-Benzoyloxycinnamaldehyde (CB-Ph) and its metabolites 2'-hydroxycinnamaldehyde (CB-OH) and 2'-hydroxycinnamic acid (CB-OH acid)

Methods: In a dose-escalating phase I study in patients with malignant solid tumor , three subjects received a single dose 500 mg CB-Ph and two subjects receives a single dose of 1000 mg CB-Ph. Plasma samples were collected at 0, 0.5, 1, 2, 4, 6, 8, 12, 24, 36, and 48 h and urine samples were collected during the intervals of -12-0, 0-6, 6-12, 12-24, and 24-48h. Population PK analysis was done using NONMEM.

Results: CB-Ph was not detected in any plasma or urine samples from the subjects throughout the time course indicating rapid conversion of CB-Ph to its metabolites, consistent with the findings in a previous animal PK study(1) . Thus Cb-OH and CB-OH acid plasma PK was analyzed using a population approach. Plasma concentrations of Cb-OH were well described by a biexponential structural model. Population parameter estimates were central volume of distribution (V1) 5.11 (BSV 65.5%) x dose (mg), peripheral volume of distribution (V2) 3.07 L (BSV fixed to 0), clearance 2.24 L/h (50.2%), and intercompartmental clearance 0.385 L/h (fixed to 0). Covariate analysis revealed no identifiable effects of age, weight, bosy surface area, renal or hepatic function on V1. The CB-OH acid formation clearance was 65.3 (97.6%) L/h, elimination clearance was 33.1 (132%) L/h, and the rate constant for intermediate compartments was 7.24 (fixed to 0) /h. CB-OH volume of distribution was fixed to the same value for central volume of distrubution.

Conclusion: Plasma data of CB-OH and CB-OH acid could be adequately described by compartmental PK models.

References:

1. Lee K, Kwon B-M, Kim K, Ryu J, Oh SJ, Lee KS, et al. Plasma pharmacokinetics and metabolism of the antitumour drug candidate 2'-benzoyloxycinnamaldehyde in rats. Xenobiotica. 2009 2009/03/01;39(3):255-65.

273

Quantitative model diagrams (QMD): a new perspective in model evaluation

Mr Benjamin Guiastrennec[1], Dr Ron J. Keizer[2], Pr Mats O. Karlsson[1]

[1]Department of Pharmaceutical Biosciences, Uppsala University, Uppsala, Sweden, [2]InsightRX, San Francisco, USA

Aims: To facilitate model communication and evaluation through intuitive visual representation of their structure, parameter values and uncertainty.

Methods: An open source R package (https://github.com/guiastrennec/modelviz) was developed for the translation of model structure from NONMEM output and scaling of parameters into diagrams, using the package DiagrammeR [1] for plotting. QMD were generated by scaling the compartment size to the distribution volume and arrow width to the corresponding clearance or rate constant. When available, parameter uncertainty or between subject variability (BSV) could be visualized using color-coded compartments and arrows.

Results: Diagrams for the standard NONMEM model library (ADVAN 1–4 and 11–12) have been fully automated. A differential equation parser has been implemented to require minimal or no user input. To illustrate the use of QMD in Pharmacometrics, three example models of various complexities were selected, including a 3-compartment model with first order absorption [2] (Figure 1), a mechanistic model [3] and a physiologically-based pharmacokinetic model [4].

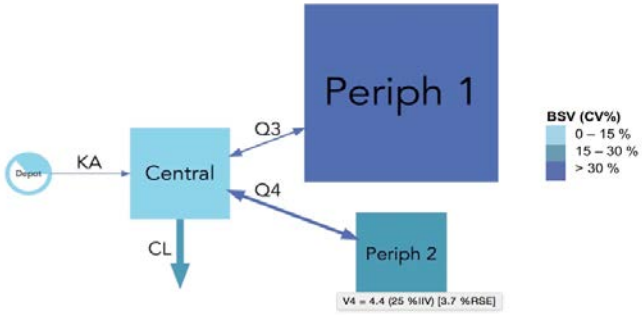

Figure 1: QMD of a 3-compartment model with first order absorption [2]. BSV is represented by the color code, bioavailability by the pie chart, volumes by the surface area of compartments and clearances by arrow width. The interactive tooltip displays arrow and compartment information.

Conclusion: QMD effectively summarized the information on model structure, compartment volume, clearance and rate constant, along with their uncertainty or BSV within a single intuitive graph. Informative representation of pharmacometric models was demonstrated to be applicable for a range of model structure and complexity and may improve model communication within and outside of the pharmacometric community.

References:

1. R. Iannone *et al*. Create Graph Diagrams and Flowcharts Using R. CRAN. 2016;v0.8.2.
2. S. Fanta *et al*. Developmental pharmacokinetics of ciclosporin – a population pharmacokinetic study in paediatric renal transplant candidates. BJCP. 2007;64(6):772–84.
3. E. Hénin *et al*. A Mechanism-Based Approach for Absorption Modeling: The Gastro-Intestinal Transit Time (GITT) Model. AAPSJ. 2012;14(2):155–63.
4. S. Björkman. Prediction of drug disposition in infants and children by means of physiologically based pharmacokinetic (PBPK) modelling: theophylline and midazolam as model drugs. BJCP. 2004;59(6):691–704.

274

Placebo effect in overactive bladder clinical studies: longitudinal model-based meta-analysis of micturitions

Dr Chihiro Hasegawa[1], Dr Tomoya Ohno[1]

[1]*Clinical Pharmacology, Translational Medicine Center, Ono Pharmaceutical Co., Ltd., Osaka, Japan*

Aims: Existing evidence from clinical trial data suggests that a positive placebo effect occurs in overactive bladder (OAB) patients (1). Researchers also confirmed that the placebo response in OAB clinical trials was substantial by a meta-analysis based on the change from baseline (CFB) outcomes at the end of the study period (2). However, the time course of the placebo response in OAB clinical trials has not been systematically investigated via model-based analysis. The aim of this study is to describe the time course of the placebo effect in OAB and quantitatively investigate the covariates for the placebo response.

Methods: We conducted a search of public data sources including new drug application (NDA) materials which had been published online for the study-level micturition frequency (MF) to develop the placebo effect model. Mean patient age, mean male proportion, baseline MF, and ethnicity (non-Japanese or Japanese) were tested as covariates. The parameter estimation was performed using NONMEM 7 (Level 1.2, ICON Development Solutions, Ellicott City, MD, USA) with the FOCE-I method.

Results: There were 17 clinical studies for anti-cholinergic (anti-muscarinic) agents and a beta-3 adrenergic agonist with 3,580 placebo-arm patients. The exponential models rather than linear ones adequately described the time course of placebo effect with the typical value of the maximum placebo effect (Pmax) of approx. 2 MF reduction/day. Ethnicity (non-Japanese or Japanese) was detected as a covariate on the rate constant for onset of the placebo effect with objective function value (OFV) reduction of 7.6 (Figure 1), which had already been suggested in clinical studies of fesoterodine, one of the anti-muscarinic agents.

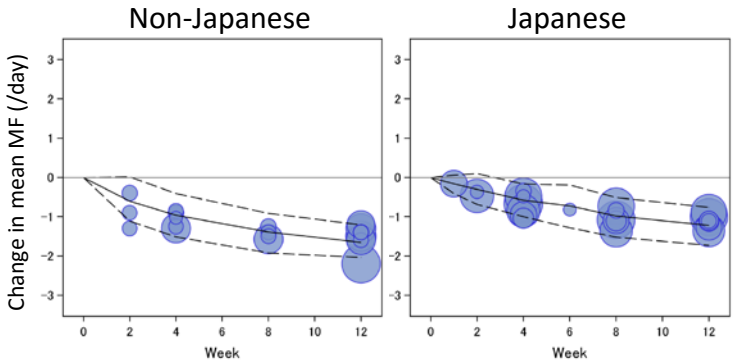

Figure 11
Visual predictive check for change in micturition frequency (MF)
Each plot shows the observed mean values (circles), predicted median (solid line), and 90% prediction (confidence) interval (5th and 95th percentiles, broken lines) versus time.
The size of circles reflects the number of patients in each study placebo arm.

Conclusion: The placebo effect in the OAB clinical trials is adequately described by an exponential model over time. The developed model could be the useful tool for the drug effect evaluation.

References:

1. Mangera A, Chapple CR, Kopp ZS, Plested M. The placebo effect in overactive bladder syndrome. Nat Rev Urol. 2011;8(9):495-503.
2. Lee S, Malhotra B, Creanga D, Carlsson M, Glue P. A meta-analysis of the placebo response in antimuscarinic drug trials for overactive bladder. BMC Med Res Methodol. 2009;9:55.

275

Population pharmacokinetic model of doxycycline plasma concentrations – pooled study data

Mr Ashley M Hopkins[1], Dr David JR Foster[1], Dr Stuart J Mudge[2], Prof Richard N Upton[1]

[1]Australian Centre for Pharmacometrics, University of South Australia, Adelaide, Australia, [2]Mayne Pharma International Pty Ltd, Adelaide, Australia

Aims: Doxycycline is a oral tetracycline antimicrobial. The literature is presently void of a significantly powered population pharmacokinetic analysis of doxycycline. Using pooled study data the aim of this study was to develop a population pharmacokinetic model of doxycycline plasma concentrations following oral doxycycline administration.

Methods: Doxycyline pharmacokinetic data was avalible from eight Phase 1 clinical trials conducted by Mayne Pharma following the administration of formulations including Doryx tablets and Doryx capsules in cross-over study designs. A population pharmacokinetic model was developed in a step-wise manner using NONMEM® 7.3. The final covariate model was developed according to a forward-inclusion ($p<0.01$) and then backward deletion ($p<0.001$) procedure.

Results: 7093 doxyclyine plasma concentrations were avaliable from 178 individuals enrolled across eight Phase 1 clinical trials. The final model was a two compartment model with two-transit absorption compartments (3 transit rate constants), and included the basic structural components: transit compartment absorption rate (KTR; 2 h^{-1}; se% 4.3), apparent clearance (CL; 4.63 L/h/70 kg FFM; se% 5), inter compartmental clearance (Q; 11.3 L/h/70 kg FFM; se% 4.1), apparent central volume (V; 55.2 L/70 kg FFM; se% 7.8) and apparent peripheral volume (V2; 49.8 L/70 kg FFM; se% 3.5). The final model was allometrically scaled for fat free mass (FFM), and had a proportional (%CV 19.6; se% 2.5) and additive (19.8 µg/L; se% 18.5) residual error model. The model had a covariance matrix with between subject variability for the parameters KTR (%CV 28.2; se% 8.3), CL (%CV 19.3; se% 6.4), V (%CV 37.6; se% 5.8) and V2 (%CV 15.1; se% 11.2). Between occasion variability was included on KTR (%CV 27.2; se% 10.5) and CL (%CV 13.5; se% 7.8). Structural covariates in the base model included formulation effects on relative bioavailability (F), absorption lag (ALAG) and KTR under the fed status. An absorption lag for the fed status (FTLAG2 = 0.203 h) was also included in the model as a structural covariate. Between study differences were included on the F, KTR, CL and V parameters. Fed status was observed to decrease F by 10.5% (se% 33.2), and the female sex resulted in a 14.4% (se% 20.4) increase in CL. *Figure 1* presents a prediction corrected visual predictive check of the final model which is consistent with a model appropriately capturing the structural and population components of a pooled study data analysis.

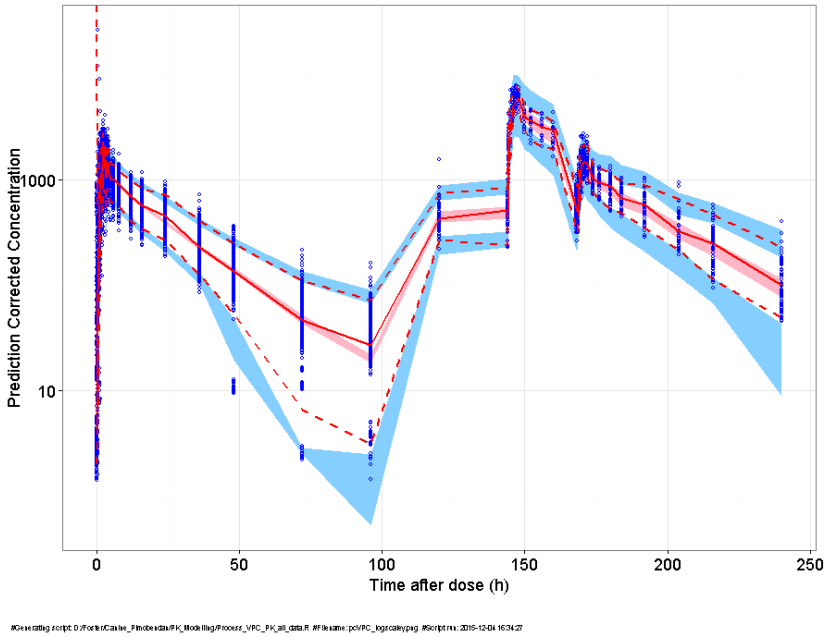

Figure 2: pcVPC of the final model for doxycycline concentrations.

Conclusion: A population pharmacokinetic model was developed to describe doxycycline plasma concentrations following single / multiple doses of oral doxycycline collected from eight clinical trials. To our knowledge this is the first and largest population pharmacokinetic analysis of doxycycline plasma concentrations following oral doxycycline administration. The model may potentially be used to critically examine and optimise doxycycline dose regimens.

276

Comparison between non-compartmental analysis and non-linear mixed effects in determining bioequivalence for two-compartment drugs

Mr Jim Hughes[1], Dr David Foster[1], Prof Richard Upton[1]

[1]*Australian Centre for Pharmacometrics, University of South Australia, Adelaide, Australia*

Aims: To develop a software tool with the ability to rapidly compare Non-Compartmental Analysis (NCA) and Non-Linear Mixed-Effect Modelling (NLMEM) methods in determining bioequivalence of two-compartment kinetic drugs and to elucidate the impact of changes in (i) random unexplained variability (RUV) at the lower limit of quantification (LLOQ), (ii) the extent of censoring data below the LLOQ and (iii) the concentration sampling times.

Methods: A tool using both R and NONMEM was developed to allow the comparison of NCA and NLMEM in multiple scenarios. The R code generated sample data, ran the NCA analysis and called NONMEM to run NLMEM on the same data. Each scenario tested included 500 bioequivalence studies, comprising of 24 subjects each. Each study had concentration-time profiles simulated where relative bioavailability (Frel), RUV at the LLOQ and LLOQ differed between scenarios. NLMEM analyses employed the M1 and M3 methods for dealing with values below the LLOQ and two methods for determining Frel: using post-hoc estimates of Frel directly or estimated from post-hoc calculations of AUC from model parameters. Finally the test/reference ratios were used to determine bioequivalence.

Results: The tool allowed for NCA and NLMEM to be run sequentially for 105 scenarios. NLMEM showed a consistent 10-20% higher accuracy and sensitivity in identifying bioequivalent drugs when compared to NCA, while NCA was found to have a higher specificity than NLMEM (1-10% higher). Increasing the LLOQ resulted in censoring of larger amounts of data and a decrease in the accuracy and sensitivity of NCA by approximately 20%, but had minimal effects on NLMEM.

Conclusion: A highly robust and automated tool has been developed that provides a platform for comparing NCA and NLMEM methods and can be used to extend beyond the scenarios evaluated here. In the situations examined it is seen that NLMEM is more robust than NCA and may have a role to play in the determination of bioequivalence, despite its lower specificity.

277

Pharmacokinetic modeling and simulation analysis of LCB01-0371, a novel oxazolidinone antibiotic

MD, PhD Hyeong-Seok Lim[1,2], PhD Yong Zu Kim[3], PhD Young Lag Cho[3], Ms Hee Sook Nam[3], MD, PhD Kyun-Seop Bae[1,2]

[1]Asan Medical Center, Seoul, South Korea, [2]University of Ulsan College of Medicine, Seoul, South Korea, [3]LegoChem Biosciences, Inc., Daejeon, South Korea

Aims: LCB01-0371 is a new oxazolidinone antibiotic with cyclic amidrazone under clinical development. It exerts its anti-bacterial activity by binding to bacterial ribosomes, thereby inhibiting protein synthesis of the bacteria. The purpose of this study was to explore the pharmacokinetics (PK) of oral LCB01-0371 in healthy Korean volunteers, to predict the plasma LCB01-0371 concentration over time on various dosing regimens of LCB01-0371 via Monte-Carlo simulation.

Methods: PK data from 110 healthy, Korean, male subjects in three phase 1 studies for LCB01-0371 were used for this analysis. The subjects received single or multiple oral doses of LCB01-0371 in 50 ~ 3,200 mg, and blood and urine were collected serially for PK. Plasma and urine concentrations of LCB01-0371 were measured using validated LC/MS-MS. PK were analyzed by nonlinear mixed effect modeling implemented in NONMEM (version 7.3).

Results: Plasma LCB01-0371 was absorbed very fast after oral administration with followed by rapid decline in plasma concentration. The LCB01-0371 concentration in plasma and amount excreted in urine over time were best described by two-compartment model (central Vd, 82.4 L; peripheral Vd, 8.59 L) with absorption lag ($ALAG_1$, 0.212 hour) and mixed zero (D_1, 0.286 hour) and first order absorption (Ka, 80.7 /hour) process. Basic goodness of fit plots, visual predictive check plots showed that the final plasma and urine PK model describe the data reasonably well.

Conclusion: The current modeling and simulation analysis characterized the pharmacokinetics of LCB01-0371 in Korean healthy normal male subjects, which will be useful in identifying the optimal dosing regimens of LCB01-0371.

278

Pharmacokinetic and pharmacodynamic modeling and simulation analysis of a novel donepezil patch formulation

MD, PhD Hyeong-Seok Lim[1,2], MD, PhD Hee Youn Choi[1,2], MD, PhD Yo Han Kim[1,2], Mr Donghyun Hong[3], Mr Seong Su Kim[3], Mr Young Kweon Choi[3], MD, PhD Kyun-Seop Bae[1,2]

[1]Asan Medical Center, Seoul, South Korea, [2]University of Ulsan College of Medicine, Seoul, South Korea, [3]iCure Pharmaceutical Incorporated, Anseong, South Korea

Aims: Donepezil is a well-known reversible noncompetitive acetylcholinesterase inhibitor for the symptomatic treatment of Alzheimer's disease (AD). The purpose of this study was to explore the pharmacokinetics (PK) of donezeil patch under clinical development using mixed effect modeling analysis, and to expore optimal dosing regimens of the donepezil patch in comparison with donepezil oral formulation.

Methods: PK data used in this analysis were from 44 Korean, healthy, male subjects in two phase 1 studies, where all the subjects received single or multiple doses of donepezil patch of 43.75, 87.5, and 175 mg, and 12 of them received single oral dose of donepezil, 10 mg followed by single dose of donepezil patch. Plasma concentrations of donepezil were measured using validated LC/MS-MS. Donepezil PK were analyzed by nonlinear mixed effect modeling implemented in NONMEM (version 7.3).

Results: The PK modeling analysis were conducted seqentially for oral formulation and patch, which describes the data of oral formulation compared to simultaneous analysis of both oral and patch formulations. PK for oral formulation was modeled first, then the PK of patch was modeled after fixing the oral absorption related parameters of absorption rate constant (ka) and absorption delay (ALAG1) as the estimates of the previous fitting, since the predose concentrations of patch was not 0. A well-stirred model with two-compartment distribution and delayed absorption was chosen as the final model for the oral formulation, where the Michaelis-Menten equation describes both first-pass effect during absorption and systemic clearance. The relative bioavailability of donepezil after patch application compared to oral dosing was described to be affected by the duration of patch application, and the study. In the basic goodness of plots, no significant trend in the model fitting was shown in PK models of both oral and patch formulations described the PK data. The final model predicted the real, observed concentration data reasonably well. The Monte-Carlo simulation for plasma donepezil concentration predicted that overall, exposure to plasma donepezil is similar between donepezil 10 mg oral dosing every 24 hours and donepezil patch 175 mg every 72 hours, and between donepezil 5 mg oral dosing every 24 hours and donepezil patch 87.5 mg every 72 hours (Figure 1).

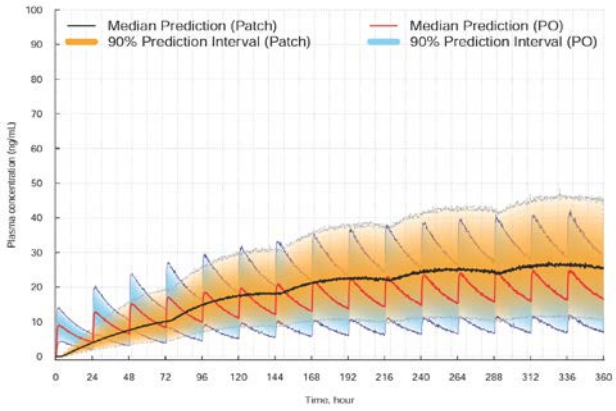

1. Donepezil 5 mg PO every 24 hours and Donepezil Patch 87.5 mg every 72 hours

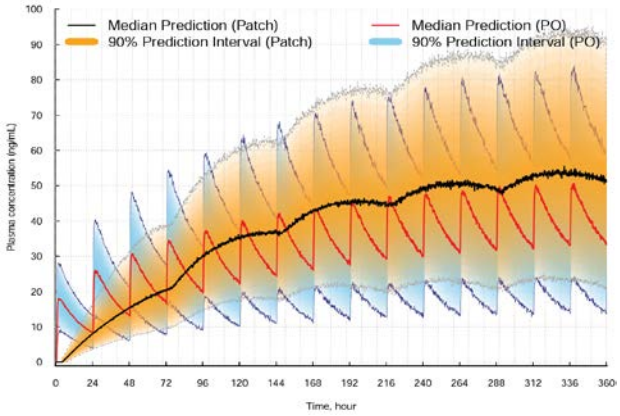

(a) Donepezil 10 mg PO every 24 hours and Donepezil Patch 175 mg every 72 hours

Figure 1. Model predicted plasma donepezil concentrations over time after donepezil oral and patch formulations

Conclusion: We developed a population PK model describing the plasma PK of donepezil patch formulation and compared it with that of donepzeil oral formulation in healthy Korean adult males. PK simulation based on the final PK model suggested that donepezil 175 mg patch every 72 hours shows similar concentration profile with oral dosing of donepezil 10 mg every 24 hours, and 87.5 mg patch every 72 hours with oral dosing of 5 mg every 24 hours.

279

Examining the predictive performance of equations to estimate glomerular filtration rate in paediatric oncology patients

Miss Carolina Llanos[1], Dr Christine Staatz[1], Miss Rachael Lawson[2], Dr Stefanie Hennig[1]

[1]The University of Queensland, Brisbane, Australia, [2]Lady Cilento Children's Hospital, Brisbane, Australia

Aims: The National Kidney Foundation guidelines recommend the use of equations to estimate glomerular filtration rate (GFR) in paediatrics and adults, some of which require serum creatinine plasma concentrations. However, serum creatinine may not always be reflective of renal function in paediatrics, as a lack of muscle mass may lead to very low serum creatinine concentrations, which may be misinterpreted as good renal function. This study aims to evaluate the predictive performance of five equations to estimate GFR in paediatric oncology patients in whom a measured GFR had been obtained from the excretion of ^{51}Cr-EDTA.

Methods: Data were collected retrospectively from the medial records of paediatric oncology patients at the Lady Cilento Children Hospital in Brisbane, Australia from 2007 to 2013. Patients had undergone a radioisotopic method to measure their GFR prior to treatment with cisplatin, carboplatin, tacrolimus, cyclosporine or a bone marrow transplant. Estimates of GFR (mL/min) for these patients were obtained from five equations suggested to be useful in children (1-4). GFR predicted by the five equations was compared to GFR measured by excretion of ^{51}Cr-EDTA and equation predictive performance was examined in terms of bias, precision and accuracy. To examine how best to handle serum creatinine concentrations <30 µmol/L which is below the assay limit of quantification these values were either replaced by 15 µmol/L, 30 µmol/L or an expected mean serum creatinine concentration based on patient age and gender according to Ceriotti et al (5).

Results: Sixty-eight children (median age 3.7 years) contributed 118 measurements of measured GRF. Measured GFR (mL/min) values ranged from 7 to 146 (median: 38.5). The equation proposed by Rhodin et al. (2) yielded the least bias, the highest precision and the highest accuracy in estimating GFR reflected by a mean prediction error, a root mean square error and a mean relative percentage prediction error of -0.13 mL/min, 12.3 mL/min and 7.96%, respectively. The Schwartz equation (1) and the equation proposed by Cole et al.(3), also performed reasonably well with a mean relative percentage prediction error of 14.6% and 25%, respectively. The least accurate model was the equation proposed by Leger et al. (4). 60% of collected serum creatinine concentrations were reported as <30 µmol/L. Setting those serum creatinine concentrations to 15 µmol/L resulted in the least accurate and the most biased estimate of GFR for all tested equations that required a measurement of serum creatinine concentration.

Conclusions: This study shows that an equation by Rhodin et al. which does not use serum creatinine concentration to estimated GRF had the best agreement with measured GFR obtained by ^{51}Cr-EDTA clearance in oncology children. This equation which describes maturation of renal function in children using total body weight and post-menstrual age avoids problems associated with serum creatinine concentrations below the assay quantification limit.

References:

1. Schwartz GJ, Munoz A, Schneider MF, Mak RH, Kaskel F, Warady BA, et al. New equations to estimate GFR in children with CKD. Journal of the American Society of Nephrology : JASN. 2009;20(3):629-37.
2. Rhodin MM, Anderson BJ, Peters AM, Coulthard MG, Wilkins B, Cole M, et al. Human renal function maturation: a quantitative description using weight and postmenstrual age. Pediatric nephrology. 2009;24(1):67-76.
3. Cole M, Price L, Parry A, Keir MJ, Pearson AD, Boddy AV, et al. Estimation of glomerular filtration rate in paediatric cancer patients using 51CR-EDTA population pharmacokinetics. British journal of cancer. 2004;90(1):60-4.
4. Leger F, Bouissou F, Coulais Y, Tafani M, Chatelut E. Estimation of glomerular filtration rate in children. Pediatric nephrology. 2002;17(11):903-7.
5. Ceriotti F, Boyd JC, Klein G, Henny J, Queralto J, Kairisto V, et al. Reference intervals for serum creatinine concentrations: assessment of available data for global application. Clinical chemistry. 2008;54(3):559-66.

280

Population pharmacokinetic model of gentamicin in paediatric oncology patients

Miss Carolina Llanos[1], Dr Christine Staatz[1], Miss Rachael Lawson[2], Dr Stefanie Hennig[1]

[1]The University of Queensland, Brisbane, Australia, [2]Lady Cilento Children's Hospital, Brisbane, Australia

Aims: To describe the population pharmacokinetics of gentamicin in paediatric febrile neutropenic patients and to identify covariates which explain pharmacokinetic variability in this population.

Methods: Data for pharmacokinetic analysis were collected retrospectively from the medical records of paediatric febrile neutropenic patients who had undergone gentamicin concentration-time profiling at the Lady Cilento Children's hospital between 2008 and 2013. A population pharmacokinetic model of gentamicin was developed using a nonlinear mixed effects modelling approach with NONMEM® software version 7.3 with an Intel FORTRAN compiler and Perl Speaks NONMEM (PSN) version 3.5.3. Typical population pharmacokinetic parameters of gentamicin as well as between-subject and between-occasion variability were estimated in these patients via the first-order estimation with interaction method. Xpose (v 4.0) and R software was used for data exploration and visualisation. One- and two-compartment disposition models with first-order elimination were tested during model building. Proportional, additive and combined error models were compared to describe residual variability. Covariates screened to assess their influence on the pharmacokinetics of gentamicin included: post-natal age (PNA), body weight (WT), fat-free mass (FFM) (1), renal function (eGFR) (2, 3) and concomitant nephrotoxic medication such as metrothexate, cyclophosphamide, ambisome, cyclosporine, cisplatin and carboplatin. Potentially influencing covariates were included in the model following a sequential forward selection and backward elimination step. Difference in objective function value (ΔOFV), visual comparison with goodness-of-fit plots and also difference in magnitude of unexplained and explained parameter variability (4) was used for model comparison. Model predictive performance was evaluated via prediction-corrected PVC (pcVPC) based on 1000 simulations.

Results: Data were collected from 423 oncology paediatric patients aged 0.21-18 years (median: 5.18 years). Gentamicin disposition was well described by a two-compartment model with first order elimination. The best base model allowed estimation of between subject variability (BSV) associated with clearance (CL), volume of the central (V_1) and peripheral (V_2) compartments, and intercompartmental clearance (Q); correlation between CL and V_1 and estimation of between occasion variability (BOV) in CL. Residual unexplained variability (RUV) was better described using a combined error model. A model that included a covariate effect of FFM on CL, V_1, Q and V_2 and PNA on CL had increased explained parameter variability on CL compared to one that included a covariate effect of eGFR (calculated using the Rhodin formula) on CL. Explained parameter variability on CL increased from 0.17 to 1.30 (L/h) when FFM was used instead of WT. Parameter estimates (BSV (%CV)) were CL (L/h/70kg): 6.33 (14.5%), V_1 (L/70kg): 22.4 (17.7%), Q (L/h/70kg): 0.69 and V_2 (L/70kg): 16.1 (29.8%). BOV (%CV) on CL was 21.8%. The proportional error component of RUV (%CV) was 35.3% and the additive error component was 0.04 mg/L.

Conclusions: FFM and PNA influence the pharmacokinetics of gentamicin in oncology paediatric patients. These covariates provided a better fit and increased explained variability on CL compared to utilising the Rhodin equation, which uses WT and PNA age to obtain eGFR . The effects of concomitant nephrotoxic medication on the pharmacokinetics of gentamicin are still to be investigated.

References:

1. Al-Sallami HS, Goulding A, Grant A, Taylor R, Holford N, Duffull SB. Prediction of Fat-Free Mass in Children. Clinical pharmacokinetics. 2015;54(11):1169-78.
2. Rhodin MM, Anderson BJ, Peters AM, Coulthard MG, Wilkins B, Cole M, et al. Human renal function maturation: a quantitative description using weight and postmenstrual age. Pediatric nephrology. 2009;24(1):67-76.
3. Schwartz GJ, Munoz A, Schneider MF, Mak RH, Kaskel F, Warady BA, et al. New equations to estimate GFR in children with CKD. Journal of the American Society of Nephrology : JASN. 2009;20(3):629-37.
4. Hennig S, Karlsson MO. Concordance between criteria for covariate model building. Journal of pharmacokinetics and pharmacodynamics. 2014;41(2):109-25.